

**THE DESIGN AND SYNTHESIS OF STRAINED TRANSITION STATE  
ANALOGUES FOR PHOSPHOTRIESTER HYDROLYSIS**

**by**

**Gabriel Hum**

**A thesis submitted in conformity with the requirements  
for the degree of Masters of Science  
Graduate Department of Chemistry  
University of Toronto**

**© Copyright by Gabriel Hum 1997**

**The author has granted a non-exclusive licence allowing the National Library of Canada to reproduce, loan, distribute or sell copies of this thesis in microform, paper or electronic formats.**

**The author retains ownership of the copyright in this thesis. Neither the thesis nor substantial extracts from it may be printed or otherwise reproduced without the author's permission.**

**L'auteur a accordé une licence non exclusive permettant à la Bibliothèque nationale du Canada de reproduire, prêter, distribuer ou vendre des copies de cette thèse sous la forme de microfiche/film, de reproduction sur papier ou sur format électronique.**

**L'auteur conserve la propriété du droit d'auteur qui protège cette thèse. Ni la thèse ni des extraits substantiels de celle-ci ne doivent être imprimés ou autrement reproduits sans son autorisation.**

0-612-29223-1

**Canada**

**The Design and Synthesis of Strained Transition State Analogues for  
Phosphotriester Hydrolysis, Masters of Science, 1997, Gabriel Hum,  
Department of Chemistry, University of Toronto**

Isomeric 2,5-di-*p*-nitrophenyl phospholanate esters were synthesized using a modified McCormack reaction. They are to be employed as novel transition state analogues (TSA's) for the hydrolysis of phosphotriesters. Antibodies raised against these haptens are intended to exert strain upon their substrates in order to exercise their catalysis by a combination of ground state destabilization and transition state stabilization. Confirmation of the strained nature of the TSA's was confirmed by determining the C-P-C bond angle by X-ray structure analysis of a 2,5-diphenyl phospholanic acid precursor. The TSA's were conjugated to carrier proteins (bovine serum albumin and keyhole limpet hemocyanin) and used for the generation of monoclonal antibodies. The corresponding bis(*p*-nitrophenyl)phosphate and *p*-nitrobenzyl-*p*-nitrophenyl phosphonate antibody substrates were also synthesized. Preliminary kinetics studies on these substrates showed that they are kinetically stable enough for screening purposes yet sufficiently labile to be susceptible to antibody catalysis.

As is customary, I would like to begin by expressing my gratitude to my research supervisor, Professor Scott D. Taylor, for his guidance, patience, and support. He has always set the highest standards, and for that I thank him.

To the members of the Taylor group, past and present, I thank them for their advice, camaraderie, and comic relief. Special mention goes to A. N. Dinaut, and my partner in crime, C. C. Kotoris, who have been there with me for the last two years both as friends and colleagues.

I thank my parents and siblings for their love, encouragement, and understanding. Their support never wavered regardless of what decisions I made. I would also like to thank my in-laws for their assistance over the past two years, which made things easier at their own sacrifice.

Finally, I would like to thank my wife, Stephanie, and daughter, Kelsey, for their infinite patience and understanding. When things are at their worst, you guys have always managed to make me smile.

<b>Abstract</b>	ii
<b>Acknowledgments</b>	iii
<b>Table of Contents</b>	iv
<b>Abbreviations</b>	vi
<b>List of Schemes</b>	viii
<b>Chapter 1 - Introduction</b>	1
<b>1.1 General Overview</b>	1
<b>1.2 Catalytic Antibodies</b>	1
<b>1.3 Antibody Catalyzed Phosphoester Hydrolysis</b>	5
<b>1.4 The Role of Strain in Bio Catalysis</b>	8
<b>1.5 Design of a Strained TSA for the Hydrolysis of Phosphotriesters</b>	13
<b>Chapter 2 - Experimental</b>	22
<b>2.1 Materials and Methods</b>	22
<b>2.2 Synthesis of Transition State Analogues</b>	23
<b>2.3 Synthesis of Substrates</b>	34
<b>2.4 Hapten Isomerization Studies</b>	37
<b>2.5 Conjugation of TSA's to Carrier Proteins</b>	38
<b>2.6 Substrate Hydrolysis Studies</b>	39
<b>Chapter 3 - Results and Discussion</b>	40
<b>3.1 Synthesis of Haptens</b>	40
<b>3.2 Hapten Isomerization Studies</b>	65
<b>3.3 Conjugation of Haptens to Proteins</b>	73
<b>3.4 Crystal Structure of trans-2,5-diphenyl phospholanic acid</b>	74

<b>Conclusions</b>	82
<b>References</b>	83
<b>Appendix A: Supplementary Crystallographic Data</b>	A(i)

## Abbreviations

approx.....	approximately
Ar.....	argon
BSA.....	bovine serum albumin
DIAD.....	diisopropylazido dicarboxylate
DMF.....	dimethyl formamide
DMSO.....	dimethyl sulphoxide
EDC.....	1-(3-methyl-amino-propyl)-3-ethyl-carbodiimide hydrochloride
eq.....	equivalent
EtOAc.....	ethyl acetate
hr.....	hour
KLH.....	keyhole limpet hemocyanin
M.....	molar
min.....	minute
NHS.....	N-hydroxy succinimide
O/N.....	overnight
PG.....	protecting group
Ph.....	phenyl group
ppm.....	parts per million
R <sub>f</sub> .....	migration distance on a TLC plate
RT.....	room temperature
TBP.....	trigonal bipyramidal

THF.....tetrahydrofuran  
TMSI.....trimethyl silyl iodide  
TS.....transition state  
TSA.....transition state analogue



## List of Schemes

Scheme	Title	Page
1	General route for generating abzymes	2
2	Substrate and TSA for carbon ester hydrolysis	4
3	Substrate and hapten for $\beta$ -fluoride elimination	5
4	Phosphate ester hydrolysis via a TBP transition state	6
5	Mechanism of catalysis by strain	9
6	Reaction coordinate diagram for an antibody strain catalyzed mechanism	10
7	Hydrolysis of cyclic and acyclic phosphate esters	12
8	Hydrolysis of phosphotriester substrates via a strain mechanism	15
9	Kalinov's <sup>30</sup> synthesis of 1-methoxy-trans-2,5-diphenylphospholanate	16
10	Synthesis of <b>25</b> and <b>26</b> by Taylor <sup>26</sup>	18
11	Synthesis of <b>13</b> and <b>14</b> by Taylor <sup>26</sup>	19
12	Retrosynthesis of <b>29</b> and <b>30</b>	42
13	Retrosynthesis of <b>29</b> and <b>30</b> via nitration of precursors	43
14	Retrosynthesis of <b>29</b> and <b>30</b> via nitration of <b>13</b> and <b>14</b>	43
15	McCormack reaction with <b>33</b>	44
16	McCormack reaction with <b>31</b> and <b>41</b>	45
17	Synthesis of <b>20</b> and <b>21</b> By Taylor <sup>26</sup>	46
18	Direct attachment of linker chain to acid chlorides	47
19	Hydrogenation of <b>20</b> and <b>21</b>	49
20	Isomerization of <b>23</b> to <b>22</b>	50
21	Nitration of ethyl esters <b>22-24</b>	55
22	Conversion of ethyl esters to acids	56
23	Synthesis of 6-hydroxy-allyl hexanoate <b>51</b>	57

24	Synthesis of <b>30</b> via an acid chloride coupling	58
25	Synthesis of <b>29</b> via an acid chloride coupling	59
26	Synthesis of <b>30</b> via a Mitsunobu coupling	60
27	Mitsunobu coupling with <b>41</b>	61
28	Mechanism of Mitsunobu coupling	62
29	Alternate mechanism for the Mitsunobu coupling	64
30	Synthesis of <b>29</b>	65
31	Conjugation of TSA's to carrier proteins	73
32	Synthesis of phosphate substrate <b>31</b>	77
33	Synthesis of phosphonate substrate <b>32</b>	78
33	Hydrolysis of substrates <b>31</b> and <b>32</b>	79

# **1 Introduction**

## **1.1 General Overview**

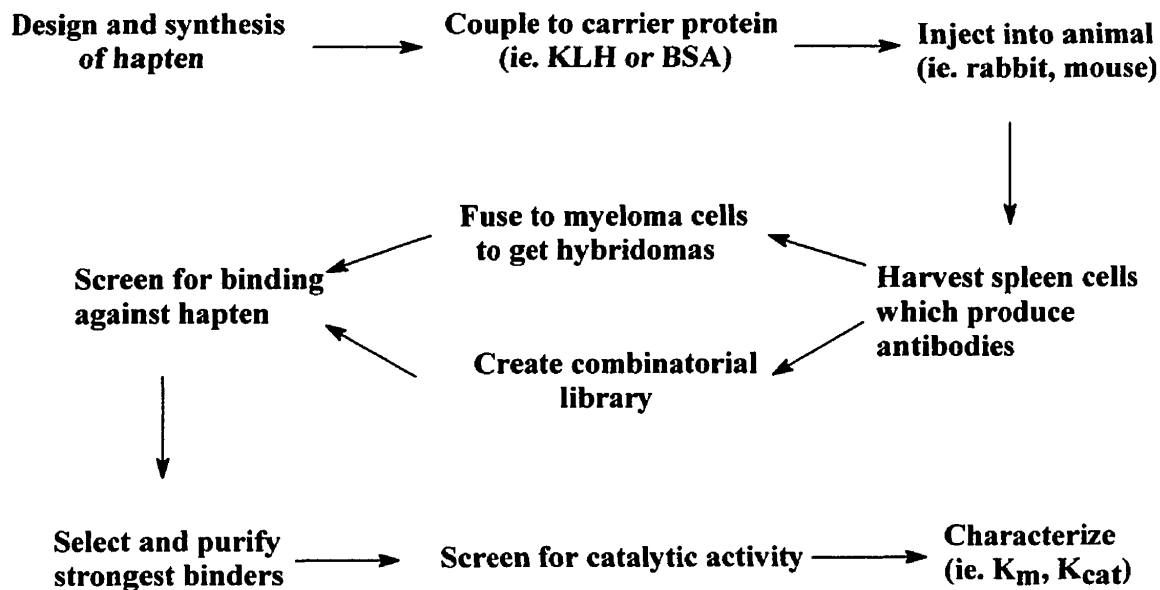
The work outlined in this thesis describes the synthesis of novel transition state analogues (TSA's) for phosphotriester hydrolysis. The TSA's are to be employed as haptens for the purpose of eliciting catalytic antibodies capable of hydrolyzing phosphotriester substrates. The TSA's described here differ from the conventional TSA design in that they are designed to elicit antibodies that exercise their catalytic effect by exerting strain upon the bound substrates. The stability of the haptens and substrates are also investigated.

## **1.2 Catalytic Antibodies**

Antibodies are agents of the immune system which are responsible for identifying and tagging foreign particles by binding to them. The strong and specific binding which antibodies are capable of are the exact properties which make it possible to create a unique class of tailor made catalysts, designed to carry out specific reactions, known as catalytic antibodies or abzymes. These catalysts are generated by taking advantage of the fact that antibodies can be raised to bind virtually any species.

Jencks<sup>1</sup> is generally credited as being the first individual to propose the concept of catalytic antibodies. He suggested that if an antibody could bind to and stabilize the transition state of a reaction, it would be able to catalyze the reaction in a manner similar to that exercised by enzymes. Since transition states have only a brief transient existence, it would be impossible to generate antibodies against the high energy intermediates themselves. Stable organic compounds which mimic the transition states (transition state analogues or TSA's)

independently realized Jencks' proposal in 1986 when they raised antibodies against phosphate and phosphonate TSA's which demonstrated abilities to hydrolyze carbonates and esters<sup>5</sup>. These reports gave rise to the field of catalytic antibodies.



**Scheme 1:** General route for generating abzymes

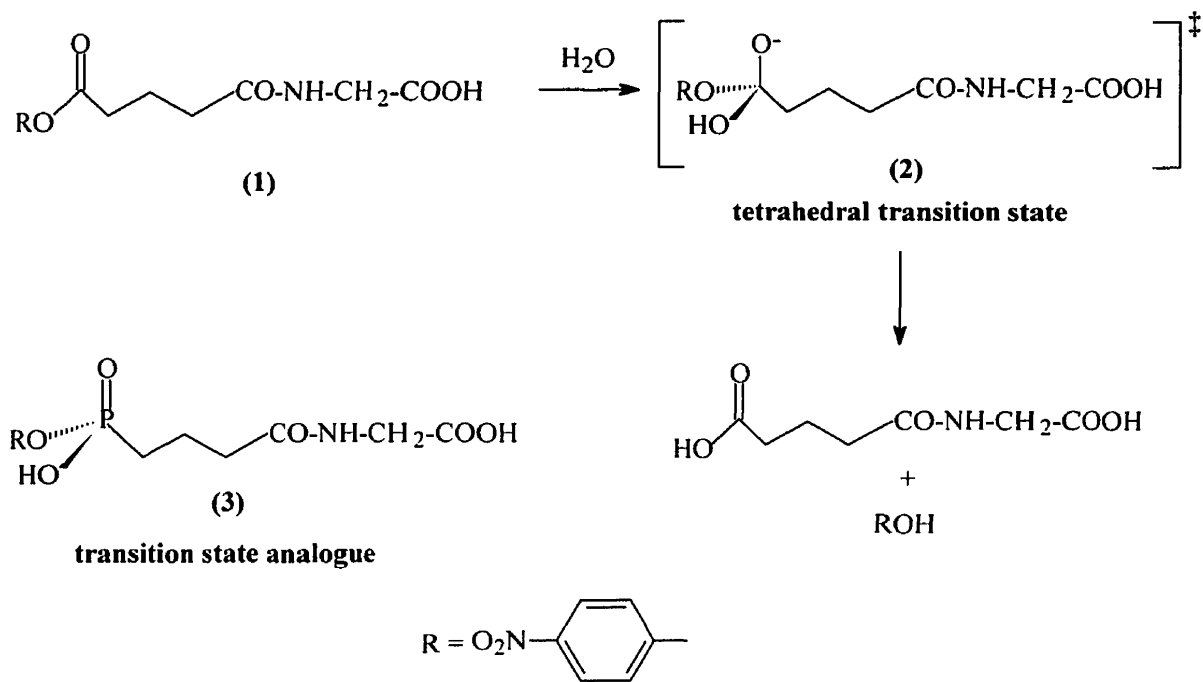
The route towards generating a catalytic antibody is outlined in Scheme 1. The first step is the design and synthesis of a compound that is supposed to either mimic the transition state of the reaction of interest or generate desirable functionalities within the abzyme binding site. Usually, these compounds are not effective in eliciting an immune response. However, they do provoke a response when attached to a large molecule such as a protein. A small molecule that is used to elicit an immune response by such means is called a hapten. Thus, the compound is attached to a carrier protein (and the compound is now a hapten). The

hapten-protein conjugate is injected into an animal (usually a mouse) several times over a period of several months to elicit an immune response. The animal's spleen is harvested in order to obtain the antibody producing cells. The spleen cells are fused with myeloma cells in order to produce hybridoma cells which produce antibodies and can be grown in cell culture. The antibodies produced by each cell line is screened for hapten binding. Due to high costs and time, only the best 20-30 antibodies with the highest affinities for the hapten are purified and screened for catalytic activity with the intended substrates. The most active abzymes are studied in detail.

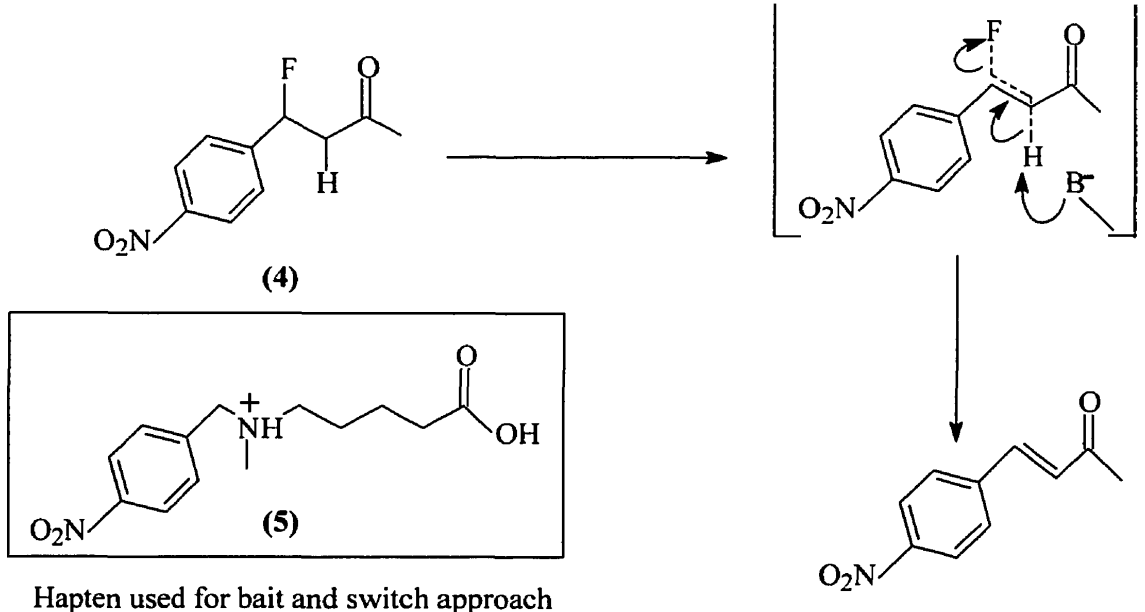
An alternative to the hybridoma route for the generation of abzymes is to construct a combinatorial antibody library. In this approach, antibodies are expressed in a bacterium such as *E.coli*. The library is designed to contain a vast number of antibodies thus increasing the likelihood that a few will actually bind the hapten and display some catalytic activity. The library is screened for hapten binding and the best binders are chosen for overexpression and characterization.

In the most common strategy for generating abzymes, the hapten is a TSA. Any antibody which recognizes the hapten could potentially bind to and stabilize the intended TS, in order to effect a rate acceleration for a reaction. An example of a catalytic antibody generated using this popular approach was reported by Tawfik and coworkers<sup>6</sup> who raised antibodies against the tetrahedral phosphonate species **3**. This species was a TSA for the hydrolysis of the ester **1** which proceeds through a tetrahedral TS **2**. The phosphonate **3** mimicked both the electrostatic and geometric properties of the TS so that antibodies which recognized the hapten **3** could also bind the negatively charged tetrahedral TS.

Another approach for obtaining catalytic antibodies is known as the bait and switch approach. This strategy differs slightly in that the hapten is not a TSA, but is rather intended to elicit specific functionalities within the antibody 'active site'. These functionalities may act to stabilize the TS by eliciting complementary residues (in terms of charge, H-bonding ability etc.). An example of this strategy is offered by Shokat et al.<sup>7</sup> who sought to catalyze the  $\beta$ -elimination of a fluoride ion from a ketone substrate (Scheme 3). The hapten they employed, **5**, contained a protonated amino group at physiological pH. The positive charge on the N-atom generated a negative charge in the antibody binding site. When the antibodies bound the substrate, **4**, the negatively charged side chain was correctly positioned to serve as a base and abstract the alpha proton in order to catalyze the elimination of the fluoride ion.



**Scheme 2:** Substrate and TSA for carbon ester hydrolysis



**Scheme 3:** Substrate and hapten for  $\beta$ -fluoride elimination

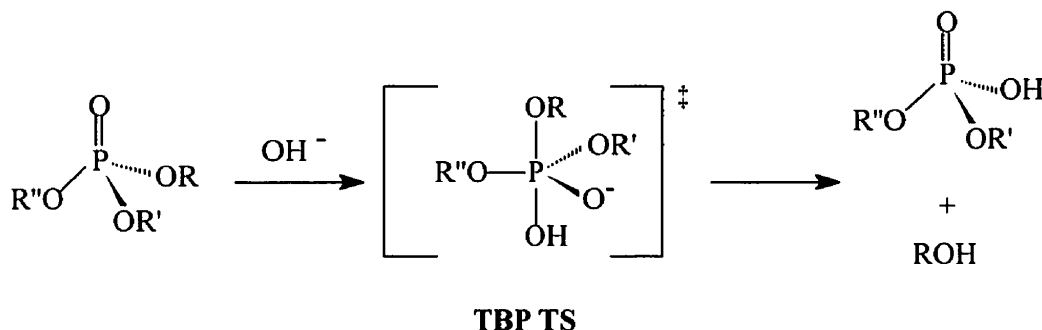
### 1.3 Antibody Catalyzed Phosphoester Hydrolysis

Though many advances have been made in the field of catalytic antibodies, the hydrolysis of phosphoesters still represents a challenge. Abzymes capable of hydrolyzing phosphoesters would be of interest for several reasons. Phosphoesters play many significant roles in biological systems. At the cellular level, phosphodiester form the backbone structures for the genetic material (RNA, DNA) as well as the means for energy transfer in the form of ATP. From a chemical viewpoint, phosphate esters have considerable kinetic stability. Any means of increasing their rate of hydrolysis would represent a step forward in understanding catalytic mechanisms.

Phosphatase abzymes have possible practical applications. In theory, abzymes capable of hydrolyzing phosphodiester could give rise to the production of customized restriction

abzymes with preprogrammed specificity's not found in nature. Many chemical weapons and insecticides (eg. sarin, tabun, paraoxon) are phosphotriesters. Phosphatase abzymes may be potentially employed as detoxification agents to neutralize such toxins within afflicted individuals. Such a therapeutic course would have the advantage of actually decomposing the toxin into harmless products rather than merely immobilizing it.

This thesis is concerned with generating abzymes capable of catalyzing the hydrolysis of phosphotriesters. The largest hurdle in generating phosphotriesterase abzymes is the difficulty in finding suitable TSA's. The hydrolysis of phosphoesters proceeds through a pentavalent trigonal bipyramidal (TBP) transition state<sup>8</sup> (Scheme 4). Species which may potentially mimic the TS, such as TBP phosphoranes, are often unstable in aqueous solution, and/or toxic which precludes their use as haptens in immunization procedures.

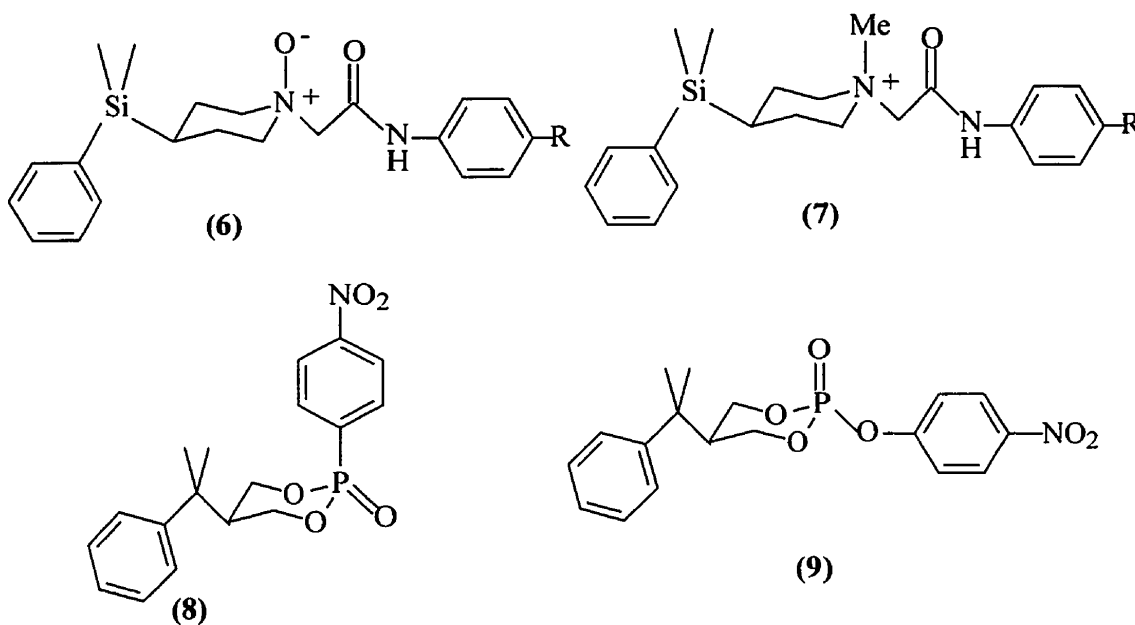


**Scheme 4:** Phosphate ester hydrolysis via a TBP transition state

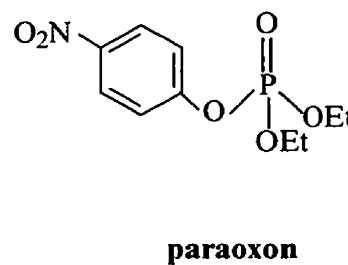
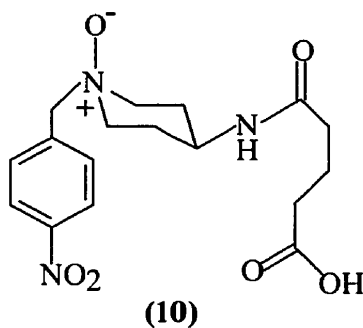
Rosenblum et al.<sup>9</sup> and Lavey et al.<sup>10</sup> have reported the generation of phosphotriesterase abzymes using a bait and switch approach. Rosenblum et al.<sup>9</sup> used compounds **6** and **7** to generate abzymes capable of hydrolyzing **8** and **9**. The charged hapten **6** is designed to



specifically elicit reactive side chains in the abzyme active site. The negatively charged O atom of the N-oxide is believed to promote the placement of a positively charged side chain in the antibody which may stabilize the developing negative charge on the apical oxygen atom of the leaving group in the TBP TS. The positive charge on the N atom elicits a negatively charged side chain in the active site which may potentially stabilize the developing partial positive charge on the phosphorous center. Hapten 7 should only generate antibodies which stabilize exclusively the positive charge at the phosphorous center. These haptens were not meant to serve as TSA's but rather as a means of investigating whether or not stabilizing the electrostatic features of the TS is sufficient to produce an efficient catalyst. The most efficient abzyme from this study was raised against 6 and catalyzed the hydrolysis of 8 with an approximate 400 fold rate enhancement.

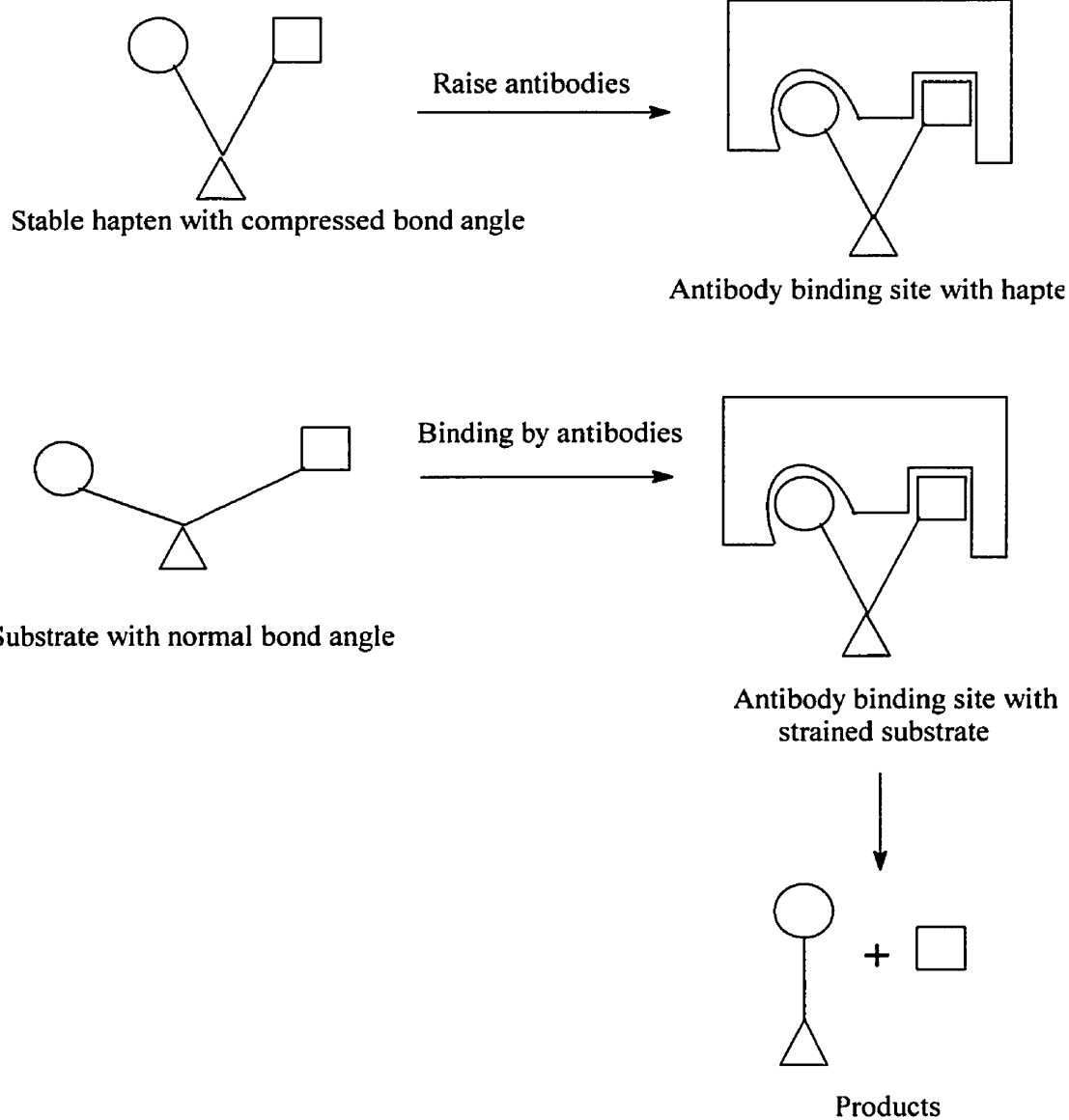


Lavey et al.<sup>10</sup> employed **10** as a hapten in order to produce abzymes capable of hydrolyzing paraoxon, an organophosphorus-based insecticide. The hapten was once again based upon an N-oxide to produce the desired side chains in the antibody binding site. However, the most efficient antibody obtained hydrolyzed paraoxon with only a 500-fold rate enhancement. Thus, in order to obtain better phosphotriesterase abzymes, alternative methods must be employed.



#### **1.4 The Role of Strain in Biocatalysis**

Abzymes have been elicited that catalyze reactions in a variety of ways. We have already mentioned how abzymes have been generated against TSA's and that it is believed that these antibodies catalyze reactions mainly by TS stabilization. Antibodies have also been generated that catalyze reactions by acting as entropy traps or are designed to have specific catalytic groups and/or co-factors in the binding site to aid in the catalytic process.<sup>5</sup> Another potential means by which abzymes could catalyze a reaction is via a combination of ground state destabilization and transition state stabilization. The general approach is outlined in Scheme 5.

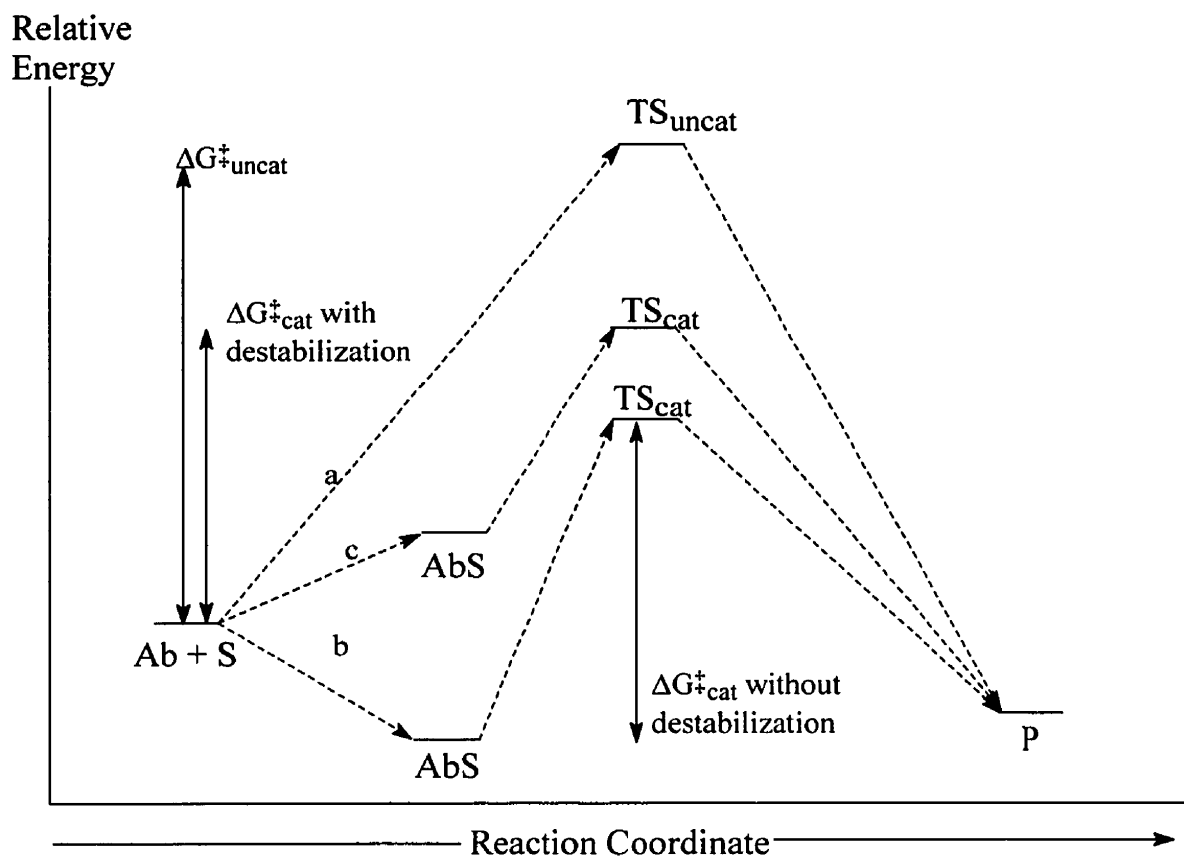


**Scheme 5:** Mechanism of catalysis by strain

The tactic is to generate antibodies against a stable hapten that is analogous to a strained form of the intended substrate yet has features of the transition state of the reaction. When the antibodies encounter the actual substrate, the antibodies will have to strain or distort

the substrate towards the transition state structure in order to bind it. Catalysis would occur by tandem ground state destabilization as well as TS stabilization. The strain is relieved when the transition state is formed. In order for such a mechanism to function, the ground state must be selectively destabilized while the TS is stabilized.

Scheme 6 outlines the difference in the energy profiles between an uncatalyzed reaction (pathway a), a reaction catalyzed by an abzyme generated using the bait and switch strategy of Lavey and coworkers (pathway b), and one catalyzed by an antibody employing a strain mechanism (pathway c). Whereas both antibodies would lower the energy of the TS, to



**Scheme 6:** Reaction coordinate diagram for an antibody strain catalyzed mechanism

decrease the energy barrier between the TS and the substrate, the strain mechanism destabilizes the ground state to bring its energy closer to that of the TS. This strategy avoids the potential ‘thermodynamic pit’ which may result if an antibody was raised against a normal, unstrained phosphoester (pathway b) or a tetrahedral hapten such as the one employed by Lavey et al.<sup>10</sup> Pathway b and c may potentially achieve TS’s of different energies, since stabilization of the TS may not be maximized by antibodies raised to a distorted ground state, but catalysis may result from either route if  $G_{\text{uncat}}^{\ddagger} > G_{\text{cat}}^{\ddagger}$ .

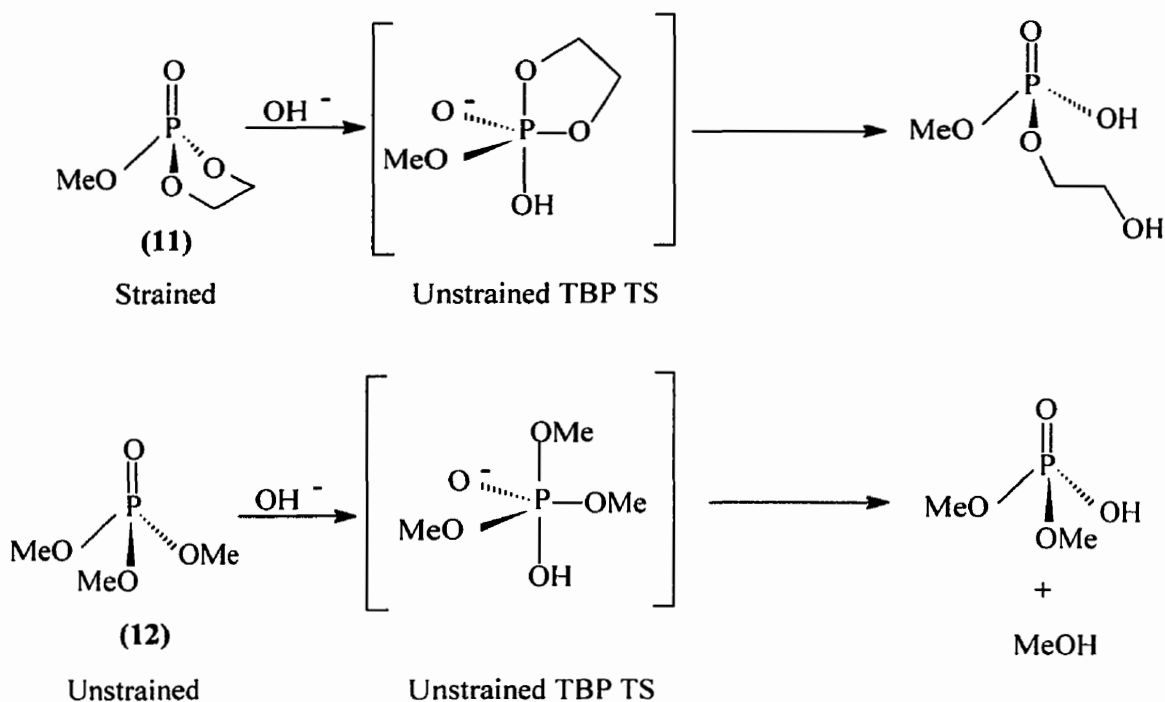
The role of strain in biocatalysis is a subject of much controversy.<sup>1,11-14</sup> According to the strain hypothesis, substrates do not fit the enzyme active sites perfectly but instead must be distorted slightly. This distortion causes the scissile bonds to weaken as well as a concomitant increase in energy of the substrate which is relieved in the transition state. Crystal structure and theoretical studies implicate the possible role of substrate distortion as a factor in the catalytic activity of the enzyme lysozyme.<sup>15,16</sup> The difficulty in properly establishing the role of strain in biocatalysis is designing the appropriate experiments which would give clear insight into the contribution of ground state destabilization.<sup>1</sup>

Experimental evidence which demonstrates the potential for abzymes to act via a strain mechanism is provided by Ghosh et al.<sup>17</sup> who demonstrated that antibodies are capable of compressing metal coordination complexes to cause chromophoric shifts. This work demonstrates that antibodies are capable of exerting strain upon small molecules.

The suggestion that antibodies could catalyze reactions via a combination of ground state strain and transition state stabilization is not a novel one. Hansen and coworkers have reported the synthesis of a hapten that is supposed to elicit antibodies that will catalyze the

hydrolysis of peptide bonds in this manner.<sup>18,19</sup> To date, these workers have yet to report any catalytic species resulting from their haptens. Possible reasons to account for this include the lack of strongly immunogenic functionalities on their haptens and the lack of data characterizing the role of strain in peptide bond hydrolysis. In addition, amide bonds are kinetically very stable and difficult to hydrolyze.

Our goal is to generate antibodies that will catalyze the hydrolysis of phosphotriesters via a combination of ground state strain and TS stabilization. There is a considerable amount

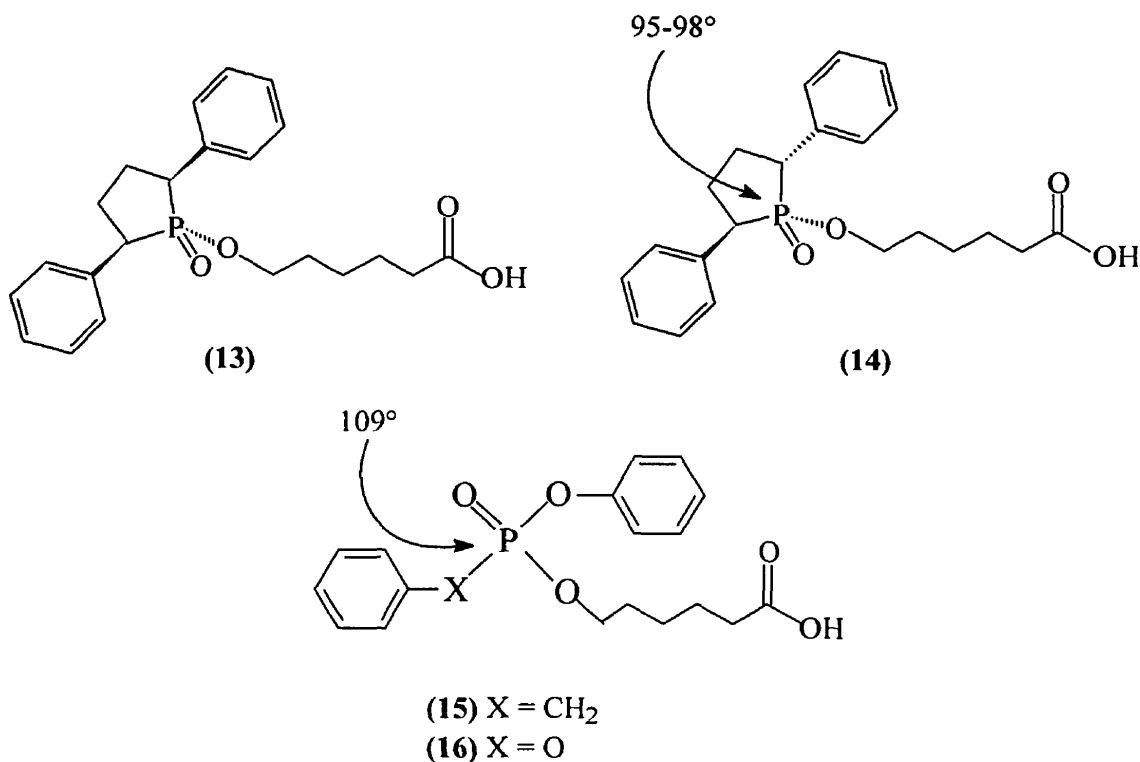


**Scheme 7:** Hydrolysis of cyclic and acyclic phosphate esters

of experimental evidence which demonstrates that strain plays a significant role in the hydrolysis of cyclic, five-membered phosphate esters. Five membered cyclic phosphate esters

are more hydrolytically labile than their acyclic counterparts. For example, Westheimer showed that methylethylenephosphate, **11**, (Scheme 7) is hydrolyzed  $10^6$  times faster than its acyclic analogue, trimethylphosphate, **12**. A significant portion of the rate acceleration is attributed to the fact that the cyclic ester is strained. The endocyclic O-P-O bond angle in **11** is  $98^\circ$ <sup>22</sup> as opposed to an unstrained ideal tetrahedral angle of  $109^\circ$ . The ring strain is relieved upon formation of the trigonal bipyramidal (TBP) transition state (Scheme 7) where the endocyclic O-P-O bond angle attains the ideal, unstrained TBP bond angle of  $90^\circ$ . The strain hypothesis is supported by calorimetric studies in which the hydrolysis of **11** is 5.9 kcal/mol more exothermic than for **12**.<sup>25</sup>

### 1.5 Design of a Strained TSA for the Hydrolysis of Phosphotriesters

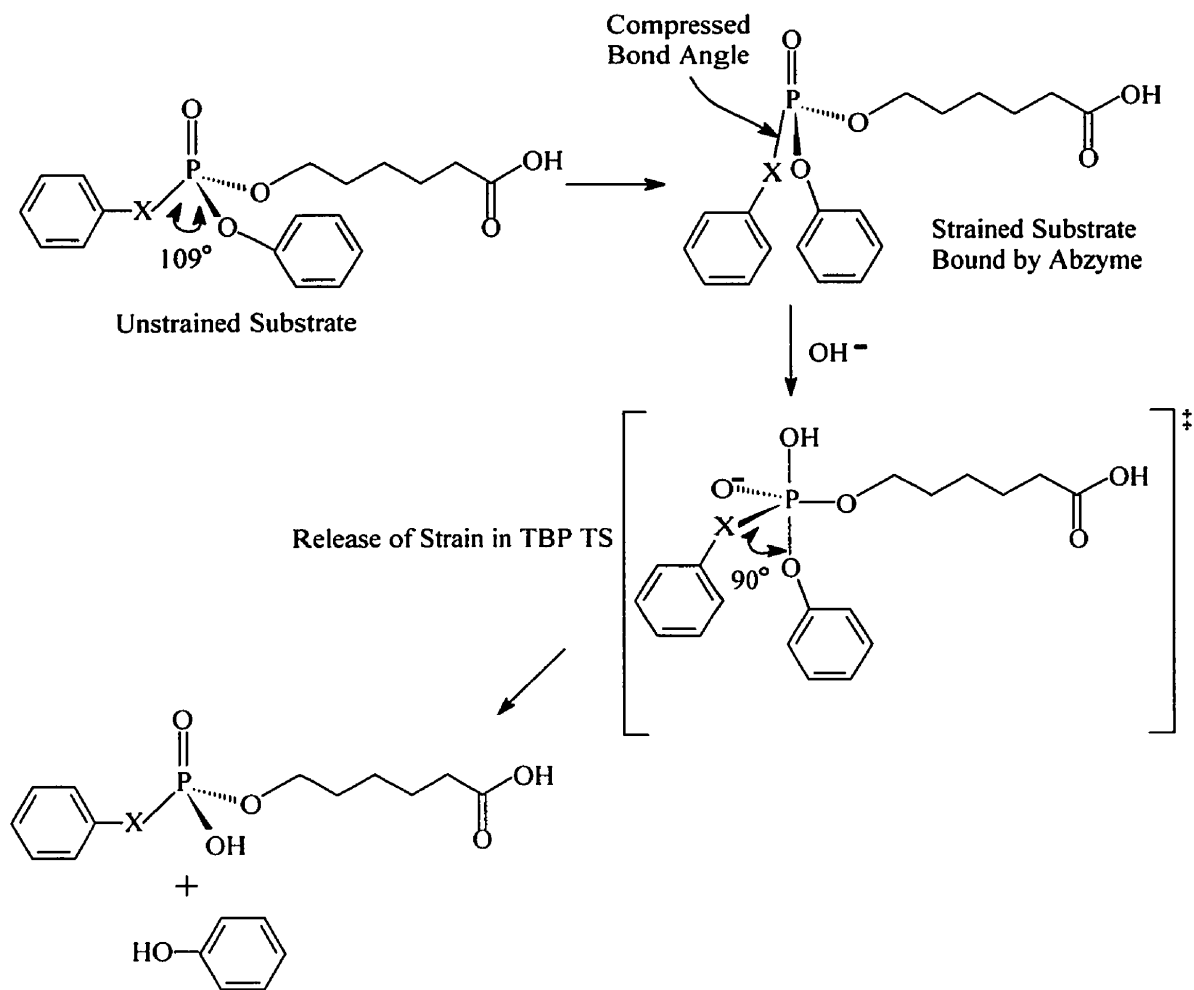


Scott D. Taylor<sup>26</sup> has recently designed and synthesized two haptens, **13** and **14**, to generate antibodies which would hydrolyze phosphotriesters, **15** and **16**, via a strain mechanism. The rationale behind the design of these haptens is as follows. First, and most importantly, the endocyclic C-P-C bond angle should be close to the strained angle of 95-98°. This is based upon crystal structures of five membered cyclic phosphates and phosphinates which have endocyclic bond angles at the phosphorous of 95-98°. <sup>22,27</sup> Second, this hapten should be highly immunogenic due to the presence of the two phenyl groups on the ring. Thus, when antibodies raised to **13** or **14** encounter structurally similar, yet unstrained phosphate ester substrates, such as **15** or **16**, the phenyl groups should be strongly recognized by the antibody. Upon binding of **15** or **16** to the antibody, the PhO-P-OPh bond angle will be compressed from the unstrained tetrahedral state (109°) to 98° (towards the optimal transition state angle of 90°) since the antibody was raised to a hapten having a compressed bond angle. This reaction is outlined in Scheme 8. Attack of hydroxide or water at phosphorus results in formation of the unstrained TBP TS.

Other aspects of the haptens are worthy of mention. First, the haptens **13** and **14** are isomeric; they differ only in the spatial arrangement of one phenyl group oriented above or below the plane of the phospholane ring (i.e. phenyl groups are cis or trans to one another). Both isomers are used in the immunization as a means to verify that the phenyl groups serve as antigenic determinants simultaneously. For example, if an antibody raised to **13** also bound **14** (or vice versa), this would imply that only one phenyl group is recognized by the antibody, and that the binding site has sufficient room to accommodate the second phenyl group regardless of its orientation (i.e. the second phenyl group would only be loosely held in the

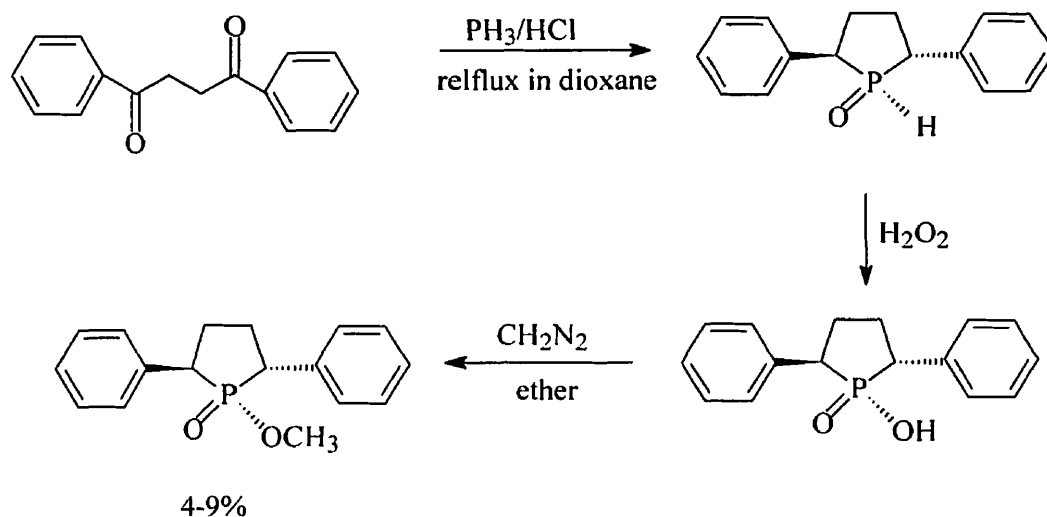


effect catalysis via a strain mechanism. Second, the longer apical bonds of the TBP TS should be accommodated in the active site since the endocyclic P-C bonds in the hapten should be approximately the same length<sup>25</sup> as apical P-O bonds in TBP oxophosphoranes.<sup>28</sup> Third, a six carbon linker chain was used to connect the hapten to a carrier protein for the immunization



**Scheme 8:** Hydrolysis of phosphotriester substrates via a strain mechanism

process. In the phenyl cis hapten, it is located on the opposite side of the phospholane ring away from the phenyl groups in order to ensure that the recognition of the phenyl rings by the antibodies is unhindered. Finally, the P=O bond is quite polar. A recent study by Prezhdo et al.<sup>29</sup> reported that the charge on the O atom of the P=O bond is -0.433 for triphenyl phosphine oxide and -0.452 for trimethyl phosphine oxide. The charge on the oxygen in our phosphinate system is expected to be in the same range. Thus, we anticipate that antibodies raised to **13** or **14** will have complementary positively charged residues in the active site which will help stabilize the negatively charged transition state formed during the hydrolysis of **15** or **16**. It is important to note that TS stabilization, in addition to ground state destabilization, must occur for catalytic activity. Straining the substrate merely prevents it from falling into a thermodynamic “pit” which would most likely be the case if the antibodies were raised to a normal, unstrained phosphate ester.

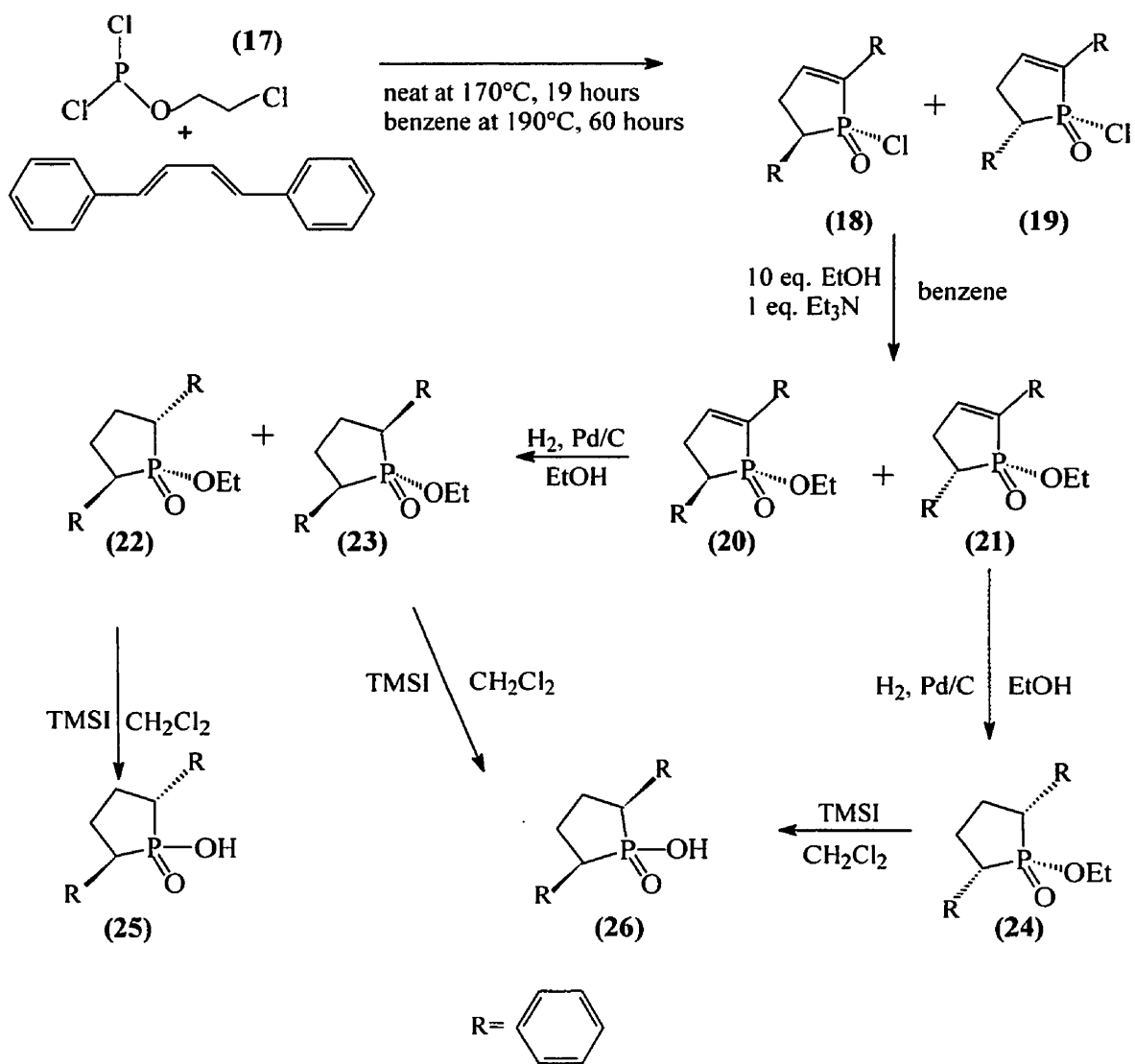


**Scheme 9:** Kalinov's synthesis of 1-methoxy-trans-2,5-diphenylphospholanate

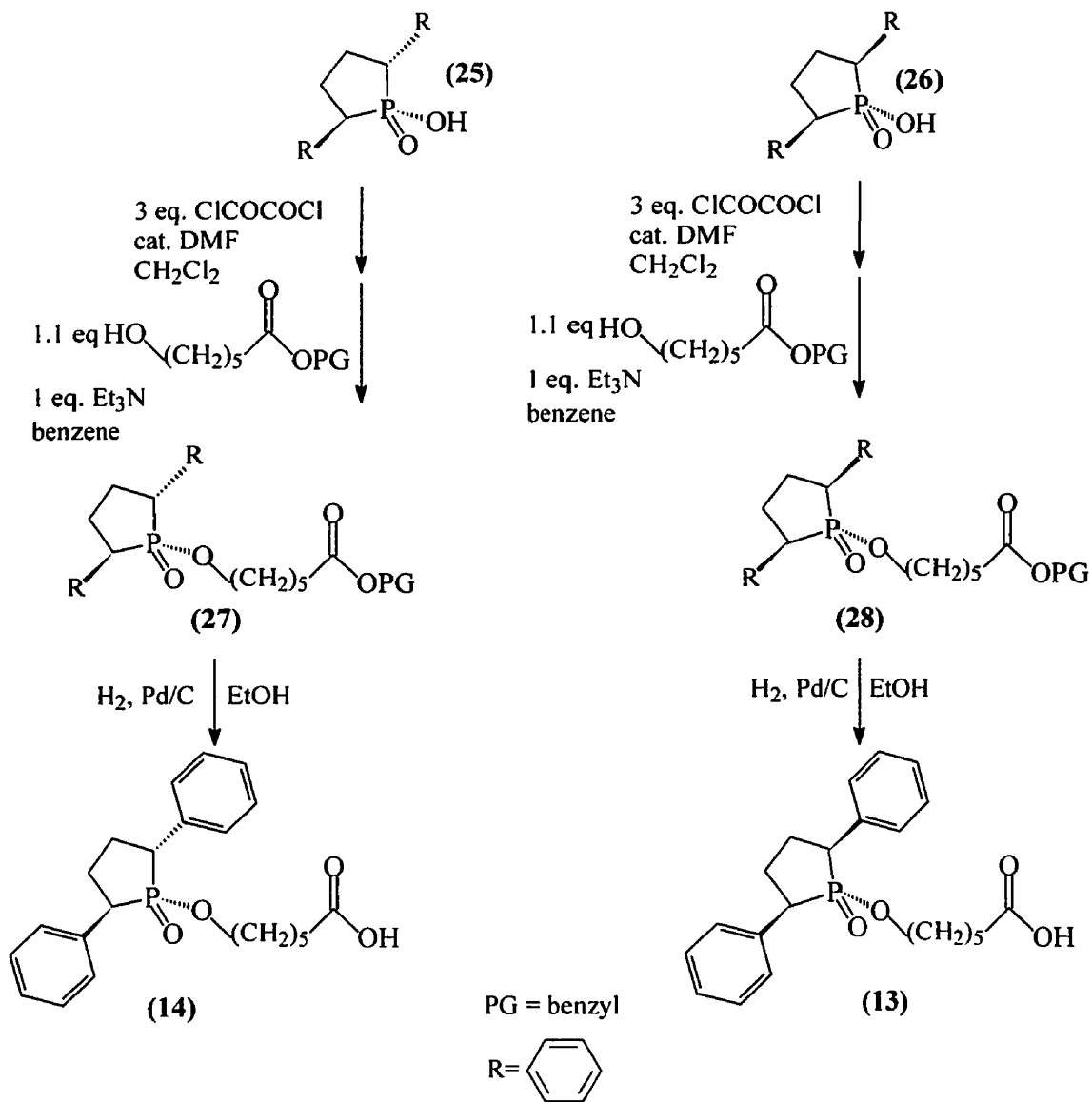
Haptens **13** and **14** are 2,5-diphenyl phospholanate esters. The only reported example of this class of compound is by Kalinov et al.<sup>30</sup> who reacted 1,4-dibenzoyl ethane with hydrogen phosphide to produce trans-2,5-diphenyl phospholanic acid (Scheme 9), which they subsequently methylated. No yield was reported for this reaction, but by using 1,4-dibenzoyl ethane as the limiting reagent, the overall yield can be calculated to be approximately 4-9% for the methyl ester. Although this gave Taylor a potential route to the trans TSA **14**, the yields were very low and a route to the cis TSA, **13**, was also necessary. It was apparent that an alternative route to this class of compounds would be required to obtain significant quantities of both **13** and **14**.

The synthesis of **13** and **14** developed by Taylor<sup>26</sup> begins in Scheme 10. It involves a McCormack reaction<sup>31</sup>, as modified by Modritz<sup>32</sup> in which phosphite **17** undergoes a 2+4 cycloaddition with 1,4-diphenyl-1,3-butadiene. The resulting acid chloride precursors **18** and **19** were esterified to form the isomeric ethoxy esters (**20** and **21**), and the phospholenes hydrogenated to give isomeric products **22**, **23**, and **24**, which were converted to the cis and trans-2,5-diphenyl phospholanic acids **26** and **25**. The acids were converted to the phosphochlorides in order to attach the benzyl protected linker chain (Scheme 11). The desired haptens were obtained upon removal of the benzyl protecting group to give **13** and **14**.

**13** and **14** were conjugated to carrier proteins and sent to the laboratory of Prof. Jeremy Lee of the Department of Biochemistry at the University of Saskatchewan. The hapten-protein conjugates were injected into mice two years ago for the purposes of eliciting monoclonal antibodies. To date, approximately fifteen monoclonal antibodies, which were

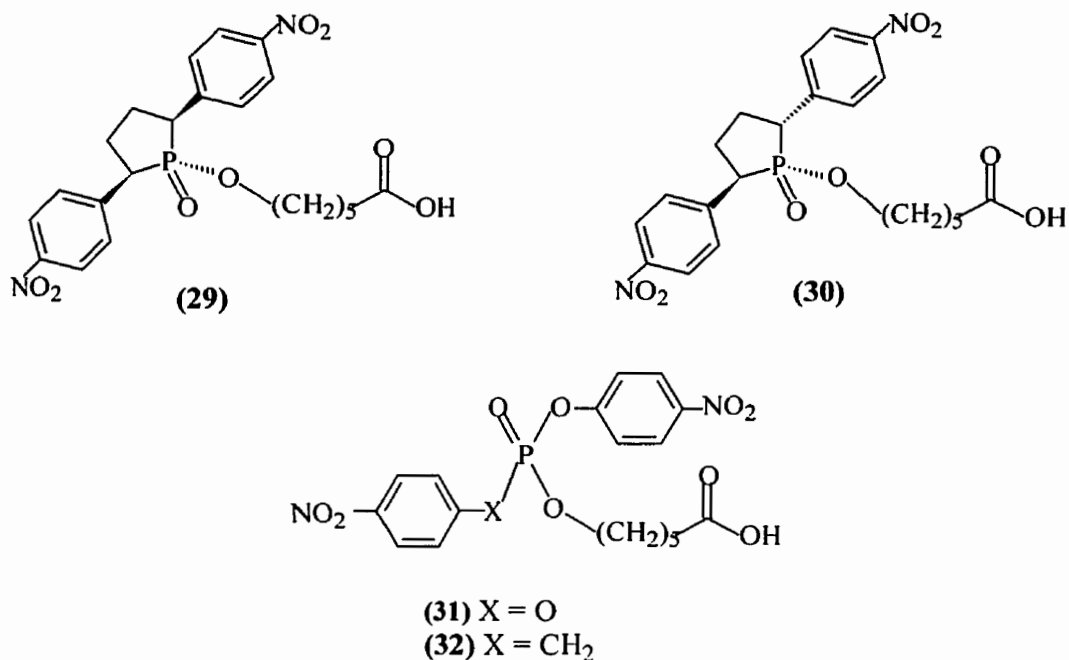


**Scheme 10:** Synthesis of 25 and 26 by Taylor<sup>26</sup>



Scheme 11: Synthesis of 13 and 14 by Taylor<sup>26</sup>

found to bind the haptens, have been raised but none have displayed any catalytic activity. However, we have found that these antibodies are unable to distinguish between **13** and **14**. This suggests that the antibodies do not bind both phenyl groups simultaneously. As a result, the antibodies bind the substrates loosely and do not compress the crucial O-P-X bond angle in the substrates enough to effect catalysis. However, we reasoned that by increasing the immunogenic properties of the haptens, catalytic species may be obtained. It is well known the *p*-nitrophenyl groups are very strong antigenic determinants. The introduction of nitro groups at the *para* position (**29** and **30**) should encourage stronger recognition of the aryl



groups in the haptens which is crucial for catalytic activity. The use of the *p*-nitrophenyl groups in the haptens has the additional advantage that esters **31** and **32** can be used as substrates which would release *p*-nitrophenol upon hydrolysis. *p*-Nitrophenol is easily

for catalytic activity. The assays may be sufficiently sensitive as to permit early rapid screens of the antibodies in order to improve the selection process. This thesis deals with the synthesis of the nitrated strained TSA's **29** and **30** and the substrates **30** and **31**.

## **2.1 Materials and Methods**

**General:** All starting materials were obtained from commercial suppliers (Aldrich Chemical Company, Oakville, Ontario, Canada or Lancaster Synthesis Incorporated, Windham, New Hampshire, USA) unless stated otherwise. Solvents were purchased from Caledon Laboratories (Georgetown, Ontario, Canada), Lancaster Synthesis Incorporated, or BDH Canada (Toronto, Canada). Tetrahydrofuran (THF) and diethyl ether were distilled over sodium metal in the presence of benzophenone. Benzene and  $\text{CH}_2\text{Cl}_2$  were distilled over calcium hydride. Ethanol was distilled over magnesium turnings. Dry chloroform was obtained by distillation over phosphorus pentoxide. All glassware was pre-dried prior to use and all liquid transfers were performed using dry syringes and needles. Silica gel chromatography was performed on 40-60 $\mu$  particle silica gel obtained from Toronto Research Chemicals (Toronto, Ontario, Canada). Melting points were obtained on a Electrothermal Inc. melting point apparatus and are uncorrected.  $^1\text{H}$  and  $^{31}\text{P}$  NMR spectra were recorded on a Varian 200-Gemini NMR machine at approximately 200 MHz, and 80 MHz respectively.  $^{13}\text{C}$  NMR spectra were recorded on a Varian-500 NMR at 126 MHz or on a Varian 200-Gemini NMR machine at 50.3 MHz. The abbreviations s, d, t, q, qt, m, dd, and b are used for singlet, doublet, triplet, quartet, quintet, multiplet, doublet of doublets and broad respectively. Coupling constants are reported in Hertz (Hz). All NMR's were run using  $\text{CDCl}_3$  as solvent unless stated otherwise. Chemical shifts ( $\delta$ ) for  $^1\text{H}$  NMR spectra run in  $\text{CDCl}_3$  and  $\text{DMSO}_d6$  are reported in ppm relative to the internal standard tetramethylsilane (TMS). Chemical shifts ( $\delta$ ) for  $^1\text{H}$  NMR spectra run in  $\text{CD}_3\text{OD}$  are reported in ppm relative to residual solvent protons



to residual solvent protons ( $\delta$  2.50). For  $^{13}\text{C}$  NMR spectra run in  $\text{CDCl}_3$ , chemical shifts are reported in ppm relative to the  $\text{CDCl}_3$  residual carbons ( $\delta$  77.0 for the central peak). For  $^{13}\text{C}$  NMR spectra run in  $\text{DMSO}_{d-6}$ , chemical shifts are reported in ppm relative to the DMSO residual carbons ( $\delta$  39.5 for the central peak). For  $^{31}\text{P}$  NMR spectra, chemical shifts are reported in ppm relative to 85% phosphoric acid (external). Electron impact (EI) mass spectra were obtained on a Micromass 70-S-250 mass spectrometer. HPLC purifications and experiments were performed on a Waters LC 450 System using Altech normal phase preparative (250 mm x 22 mm i.d. with 10  $\mu$  Econosil silica, cat. 6259) or analytical (250 mm x 4.6 mm i.d. with 10  $\mu$  Econosil silica, cat. 60090) HPLC columns. Kinetic analyses on antibody substrates were performed on a Cary 1 UV spectrophotometer.

## **2.2 Synthesis of Transition State Analogues**

**Cis 2'-chloroethyl-2,5-di-*p*-nitrophenyl-2-phospholenate and trans 2'-chloroethyl 2,5-di-*p*-nitrophenyl-2-phospholenate (44 and 45):** 1,4-di-*p*-nitrophenyl-1,3-butadiene (1.19 g, 4 mmol, 1 eq.) and 2,6-di-*t*-butyl-4-methyl phenol (40 mg, 4.5 mol %) were weighed into a 25 mL ACE Glass pressure tube equipped with a stir bar and then thoroughly flushed with Ar. Chloroform (6 ml) was added followed by ethylene chlorophosphite (0.0356 mL, 506 mg, 4 mmol, 1 eq.). The reaction vessel was sealed and heated in a oil bath at 180 °C with vigorous stirring for 72 hr. **CAUTION: This procedure should only be performed in a fume hood behind a blast shield.** Upon cooling, the crude mixture was diluted with chloroform (50 mL) and washed with 5%  $\text{NaHCO}_3$  (3 x 100 mL), 0.1N HCl (3 x 100 mL), and saturated brine (2 x 100 mL) and then dried ( $\text{MgSO}_4$ ). After removal of the solvent by

EtOAc:hexanes, 7:3) which allowed for the separation of **44** ( $R_f = 0.4$ ) and **45** ( $R_f = 0.7$ ) but did not yield pure material. Pure product was obtained by subjecting each impure isomer to further purification. **44** was purified by silica gel chromatography (EtOAc:hexanes, 9:1,  $R_f = 0.5$ ), pale yellow solid (102 mg, 6.2%);  $^1\text{H}$  NMR  $\delta$  2.96-3.12 (1 H, m), 3.21-3.49 (3 H, m), 3.62-3.92 (2 H, m), 3.98-4.14 (1 H, m), 7.31 (0.5 H, t,  $J = 2.6$  Hz), 7.57 (2.5 H, dd,  $J = 2.2$  Hz,  $J = 8.8$  Hz), 7.89 (2 H, d,  $J = 8.8$  Hz), 8.27 (4 H, d,  $J = 8.8$  Hz);  $^{31}\text{P}$  NMR  $\delta$  57.43 (s). **45** was purified by silica gel chromatography (EtOAc:hexanes, 3:2,  $R_f = 0.6$ ), pale yellow solid (81 mg, 4.8%);  $^1\text{H}$  NMR  $\delta$  2.88-3.06 (1 H, m), 3.29-3.53 (1 H, m), 3.63 (2 H, t,  $J = 5.2$  Hz), 3.69-3.84 (1 H, m), 4.14-4.48 (2 H, m), 7.28 (0.5 H, t,  $J = 2.5$  Hz), 7.52 (2.5 H, dd,  $J = 1.7$  Hz,  $J = 7.0$  Hz), 7.83 (2 H, d,  $J = 8.8$  Hz), 8.25 (4 H, dd,  $J = 4.4$  Hz,  $J = 5.1$  Hz);  $^{31}\text{P}$  NMR ( $\text{CDCl}_3$ )  $\delta$  58.74 (s).

**Trans and cis ethyl-2,5-diphenyl-2-phosphenate (20 and 21):** 1,4 diphenyl-1,3-butadiene (2.06 g, 10 mmol, 1eq.) was combined with 2,6-di-tert-butyl-4-methyl phenol (10 mg, 2 mol %) in a 12 mL ACE Glass pressure tube equipped with a stir bar and then flushed thoroughly with Ar. Phosphorous trichloride (0.545 mL, 6.33 mmol, 0.66 eq.) and tris(2-chloroethyl) phosphite (0.635 mL, 3.33 mmol, 0.33 eq.) was added to the tube under a stream of Ar. The glass bomb was rapidly sealed and the thick, mainly solid mixture was vigorously shaken for about 30 seconds to mix the contents. The tube was immersed in an oil bath, stirred vigorously, and slowly heated to 170°C and maintained at this temperature for 19 hr during which time the solid diene melted and the solution reaction became a dark orange colour. **CAUTION: This procedure must be performed in a fume hood behind a blast**

equal magnitude at 68.6 and 69.7 ppm, which is indicative of cyclic phosphinylchlorides.<sup>33</sup> After removing the oil bath and allowing the tube to cool to room temperature, the tube was fitted with a septum and dry benzene (20 mL) was added to the crude reaction mixture. The solution was transferred very slowly over a period of 30 min via syringe to an ice cold solution of dry ethanol (5.8 mL, 100 mmol, 10 eq.) and triethylamine (1.7 mL, 10 mmol, 1 eq.) in dry benzene (20 mL) and the reaction was stirred overnight at room temperature under Ar. The volume of the crude reaction mixture was reduced to one quarter by rotary evaporation and diluted with ether (75 mL) which resulted in the precipitation of triethylamine hydrochloride which was removed by suction filtration. The filter cake was washed with ether and the filtrate was washed with 0.1 N HCl (3 x 50 mL), 5% NaHCO<sub>3</sub> (3 x 50 mL), brine (3 x 50 mL) and then dried (MgSO<sub>4</sub>) and concentrated *in vacuo* to yield a crude orange oil which was subjected to silica gel column chromatography. **20** was obtained (R<sub>f</sub> = 0.40, CH<sub>2</sub>Cl<sub>2</sub>:EtOAc, 9:1) as a white solid (577 mg, 19.2% yield): mp 82-86 °C; <sup>1</sup>H NMR δ 1.23 (3 H, t, J = 6.9 Hz), 2.81-2.96 (1 H, m), 3.10-3.54 (2 H, m), 3.98-4.23 (2 H, m), 7.03 (1 H, t, J = 3.3 Hz), 7.42 (8 H, m), 7.65 (2 H, d, J = 6.2 Hz); <sup>31</sup>P NMR δ 60.41 (s); <sup>13</sup>C NMR δ 142.20 (d, J = 36.1), 138.35 (br d), 136.95 (d, J = 4.6 Hz), 133.59 (d, J = 9.1 Hz), 128.70, 128.39 (d, J = 11.5 Hz), 126.96, 126.68 (d, J = 5.5 Hz), 61.58 (d, J = 6.4 Hz), 42.28 (d, J = 92.8 Hz), 35.57 (d, J = 17.8 Hz), 16.66 (d, J = 5 Hz); MS, m/z (relative intensity) 298 (64), 270 (36), 205 (100), 104 (31), 91 (41), 77 (30). **21** was obtained (R<sub>f</sub> = 0.60, CH<sub>2</sub>Cl<sub>2</sub>:EtOAc, 9:1) as a white solid (533 mg, 17.8% yield): mp 102-108 °C; <sup>1</sup>H NMR δ 0.91 (3 H, t, J = 5.9 Hz), 2.84-3.93 (5.5 H, m), 7.08 (0.5 H, t, J = 3.75 Hz), 7.35 (8 H, m), 7.71 (2 H, d, J = 7 Hz);

135.20, 133.14 (br d), 128.70 (d, J = 6.2 Hz), 128.34, 126.92, 126.66 (d, J = 3.7), 61.58 (d, J = 6.4), 43.44 (d, J = 90.6), 33.19 (d, J = 16.4) 16.16; MS, m/z (relative intensity) 298 (100), 270 (66), 254 (47), 205 (50), 194 (83), 91 (43), 77 (30).

**Meso cis ethyl-cis-2,5-diphenyl phospholanate (24):** A solution of **21** (820 mg, 2.75 mmol) in ethanol (20 mL) containing 10% Pd/C (60 mg) was hydrogenated overnight at 30 psi under a H<sub>2</sub> atmosphere using a Parr hydrogenation apparatus. The Pd catalyst was removed by filtration and the filtrate concentrated *in vacuo* leaving a pale yellow solid. Column chromatography (silica, 100 % EtOAc, R<sub>f</sub> = 0.40) yielded pure **24** as a white solid (674 mg, 82 % yield): mp 133-137 °C; <sup>1</sup>H NMR δ 0.64 (3 H, t, J = 7 Hz), 2.42 (4 H, m), 3.22-3.54 (4 H, m), 7.31 (10 H, m); <sup>31</sup>P NMR δ 65.14 (s); <sup>13</sup>C NMR δ 135.54 (d, J = 5.5 Hz), 128.41, 127.94 (d, J = 3.7 Hz), 126.63, 61.20 (d, J = 7.4 Hz), 43.96 (d, J = 82.4 Hz), 27.45 (d, J = 12.8 Hz), 15.90; MS, m/z (relative intensity) 300 (64), 206 (48), 196 (18), 104 (100), 91 (29), 78 (25).

**Meso trans ethyl cis-2,5-diphenyl phospholanate (23) and racemic ethyl trans-2,5-diphenyl phospholanate (22):** A solution of **20** (1.530 g, 5.03 mmol) in ethanol (20 mL) containing 10% Pd/C (100 mg) was hydrogenated overnight at 30 psi under a H<sub>2</sub> atmosphere using a Parr hydrogenation apparatus. The Pd catalyst was removed by filtration and the filtrate concentrated *in vacuo* leaving a pale yellow oil which was subjected to column chromatography (silica, CH<sub>2</sub>Cl<sub>2</sub>:EtOAc, 90:10). **23** was obtained (R<sub>f</sub> = 0.50) as a white solid (1.10g, 72 % yield): mp 102-108 °C; <sup>1</sup>H NMR (CDCl<sub>3</sub>) δ 0.93 (3 H, t, J = 7.2 Hz), 2.07-2.60 (4 H, m), 3.09-3.52 (3 H, m), 3.66-3.85 (1 H, m), 7.35 (10 H, cm); <sup>31</sup>P NMR δ 61.73 (s); <sup>13</sup>C

43.59 (d,  $J = 85.1$  Hz), 29.57 (d,  $J = 14.6$  Hz), 16.69; MS,  $m/z$  (relative intensity) 300 (87), 206 (42), 196 (36), 104 (100), 91 (28), 78 (22). **22** was obtained ( $R_f = 0.30$ ) as a white solid (432.9 mg, 27 % yield): mp 68-72 °C;  $^1\text{H}$  NMR  $\delta$  1.24 (3 H, t,  $J = 7.1$  Hz), 2.33-2.46 (4 H, m), 3.21-3.37 (2 H, m), 4.00 (2 H, m), 7.35 (10 H, m);  $^{31}\text{P}$  NMR  $\delta$  62.37 (s);  $^{13}\text{C}$  NMR  $\delta$  136.69 (bd), 136.22 (d,  $J = 2.7$  Hz), 128.76, 128.56, 128.14 (d,  $J = 4.6$  Hz), 126.81, 61.24 (d,  $J = 7.3$  Hz), 46.68 (d,  $J = 84.1$  Hz), 45.50 (d,  $J = 86.9$  Hz), 30.40 (d,  $J = 12.8$  Hz), 27.85 (d,  $J = 9.0$  Hz), 16.26 (d,  $J = 4.6$  Hz); MS,  $m/z$  (relative intensity) 300 (91), 206 (41), 196 (26), 104 (100), 91 (30), 78 (20). Overall yield was 99 %.

**General procedure for the preparation of ethyl 2,5-di-*p*-nitrophenyl phospholanate esters (38-40):** To an ice cold solution of **22**, **23** or **24** (100 mg, 0.33 mmol, 1 eq.) in  $\text{H}_2\text{SO}_4$  (1.5 mL) was added a solution of  $\text{HNO}_3:\text{H}_2\text{SO}_4$  (1:1, 0.0180 mL, 0.86 mmol, 2.6 eq.  $\text{HNO}_3$ ) dropwise of a period of 1 min. The reaction was stirred at 0 °C for 30 min and then poured into a beaker containing ice which upon melting left a suspension.  $\text{CHCl}_3$  (20 mL) was added and the two layers were separated. The aqueous layer was further extracted with  $\text{CHCl}_3$  (3 x 20 mL) and the combined organics phases were washed with brine (2 x 30 mL), dried ( $\text{MgSO}_4$ ) and concentrated *in vacuo* leaving an oily solid residue. Pure **38-40** was obtained by either silica gel chromatography or recrystallization of the crude residue.

**Meso cis-ethyl cis-2,5-di-*p*-nitro-phenyl phospholanate (38):** Purified by silica gel chromatography (EtOAc,  $R_f = 0.3$ , 75 % yield); white solid; mp 178-184 °C;  $^1\text{H}$  NMR  $\delta$  0.65 (3 H, t,  $J = 7$ ), 2.45 (4 H, m), 3.38 (2 H, m), 3.59 (2 H, m), 7.51 (4 H, dd,  $J = 2.2$  Hz,  $J = 9.1$  Hz), 8.21 (4 H, d,  $J = 8.8$  Hz);  $^{31}\text{P}$  NMR  $\delta$  59.9 (s);  $^{13}\text{C}$  NMR  $\delta$  147.28, 143.54 (d,  $J = 8.2$

7.9 Hz), 15.94 (d, J = 3.7 Hz).

**Meso trans ethyl cis-2,5-di-*p*-nitrophenyl phospholanate (39):** Purified by recrystallization in EtOAc/hexane (64 % yield); white solid; mp 192-197 °C; <sup>1</sup>H NMR δ 1.24 (3 H, t, J = 7.2 Hz), 2.45 (6 H, m), 3.40 (2 H, m), 4.03 (2 H, m), 7.52 (4 H, dd, J = 2 Hz, J = 7 Hz), 8.22 (4 H, d, J = 8.7 Hz); <sup>31</sup>P NMR δ 60.49 (s); <sup>13</sup>C (CDCl<sub>3</sub>) δ 147.32, 144.16 (d, J = 5.4 Hz), 129.45, 123.73, 62.26 (d, J = 7.3 Hz), 43.66 (d, J = 86.1 Hz), 29.31 (d, J = 12.8 Hz), 16.60.

**Ethyl trans-2,5-di-*p*-nitrophenyl phospholanate (40):** Purified by silica gel chromatography (EtOAc:hexanes, 4:1, R<sub>f</sub> = 0.70, 55 % yield); white solid; mp 182-186 °C; <sup>1</sup>H NMR δ 0.98 (3 H, t, J = 7 Hz), 2.22 (2 H, m), 2.56 (2 H, m), 3.45 (3 H, m), 3.83 (1 H, m), 7.54 (4 H, dd, J = 8 Hz, J = 2.1 Hz), 9.24 (4 H, d, J = 8.4 Hz); <sup>31</sup>P NMR 59.7 (s); <sup>13</sup>C NMR δ 147.32, 144.00, 143.46 (br d, J = 13.8 Hz), 129.45 (d, J = 5.5 Hz), 128.90, 123.73, 62.10 (d, J = 5.4 Hz), 46.7 (d, J = 84.2 Hz), 45.5 (d, H = 86.1 Hz), 30.37, (d, J = 11 Hz), 27.73 (d, J = 11 Hz.), 16.30.

**General procedure for the synthesis of phospholanic acids (25, 26, 41 and 42) from ethyl phosphololanate esters (22-24 and 38-40):** Trimethyl silyl iodide (1.2 eq) was added dropwise to a solution of the ester in dry CH<sub>2</sub>Cl<sub>2</sub> (approx. 1 mmol ester/mL of solvent) and the reaction stirred for 2 hr under an Ar atmosphere. Additional CH<sub>2</sub>Cl<sub>2</sub> was added and the product was extracted into a 0.1 N sodium hydroxide solution. The two layers were separated and the aqueous layer acidified to pH 2 (pH paper) with 6 N hydrochloric acid which resulted in the formation of the desired acid product as a precipitate. The product was

**trans-2,5-diphenyl phospholanic acid (25):** (90% yield); white solid; mp 220-223 °C; <sup>1</sup>H NMR (CD<sub>3</sub>OD) δ 2.10-2.59 (4 H, m), 3.22-3.42 (2 H, m), 7.20-7.42 (10 H, m); <sup>31</sup>P NMR (CD<sub>3</sub>OD) δ 63.49; <sup>13</sup>C (DMSO-d<sub>6</sub>) δ 138 (d, J = 4.6 Hz), 128.51 (d, J = 4.6 Hz), 128.06, 126.04, 45.46 (d, J = 85.1 Hz), 28.85 (d, J = 11 Hz), MS, m/z (relative intensity) 272 (46), 168 (18), 104 (100), 91 (28), 78 (25).

**cis-2,5-diphenyl phospholanic acid (26):** (90% yield); white solid; mp 165-172 °C; <sup>1</sup>H NMR (DMSO-d<sub>6</sub>) δ 2.13-2.44 (4 H, m), 3.20-3.37 (2 H, m), 7.16-7.39 (10 H, m); <sup>31</sup>P NMR (DMSO-d<sub>6</sub>) δ 60.32 (s); <sup>13</sup>C (DMSO-d<sub>6</sub>) δ 138 (d, J = 6.5 Hz), 128.42 (d, J = 5.5 Hz), 128.08, 126.01, 43.23 (d, J = 84.2 Hz), 27.61 (d, J = 12.9 Hz); MS, m/z (relative intensity) 272 (57), 168 (23), 104 (100), 91 (24), 78 (25).

**cis-2,5-di-*p*-nitrophenyl phospholanic acid (41):** (90 % yield); light brown solid; mp 278-281 °C; <sup>1</sup>H NMR (DMSO-d<sub>6</sub>) δ 2.06-2.48 (4 H, m), 3.45-3.64 (2 H, m), 7.62 (4 H, d, J = 7.3 Hz), 8.22 (4 H, d, J = 8.8 Hz); <sup>31</sup>P NMR (DMSO-d<sub>6</sub>) δ 59.17 (s); <sup>13</sup>C (DMSO-d<sub>6</sub>) δ 146.24, 129.56 (d, J = 4.5 Hz), 123.15, 43.71 (d, J = 82.4 Hz), 28.52 (d, J = 3.3 Hz).

**trans-2,5-di-*p*-nitrophenyl phospholanic acid (42):** (90 % yield); yellow solid; mp 270-275 °C; <sup>1</sup>H NMR (DMSO-d<sub>6</sub>) δ 2.04-2.45 (4 H, m), 3.40-3.64 (2 H, m), 7.62 (4 H, d, J = 5.8 Hz), 8.27 (4 H, d, J = 5.8 Hz); <sup>31</sup>P NMR (DMSO-d<sub>6</sub>) δ 58.60 (s); <sup>13</sup>C (DMSO-d<sub>6</sub>) δ 146.26, 129.68 (d, J = 5.4 Hz), 123.17, 45.68 (d, J = 82.2 Hz), 28.54 (d, J = 10 Hz).

**Allyl-6-hydroxy-hexanoate (51):** To a solution of tetrabutyl ammonium hydroxide (20% w/w, 50 mL, 39 mmol, 1 eq.) was dissolved ε-caprolactone (4.40g, 39 mmol, 1 eq.). This mixture was stirred at 65 °C for six hr after which the water was removed by high

which resulted in the formation of a white solid. The crude salt (3.74g, 10 mmol) was dissolved in dry DMF (15 mL) and allyl chloride (0.895 mL, 11 mmol, 1.1 eq) was added and the solution stirred overnight at room temperature. The reaction was diluted with water (75 mL) and extracted with EtOAc (4 x 50mL). The organic phase was washed with 5% NaHCO<sub>3</sub> (3 x 250 mL), sat. brine (3 x 250 mL), dried (MgSO<sub>4</sub>) and concentrated by rotary evaporation. Silica gel chromatography (EtOAc:hexane, 3:2, R<sub>f</sub> = 0.4) on the crude residue yielded pure **51** as a clear colourless oil (1.58g, 90%). <sup>1</sup>H NMR δ 1.39-1.68 (6 H, m), 2.29 (2 H, t, J = 7.3 Hz), 3.55 (2 H, t, J = 6.4 Hz), 4.49 (2 H, d, J = 5.8 Hz), 5.28 (2 H, t, J = 10.3 Hz), 5.57-5.91 (1 H, m).

**Allyl 6'-hydroxy(trans 2,5-di-*p*-nitrophenyl phospholanate) hexanoate (52):** **42** (250 mg, 0.69 mmol, 1 eq.) was suspended in dry CH<sub>2</sub>Cl<sub>2</sub> (5 mL). Oxalyl chloride (0.180 mL, 2.07 mmol, 3 eq.) was added dropwise over a period of 1 min and the reaction stirred for 3 hr under argon. The solvent was removed by rotary evaporation and the crude acid chloride dried under high vacuum overnight. The crude acid chloride was suspended in dry benzene (1 mL). A solution of **51** (119 mg, 0.69 mmol, 1 eq.) and 2,6-lutidine (0.81 mL, 0.69 mmol, 1 eq.) was added dropwise over a period of 2 min and the reaction was stirred for 48 hr. The solution was diluted with ether which resulted in the precipitation of lutidine hydrochloride which was removed by vacuum filtration. The filtrate was concentrated by rotary evaporation. Silica gel column chromatography (EtOAc:hexanes, 3:2, R<sub>f</sub> = 0.3) yielded pure **52** (104 mg, 29 % yield): clear colourless oil; <sup>1</sup>H NMR δ 1.04-1.55 (6 H, b m), 2.09-2.75 (6 H, b m), 3.20-3.85 (4 H, b m), 4.38 (2 H, d, J = 5.5 Hz), 5.23 (2 H, t, J = 14.1 Hz), 5.57 (1 H, m), 7.51 (4 H,



**Allyl trans 6'-hydroxy(cis 2,5-di-*p*-nitrophenyl phospholanate) hexanoate (53):** **41** (273 mg, 0.75 mmol, 1 eq.) was suspended in dry CH<sub>2</sub>Cl<sub>2</sub> (1.55 mL). Oxalyl chloride (0.197 mL, 2.25 mmol, 3 eq.) was added dropwise over a period of 1 min and the reaction stirred for 3 hr under argon. The solvent was removed by rotary evaporation and the crude acid chloride dried under high vacuum overnight. The crude acid chloride was suspended in dry benzene (1 mL). A solution of **51** (143 mg, 0.69 mmol, 1 eq.) and 2,6-lutidine (0.86 mL, 0.75 mmol, 1 eq.) was added dropwise over a period of 2 min and the reaction was stirred for 24 hr. The solution was diluted with ether which resulted in the precipitation of lutidine hydrochloride which was removed by vacuum filtration. The filtrate was concentrated by rotary evaporation. Silica gel column chromatography (CH<sub>2</sub>Cl<sub>2</sub>:EtOAc, 7:3, R<sub>f</sub> = 0.8) yielded pure **52** as a clear colourless oil (56 mg, 20 % yield), <sup>1</sup>H NMR δ 1.21-1.74 (6 H, b m), 2.23-2.64 (6 H, b m), 3.34-3.54 (2 H, b m), 3.85-3.97 (2 H, m), 4.58 (2 H, d, J = 5.5 Hz), 5.25 (2 H, t, J = 13.4 Hz), 5.80-5.98 (1 H, b m), 7.52 (4 H, dd, J = 8.8 Hz, J = 1.9 Hz), 8.20 (4 H, d, J = 8.8 Hz); <sup>31</sup>P NMR δ 60.68 (s).

**6'-hydroxy-(2,5-trans-di-*p*-nitrophenyl-phospholanate) hexanoic acid (30) via deprotection of 52:** To a solution of **52** (50 mg, 0.097 mmol, 1 eq.) dissolved in dry CH<sub>2</sub>Cl<sub>2</sub> (1.5 mL) was added tetrakis(triphenylphosphine) palladium (0.4 mg, 0.007 mmol, 7.5 mol %), and pyrrolidine (0.0081 mL, 0.097 mmol, 1 eq.). The reaction was stirred for 90 min followed by removal of the solvent by rotary evaporation. The crude was suspended in water (15 mL) and acidified to pH 2 (pH paper) with 6 N HCl. The aqueous solution was extracted with ether (5 x 15 mL), dried (MgSO<sub>4</sub>), and evaporated to dryness. Silica gel column

clear oil (40 mg, 60%):  $^1\text{H}$  NMR  $\delta$  1.09-1.65 (6 H, m), 2.05-2.75 (6 H, m), 3.17-3.98 (4 H, m), 7.52 (4 H, m), 8.22 (4 H, m);  $^{31}\text{P}$  NMR  $\delta$  60.58 (s).

**Deprotection attempt: 29 from 53 via removal of allyl protecting group:** To a solution of **53** (50 mg, 0.097 mmol, 1 eq.) dissolved in dry  $\text{CH}_2\text{Cl}_2$  (1.5 mL) was added tetrakis(triphenylphosphine) palladium (0.4 mg, 0.007 mmol, 7.5 mol %), and pyrrolidine (0.0081 mL, 0.097 mmol, 1 eq.). The reaction was stirred for 60 min followed by removal of the solvent under reduced pressure. The crude was suspended in water (15 mL) and acidified to pH 2 (pH paper) with 6 N HCl. The aqueous solution was extracted with ether (5 x 15 mL), dried ( $\text{MgSO}_4$ ), and evaporated to dryness. Due to isomerization of **29** to **30**, it was not possible to isolate pure **29** by this procedure.

**Tert-butyl 6'-hydroxy-(trans-2,5-di-*p*-nitrophenyl-phospholanate) hexanoate (55) via the Mitsunobu procedure:** Tert-butyl-6-hydroxyhexanoate<sup>34</sup> (39 mg, 0.21 mmol, 1.5 eq), **42** (50 mg, 1.4 mmol, 1.5 eq.), triphenylphosphine (54.3 mg, 0.21 mmol, 1.5 eq.), and diisopropylazidodicarboxylate (DIAD) (0.041 mL, 0.21 mmol, 1.5 eq.) were dissolved in dry THF (1.5 mL). The solution was stirred for 30 min at room temperature followed by removal of the solvent by rotary evaporation. Silica gel column chromatography (EtOAc:hexane, 1:1,  $R_f = 0.5$ ) of the crude residue yielded pure **55** as a clear colourless oil (47.5 mg, 64%):  $^1\text{H}$  NMR  $\delta$  1.00-1.48 (15 H, m), 2.00-2.74 (6 H, m), 3.19-3.86 (4 H, m), 7.45-7.58 (4 H, m), 8.23 (4 H, dd,  $J = 0.9$  Hz,  $J = 6.9$  Hz);  $^{31}\text{P}$  NMR  $\delta$  59.77 (s),  $^{13}\text{C}$   $\delta$  172.42, 147.41, 143.84 (d,  $J = 3.7$  Hz), 143.21 (d,  $J = 6.4$  Hz), 129.50 (d,  $J = 5.5$  Hz), 128.82 (d,  $J = 4.6$  Hz), 123.80, 123.77, 80.08, 65.77 (d,  $J = 7.3$  Hz), 46.83 (d,  $J = 83.3$  Hz), 45.51 (d,  $J = 86$  Hz), 35.17, 30.50, 30.24,

**6'-hydroxy (trans 2,5-di-*p*-nitrophenyl phospholanate) hexanoic acid (30) via deprotection of 55:** **55** (35 mg, mmol) was dissolved in 20% TFA/CH<sub>2</sub>Cl<sub>2</sub> (1.5 mL) and stirred overnight at room temperature. The CH<sub>2</sub>Cl<sub>2</sub> and TFA was removed by rotary evaporation. Silica gel chromatography (EtOAc:hexanes, 4:1, R<sub>f</sub> = 0.5 ) on the crude residue yielded pure **30** as a clear colourless oil (25 mg, 80%): <sup>1</sup>H NMR δ 1.09-1.65 (6 H, m), 2.05-2.75 (6 H, m), 3.17-3.98 (4 H, m), 7.52 (4 H, m), 8.22 (4 H, m), <sup>31</sup>P NMR δ 60.58 (s); <sup>13</sup>C NMR δ 175.92, 147.44, 143.65 (d, J = 3.7 Hz), 143.11 (d, J = 6.4 Hz), 129.53 (d, J = 5.5 Hz), 128.87 (d, J = 3.7 Hz), 123.82, 65.83 (d, J = 7.3 Hz), 46.64 (d, J = 84.2 Hz), 45.50 (d, J = 85.1 Hz), 33.23, 30.33, 30.02, 24.80, 24.02.

**Meso trans tert-butyl 6'-hydroxy(cis-2,5-diphenyl-phospholanate) hexanoate (60):** To a solution of **26** (120 mg, 0.55 mmol, 1 eq.) in dry CH<sub>2</sub>Cl<sub>2</sub> (2 mL) was added oxalyl chloride (0.144 mL, 1.65 mmol, 3 eq.) dropwise over a period of 1 min and the solution was stirred for 3 hr. The solvent was removed by rotary evaporation and the crude acid chloride subjected to high vacuum for 12 hr. The crude acid chloride was dissolved in dry benzene (1 mL) and a solution of tert-butyl-6-hydroxy hexanoate<sup>34</sup> (125 mg, 0.66 mmol, 1.1 eq.) and triethylamine (0.100 mL, 0.72 mmol, 1.2 eq.) in dry benzene (1 mL) was added dropwise over a period of 2 min and the reaction was stirred for 24 hr. Ether was added which resulted in the precipitation of triethylamine hydrochloride which was removed by vacuum filtration and the filtrate was concentrated by rotary evaporation. Silica gel chromatography (CH<sub>2</sub>Cl<sub>2</sub>:EtOAc, 90:10, R<sub>f</sub> = 0.6) on the crude residue yielded pure **60** as a clear colourless oil (140 mg, 57%). <sup>1</sup>H NMR δ 1.23-1.65 (15 H, m), 2.18 (2 H, t, J = 7.3 Hz), 2.40 (4 H, m), 3.29

137.07 (d, J = 4.6 Hz), 128.75, 128.63, 128.50, 126.68, 79.92, 65.18 (d, J = 6.5), 43.51 (d, J = 86.0 Hz), 35.39, 30.49 (d, J = 5.5 Hz), 29.51 (d, J = 14.7 Hz), 28.15, 25.13, 24.62, 21.78.

**Meso trans 6'-hydroxy(cis 2,5-di-*p*-nitro-phenyl-phospholanate) hexanoic acid (29) via nitration of 60:** **60** (120 mg, 0.27 mmol, 1 eq.) was dissolved in 0.5 mL of H<sub>2</sub>SO<sub>4</sub> at 0 °C. A solution of HNO<sub>3</sub>/H<sub>2</sub>SO<sub>4</sub> (1:1, 0.062 mL, 2.6 eq. HNO<sub>3</sub>) was added and the reaction was stirred at 0 °C for 30 min. The reaction was poured into a beaker containing ice which upon melting left a suspension. CHCl<sub>3</sub> (5 mL) was added and the two layers were separated. The aqueous layer was further extracted with CHCl<sub>3</sub> (4 x 10 mL) and the combined organics were washed with brine (2 x 15 mL), dried (MgSO<sub>4</sub>) and concentrated *in vacuo* leaving an oily of solid residue. Attempts to obtain pure product by subjecting the crude residue to silica gel flash chromatography were unsuccessful. Final purification of the desired product could only be accomplished using HPLC with an Alltech normal phase HPLC column (EtOAc:hexane, 7:3, retention time = 18 min) to give **29** as a clear colourless oil (51 mg, 44 %): <sup>1</sup>H NMR δ 1.23-1.68 ( 6H, m), 2.24 (2 H, t, J = 7 Hz), 2.35-2.60 ( 4 H, m), 3.35-3.57 ( 2 H, m), 3.87-4.03 (2 H, dd, J = 6.6 Hz, J = 7.7 Hz), 7.52 (4 H, dd, J = 1.8 Hz, J = 6.9 Hz), 8.19 (4 H, dd, J = 8.4 Hz); <sup>31</sup>P NMR (CDCl<sub>3</sub>) δ 61.54 (s); <sup>13</sup>C NMR δ 176.79, 147.28, 143.97 (d, J = 7.3 Hz), 129.46 (d, J = 5.5 Hz), 123.84, 66.23 (d, J = 7.3 Hz), 43.56 (d, J = 84.2 Hz), 33.48, 30.30 (d, J = 5.5 Hz), 29.26 (d, J = 14.7 Hz), 24.96, 24.1.

### 2.3 Synthesis of Substrates

**6-bis(*p*-nitrophenyl) phosphate hexanoic acid (31):** To a solution of tert-butyl-6-

bis(*p*-nitrophenyl)-phosphate (150 mg, 0.44 mmol, 1 eq.), triphenyl phosphine (173 mg, 0.66 mmol, 1.5 eq.), and diisopropyl-azido-dicarboxylate (DIAD) (130  $\mu$ l, 130 mg, 0.66 mmol, 1.5 eq.). This reaction was stirred under argon for 30 min. The solvent was removed by rotary evaporation and the crude oil chromatographed on silica gel (CH<sub>2</sub>Cl<sub>2</sub>:EtOAc, 95:5, R<sub>f</sub> 0.7). Due to slow product breakdown, it was not possible to separate the tert-butyl-6-bis(*p*-nitrophenyl) phosphate hydroxy hexanoate product from trace amounts of *p*-nitrophenol. For this reason, the impure product was deprotected in a 1 mL solution of 20% trifluoroacetic acid:CH<sub>2</sub>Cl<sub>2</sub> overnight. The solvent was removed by rotary evaporation and the 6-bis(*p*-nitrophenyl) phosphate hexanoic acid product, a clear oil, was obtained by silica gel chromatography in (hexanes:EtOAc, 50:50, R<sub>f</sub> 0.2) (126 mg, 73% overall yield). <sup>1</sup>H NMR  $\delta$  1.20-1.74 (7 H, m), 2.35 (2 H, t, J = 7 Hz), 4.34 (2 H, q, J = 6.6 Hz), 7.40 (4 H, d, J = 9.2 Hz), 8.26 (4 H, d, J = 7.3 Hz); <sup>31</sup>P NMR  $\delta$  -15.53 Hz (s).

**Dimethyl-*p*-nitrobenzyl phosphonate (63):** To *p*-nitro benzyl bromide (3 g, 13.8 mmol, 1 eq.) in dry benzene (4 mL) was added trimethyl phosphite (6 mL, 5.70 g, 45 mmol, 3.5 eq.). The reaction was refluxed overnight. Removal of excess trimethyl phosphite was performed by hi-vacuum distillation. The remaining crude was purified on silica gel in EtOAc (R<sub>f</sub> 0.5) to give the product which appeared as a thick red oil (3.08 g, 90%). <sup>1</sup>H NMR  $\delta$  3.26 (2 H, d, J = 22.3 Hz), 3.71 (6 H, d, J = 10.9 Hz), 7.47 (2 H, dd, J = 2.6 Hz, J = 8.8 Hz), 8.19 (2 H, d, J = 8.8 Hz); <sup>31</sup>P NMR  $\delta$  24.47 (s).

**Methyl-*p*-nitrobenzyl phosphonic acid (64):** A solution composed of **63** (2.5 g, 10.2 mmol, 1 eq.) and sodium iodide (2.29 g, 15.3 mmol, 1.5 eq.) in butanone (60 mL) was

salt product was dissolved in water (10 mL), and the solution acidified to pH 2 with concentrated hydrochloric acid (approx. 4 ml). The product precipitated out of solution and was obtained by vacuum filtration (2.00 g, 90%): white solid;  $^1\text{H}$  NMR  $\delta$  3.19 (2 H, d,  $J = 22.8$  Hz), 3.59 (3 H, d, 11.3 Hz), 7.44 (2 H, dd,  $J = 2.5$  Hz,  $J = 8.8$  Hz), 8.17 (2 H, d, 8 Hz);  $^{31}\text{P}$  NMR  $\delta$  26.0 (s).

**Methyl-*p*-nitrophenyl-*p*-nitrobenzyl phosphonate (65):** **64** (1 g, 4.33 mmol, 1 eq.) was suspended in dry  $\text{CH}_2\text{Cl}_2$  (40mL). To the suspension was added *p*-nitrophenol (722 mg, 5.19 mmol, 1.2 eq.) and ethyldiisopropyl carbodiimide coupling agent (995 mg, 5.19 mmol, 1.2 eq.). The reaction was stirred under argon for 72 hr. Additional  $\text{CH}_2\text{Cl}_2$  (60 mL) was added to dilute the reaction. The organic layer was washed with aliquots of 5%  $\text{NaHCO}_3$  (3 x 150 mL), 0.1 N HCl (3 x 150 mL), and saturated brine (3 x 150 mL) before being dried ( $\text{MgSO}_4$ ). The product, a white solid, was purified by recrystallization in hexanes-EtOAc (987 mg, 64%).  $^1\text{H}$  NMR  $\delta$  3.48 (2 H, d,  $J = 22.7$  Hz), 3.82 (3 H, d,  $J = 11.3$  Hz), 7.28 (2 H, d,  $J = 8.1$  Hz), 7.52 (2 H, d,  $J = 2.5$  Hz), 8.20 (4 H, d,  $J = 8.8$  Hz),  $^{31}\text{P}$  NMR ( $\text{CDCl}_3$ )  $\delta$  20.77 (s).

***p*-Nitrophenyl-*p*-nitrobenzyl-phosphonic acid (66):** **65** (600 mg, 1.7 mmol, 1 eq.) was dissolved in butanone (8 mL) with lithium bromide (221 mg, 2.55 mmol, 1.5 eq.). The reaction was refluxed overnight. The lithium salt product was obtained by cooling the solution and isolating the precipitate by vacuum filtration. The lithium salt was dissolved in water (60 mL) and the solution was acidified with 6 N HCl (approx. 6 ml) to pH 2. The resulting white precipitate was isolated by vacuum distillation and dried under vacuum (536

H, d, J = 7.62 Hz), 8.23 (4 H, t, J = 8.8 Hz); <sup>31</sup>P NMR (DMSO-d<sub>6</sub>) δ 21.73 (s).

**6-Hydroxy-*p*-nitrophenyl-*p*-nitro-benzyl-phosphate-hexanoic acid (32):** To a solution of tert-butyl-6-hydroxy-hexanoate<sup>34</sup> (156 mg, 0.83 mmol, 1.5 eq.) in dry tetrahydrofuran (1.5 ml) was added **66** (180 mg, 0.55 mmol, 1 eq.), triphenyl phosphine (218 mg, 0.83 mmol, 1.5 eq.), and diisopropylazodicarboxylate (DIAD) (180 ul, 0.83 mmol, 1.5 eq.). The reaction was stirred for 1 hour. The solvent was removed by rotary evaporation and the crude purified by silica gel chromatography in EtOAc:hexanes (60:40). Due to decomposition of the product upon the column and persistent traces of *p*-nitrophenol impurities, crude **67** was used in the deprotection step. The crude product was stirred in 1 mL solution of 20% trifluoroacetic acid in CH<sub>2</sub>Cl<sub>2</sub> overnight. The solvent was removed by rotary evaporation and the product chromatographed on silica gel (EtOAc:hexanes, 80:20, R<sub>f</sub> 0.4) (61 mg, 24%, not optimized). Clear colourless oil; <sup>1</sup>H NMR δ 8.20 (4 H, d, J = 8.8 Hz), 7.51 (2 H, dd, J = 2.6 Hz, J = 9.8 Hz), 7.29 (2 H, d, J = 9.6 Hz), 4.15 (2 H, m), 3.52 (2 H, J = 22.7 Hz), 2.30 (2 H, t, J = 7.2 Hz), 1.62 (4 H, m), 1.33 (2 H, m); <sup>31</sup>P NMR (CDCl<sub>3</sub>) δ 19.7 (s).

#### **2.4 Hapten Isomerization Studies**

**General Procedure:** Solutions of 500 μM of the cis TSA **29** were made up in the appropriate media as indicated below and partitioned into 0.5 mL aliquots. At arbitrary time intervals, reaction aliquots were quenched with 1 M HCl and extracted with EtOAc. Aliquots of the EtOAc layer were analyzed on an analytical normal phase column in order to determine the relative proportions of the cis and trans isomers. HPLC analysis was performed on a

EtOAc at 1.0 mL/min over 5 min and switching to 2.0 mL/min at 6 min. The UV detector was set at 280 nm.

0.1 N NaOH: A 500  $\mu$ M solution of **29** in 0.10 N NaOH was prepared and partitioned into 0.5 mL aliquots. Reaction aliquots were quenched with 100  $\mu$ l of 1 M HCl and extracted with 0.5 mL of EtOAc for the purposes of analysis at time intervals of 10 min, 1 hr and 24 hr.

pH 7.5: A 500  $\mu$ M solution of **29** in 20 mM sodium phosphate buffer was prepared and partitioned into 0.5 mL aliquots. Reaction aliquots were quenched with 40  $\mu$ l of 1 M HCl and extracted with 0.5 mL of EtOAc for the purposes of analysis after incubation periods of 25 min, 1, 3, 7 and 11 days .

pH 8.5: A 500  $\mu$ M solution of **29** in 20 mM sodium bicarbonate buffer was prepared and partitioned into 0.5 mL aliquots. Reaction aliquots were quenched with 40  $\mu$ l of 1 M HCl and extracted with 0.5 mL of EtOAc for the purposes of analysis after incubation periods of 20 min, 4 days and 8 days.

## **2.5 Conjugation of TSA's to Carrier Proteins**

The following general procedure<sup>54</sup> was used to couple the cis and trans TSA's to BSA and KLH. In brief, the hapten (6.4 mg, 0.013 mmol) was dissolved in DMF:water (60:40) (3 mL). To this was added sulfo-NHS (3.5 mg, 0.016 mmol) and EDC coupling agent (3.1 mg, 0.016 mmol). This reaction was stirred at room temperature for 3 hr. The reaction was divided into two 1.5 mL aliquots. One aliquot was added to a solution of BSA (6.3 mg) in 50 mM potassium phosphate buffer at pH 7.5 (3 mL) and the other to a solution of KLH (6.1 mg)



in potassium phosphate buffer at pH 7.5 (3 mL). These reactions were shaken at 4 °C overnight.

The unconjugated hapten was removed by dialysis (6 x 1L, 3 hrs each) in 50 mM potassium phosphate at pH 7.5. The extent of conjugation was determined by first measuring the concentration of BSA followed by the determination of the number of free lysines by the method of Habeeb.<sup>35</sup>

## **2.6 Substrate Hydrolysis Studies**

The substrate hydrolysis studies were performed in a sodium bicarbonate buffer at pH 9.0. A 20  $\mu$ L aliquot of a 1 mM stock solution of each of the substrates **31** and **32** in DMF was diluted to 1 mL in the assay buffer in 1 mL quartz UV cuvettes at a final concentrations of 20  $\mu$ M substrate and 20 mM sodium bicarbonate buffer. A Cary 1B UV/VIS spectrophotometer (Varian) was used to collect data. Absorbance readings were recorded every thirty minutes for approximately 48 hr. The data was fitted to a first order rate equation using the Grafit<sup>36</sup> software package. The half-life of each substrate under the experimental conditions was calculated by averaging the rate constant from duplicate assays and using the equation  $t_{1/2} = (\ln 2)/k$ .

### 3.1 Synthesis of Haptens

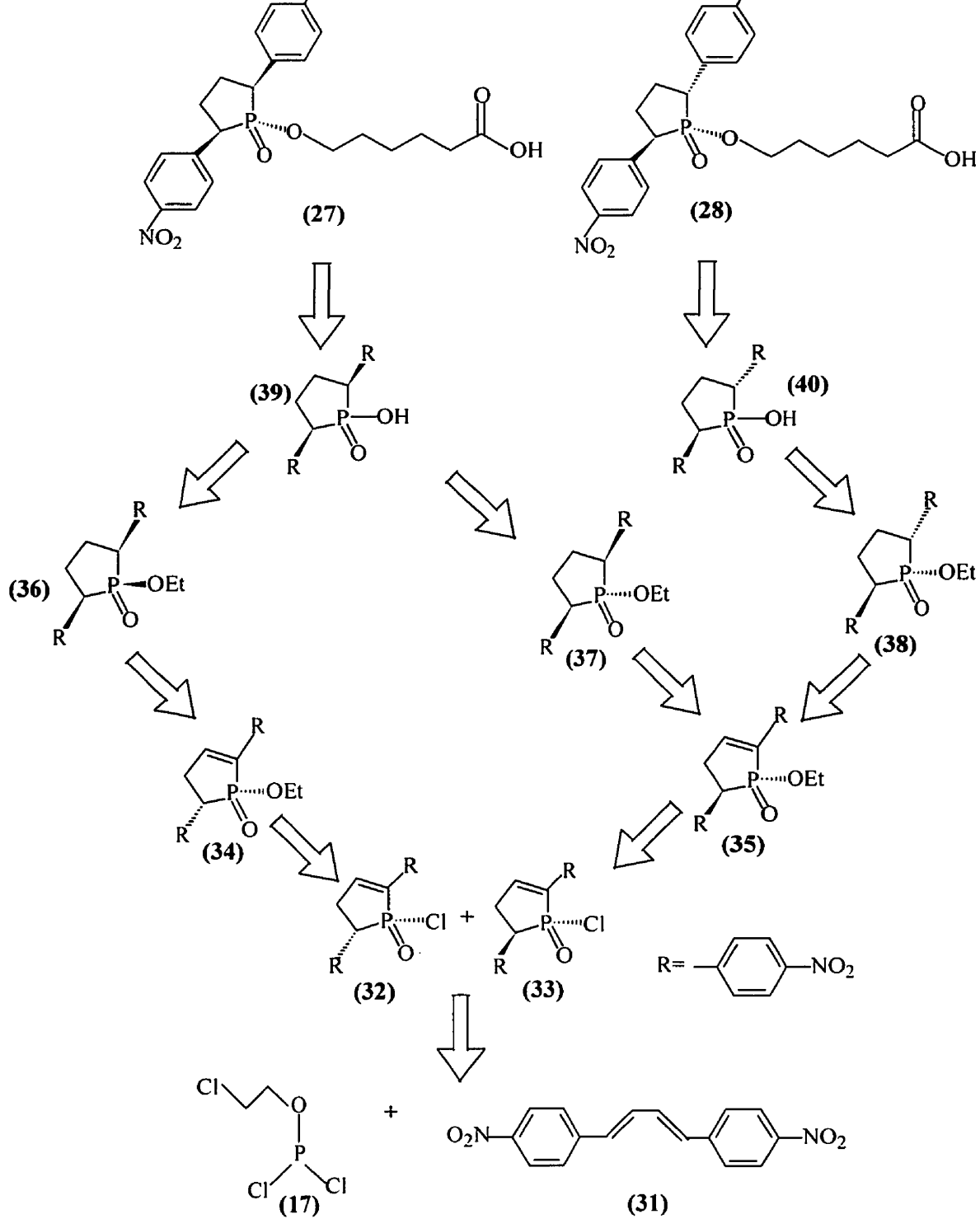
We envisioned two strategies towards the synthesis of the desired TSA's **29** and **30**. One approach, shown in Scheme 12 as a retrosynthesis, was to employ the nitrated diene **33**,<sup>37</sup> in a McCormack reaction with 2-chloroethyl dichlorophosphite **17**. This method was based upon the success achieved by Taylor<sup>26</sup> with the synthesis of the unnitrated TSAs using 1,4-diphenyl-1,3-butadiene (Schemes 10 and 11). Assuming that the double bond would isomerize to the 2 position in the phospholane ring, as was the case with the synthesis of **18** and **19**, we would obtain the isomeric phosphinyl chlorides **34** and **35** (Scheme 12). Crude **34** and **35** would be reacted with ethanol would give the desired isomeric cyclic phosphinate esters **36** and **37**. The next step, hydrogenation of the double bond to produce the isomeric esters **38-40**, would have to be performed with a reagent or catalyst that would also not result in the reduction of the nitro groups to amino groups. The reduction of double bonds in the presence of nitro groups has been reported using Wilkinson's catalyst<sup>38</sup> and we anticipated that this would work successfully here. Once isomers **38-40** were formed, the desired haptens would be synthesized using a procedure similar to that developed by Taylor (for the synthesis of the unnitrated TSAs **13** and **14**) in which the isomeric esters (**38-40**) are separated and converted to the acids **41** and **42** which are converted into the desired TSAs.

An alternative approach would be to nitrate the phenyl rings after construction of the phospholane ring. For example, we would synthesize the unnitrated esters **22-24** using Taylor's procedure (see Scheme 10) and then attempt to selectively bis-nitrate these species at the *para*-position to form the nitrated esters **38-40** (Scheme 13). Isomers **38-40** would be

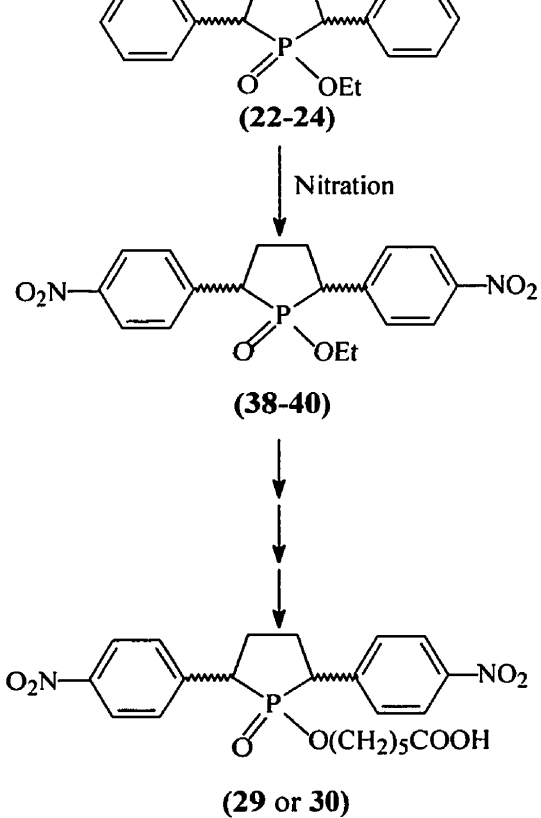
synthesize the unnitrated haptens **13** and **14** using Taylor's procedure (see Scheme 10 and 11) and then attempt to nitrate these species directly to form the nitrated haptens (Scheme 14).

The latter routes (Schemes 13 or 14) involves a bis-nitration of the phenyl rings at the *para*-position. We reasoned that specifically nitrating *both* phenyl rings exclusively at the *para*-position would be difficult. In all likelihood, we reasoned that we would obtain a complex mixture of *ortho*- and *para*-substituted products which would be difficult to purify. Consequently, we decided to construct **29** and **30** via the former route (Scheme 12).

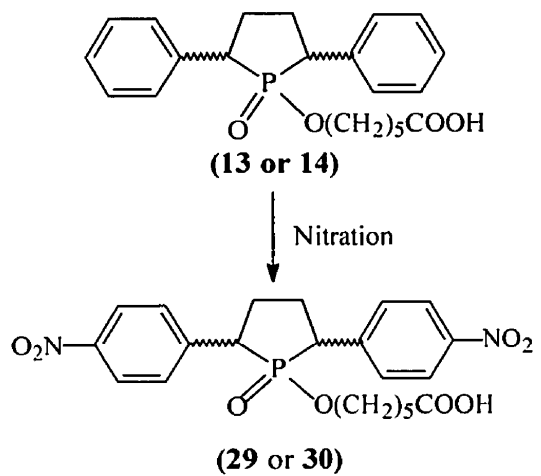
We chose to perform the McCormack reaction with the nitrated diene **33** using the methodology developed by Taylor<sup>26</sup> for the synthesis of the unnitrated phospholenate esters **20** and **21** (Scheme 10). However, Taylor performed this reaction neat and indeed, most McCormack reactions are performed neat and a solvent rarely used. McCormack reactions performed in a solvent tend to proceed much slower. However, with **33**, this was not possible due to the very high melting point of this diene (254 °C). Consequently, we attempted the McCormack reaction using benzene as solvent since benzene has been used successfully as a solvent in McCormack reactions.<sup>39</sup> The reaction was performed in a pressure tube at 190 °C for three days (Scheme 15) and the resulting crude reaction mixture reacted with ethanol in benzene in the presence of a tertiary base. This procedure failed to produce the desired products. The failed reaction could be attributed to a number of factors. The presence of the *p*-nitro groups deactivate the diene to make it less susceptible to reactions with the dienophile thus slowing the rate of the cycloaddition reaction. In addition, the phosphite can react with the NO<sub>2</sub> groups to form unwanted side products. The reaction of phosphites with nitro groups



**Scheme 12: Retrosynthesis of 29 and 30**

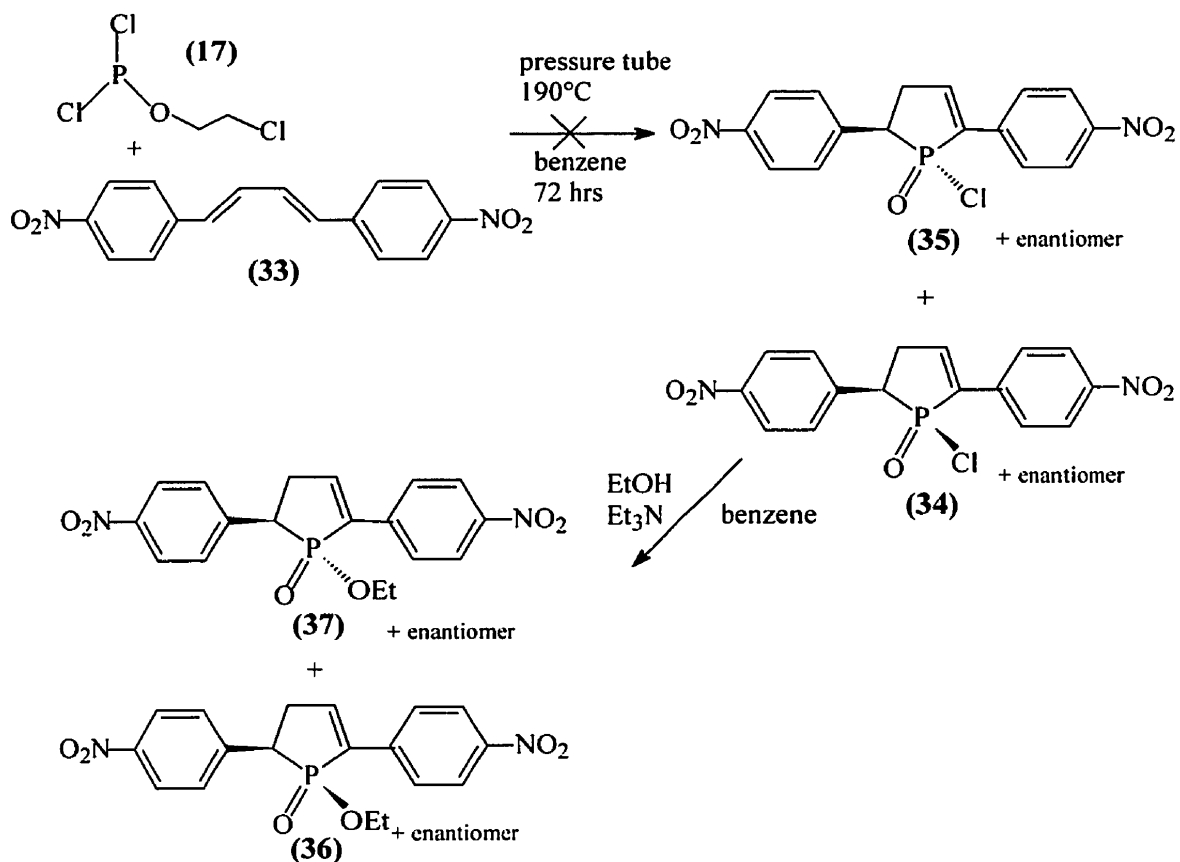


**Scheme 13:** Retrosynthesis of **29** and **30** via nitration of precursors



**Scheme 14:** Retrosynthesis of **29** and **30** via nitration of **13** and **14**

byproducts. This is not unusual for a McCormack reaction performed at high temperature.<sup>42</sup>

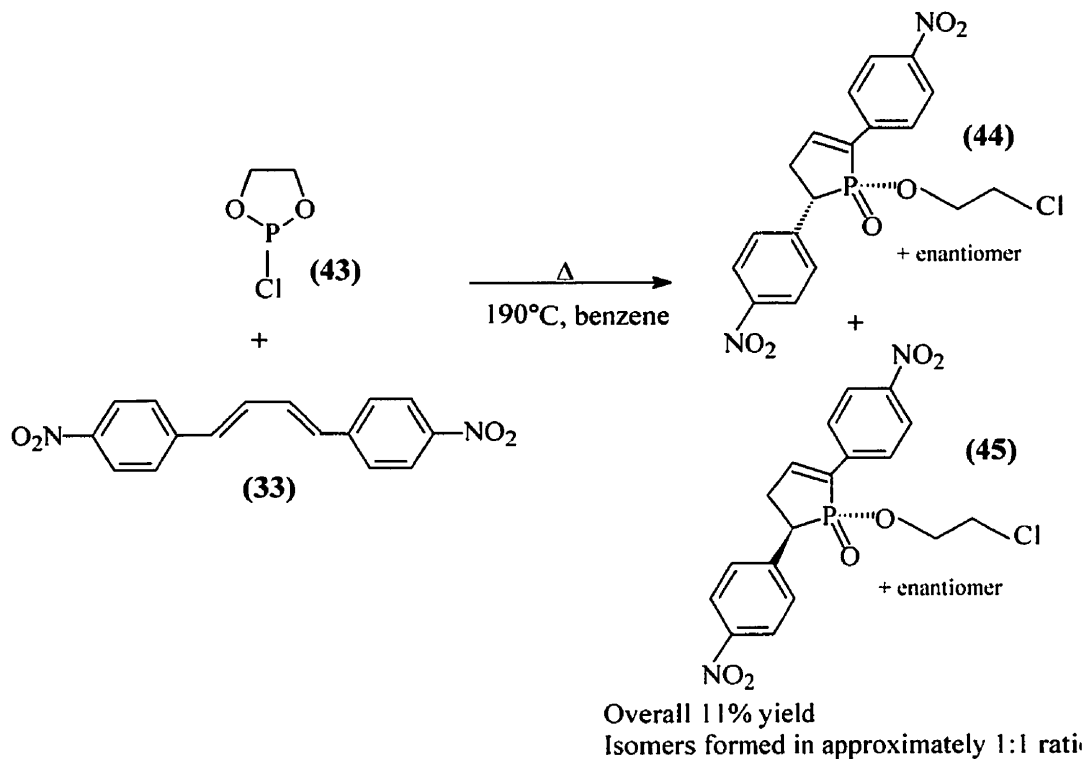


**Scheme 15:** McCormack reaction with 33

To counter these problems, we attempted the McCormack reaction using ethylene chlorophosphite (43 in Scheme 16) as the dieneophile since it has been reported to undergo the McCormack reaction more readily than acyclic phosphites.<sup>43-45</sup> This was indeed the case and the yield did improve but only to 11% (Scheme 16). Again, the deactivating effects of the nitro groups and their well-known ability to react with phosphites are the most likely reasons

what phosphite we used and therefore, obtaining a reasonable yield employing the nitrated diene was going to be very difficult.

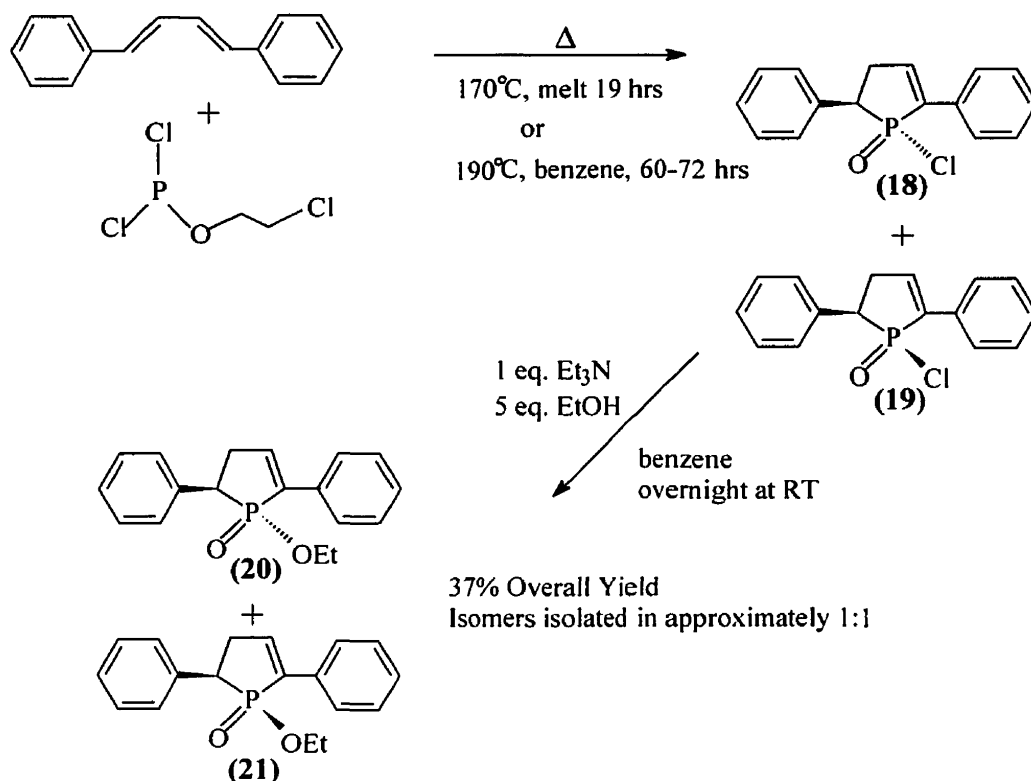
Due to the very low yields obtained using the nitrated diene, we decided to attempt to



**Scheme 16:** McCormack reaction with 31 and 41

synthesize the TSAs using the approach outlined in Scheme 13 or 14. The first step was to synthesize the isomeric esters 20 and 21 using the procedure developed by Taylor outlined in Scheme 17. Thus, 1,4-diphenyl-1,3-butadiene and 2-chloroethyl-dichlorophosphite (generated *in situ* between  $\text{PCl}_3$  and  $\text{P}(\text{OCH}_2\text{CH}_2\text{Cl})_3$ ) were reacted in a pressure tube at 160-

in the presence of triethylamine. This produced the two isomeric esters **20** and **21** in an overall yield of 25-33%. Although Taylor performed the reaction neat (which works reasonably well) we also found that benzene could be used as a solvent as was the case when performing the reaction with the nitrated diene. Although the use of the solvent requires a higher reaction temperature of 190 °C and a longer reaction time of 60-72 hours, the amount of polymeric byproducts formed is significantly decreased which simplifies the workup. The yields are also slightly higher (30-39%).

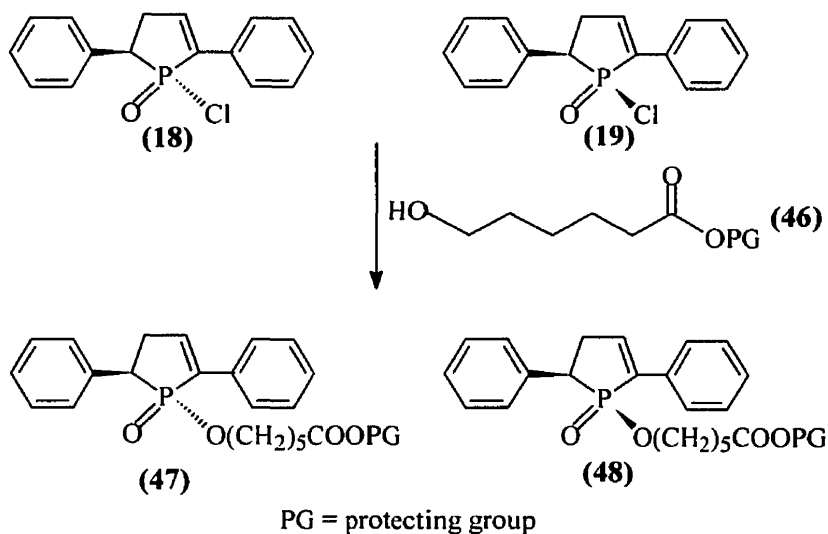


**Scheme 17:** Synthesis of **20** and **21** by Taylor<sup>26</sup>

In theory, the linker chain could have been attached by reacting the crude acid



previous work by Taylor<sup>26</sup> indicated that separation of the isomers resulting from this reaction, **47** and **48**, was very difficult and Taylor was unable to separate and purify these species. Consequently, we decided to work with the isomeric ethyl esters, **20** and **21**, since the resulting isomers could be readily purified and separated by chromatography.



**Scheme 18:** Direct attachment of linker chain to acid chlorides

The stereochemical relationship between the cis, **21**, and trans, **20**, isomers could be assigned on the basis of the <sup>1</sup>H NMR signals. In **20**, where the phenyl and ethoxy group are on opposite sides of the ring, both methylene protons (H<sub>a</sub>) of the ethoxy groups appear as a complex multiplet in the chemical shift range of 3.9-4.3 ppm (Figure 1A). This chemical shift range is typical for methylene protons in ethyl phosphinates. However, in the phenyl-ethoxy cis isomer **21**, the two methylene protons (H<sub>a</sub> and H<sub>b</sub>) of the ethoxy group have very different

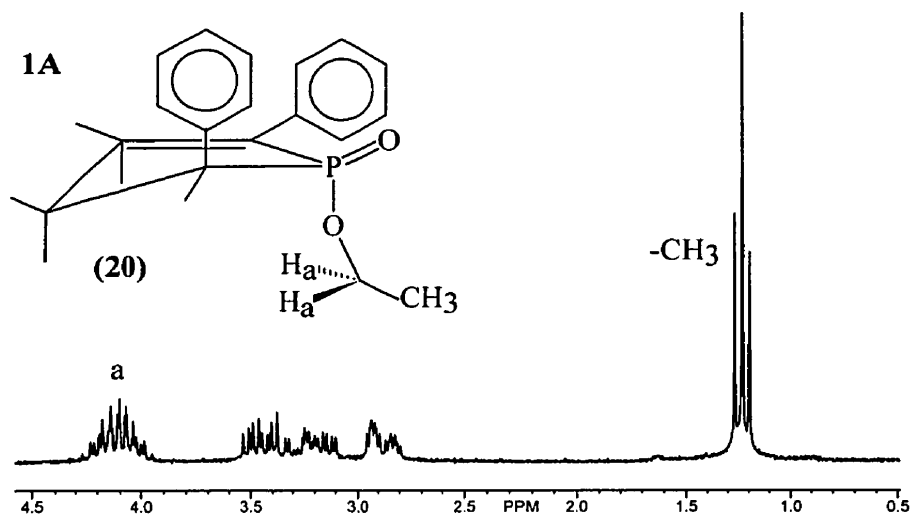
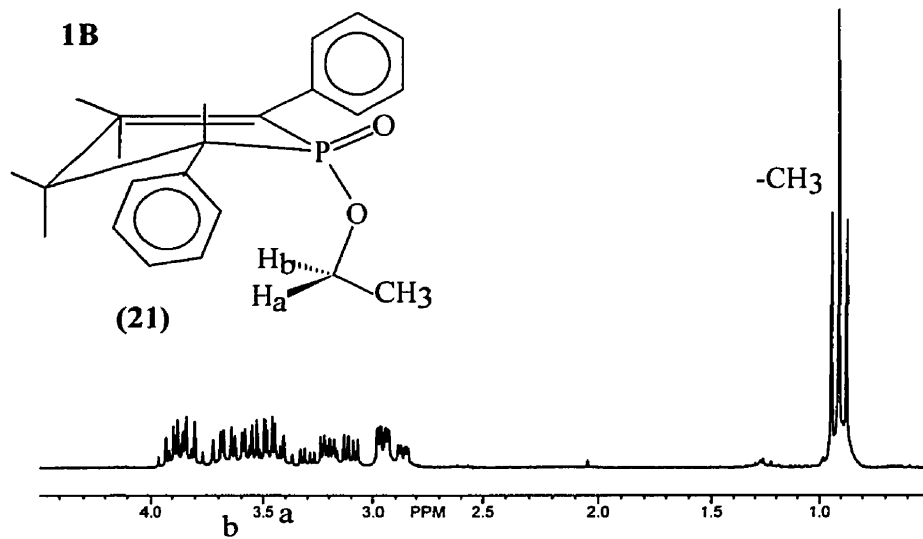
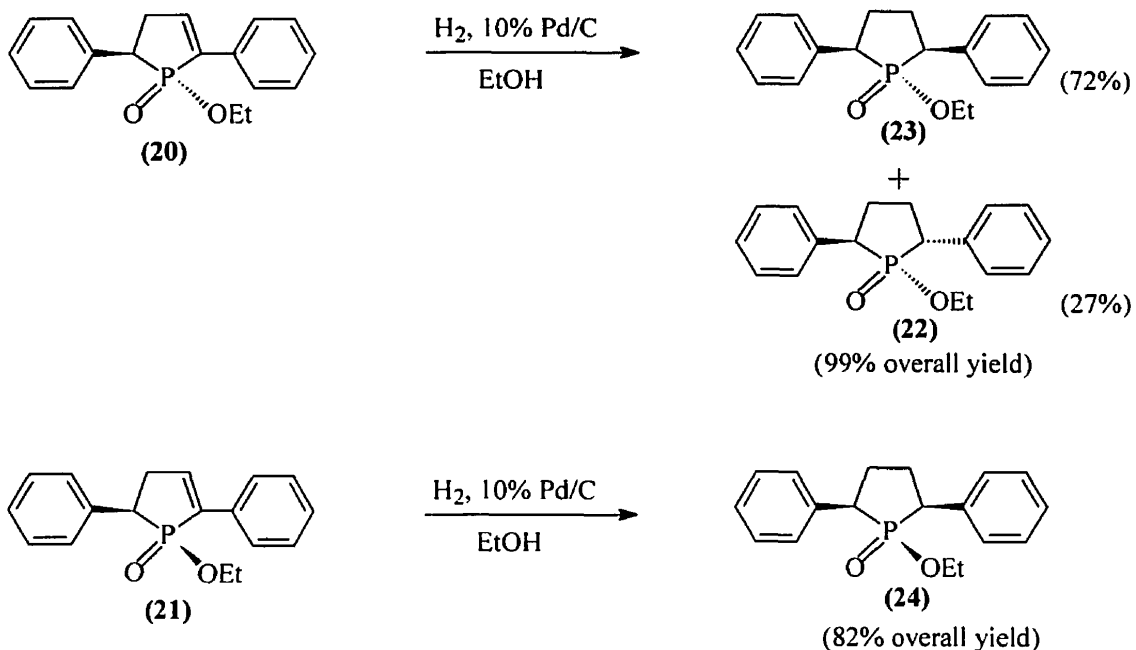


**Figure 1:** Differences in  $^1\text{H}$  NMR spectra of isomers **20** and **21**

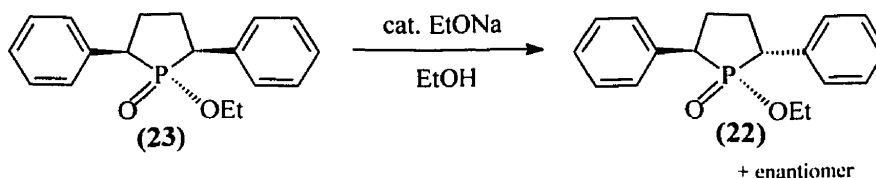
$H_a$ , appears as a complex multiplet at 3.4-3.6 ppm considerably further upfield than that found in a 'typical' ethoxy phosphinate. This is because it is oriented close to the face of the phenyl ring (at the 5-position) and therefore experiences a shielding effect. The other methylene proton  $H_b$ , has an almost 'normal' chemical shift range of 3.7-3.9 ppm (Figure 1B) because it is oriented away from the face of the phenyl ring. This phenomenon does not occur with the trans ester **20** because the phenyl group at the 5-position on the ring and the ethoxy group are on opposite sides of the phospholane ring. Bodalski *et al.*<sup>46</sup> reported observing similar phenomenon in 2-phenyl-2-phospholene-1-oxides.



**Scheme 19: Hydrogenation of **20** and **21****

**20** and **21**. Hydrogenation (10 % Pd/C) of the cis phospholanate ester, **21**, yielded the “all cis” phospholanate ester **24** (both phenyl groups and the ethoxy group cis to one another) exclusively in 84 % yield (Scheme 19). Thus, as expected, the hydrogen approaches exclusively from the side opposite the two phenyl and ethoxy groups which is the least sterically hindered side. Hydrogenation of **20** gave mainly the “phenyl-cis” phospholanate ester, **23**, (the two phenyl groups cis to one another and the ethoxy group trans to the phenyl groups) and the desired “phenyl-trans” phospholanate ester, **22**, was formed as the minor product indicating that the more distant but larger phenyl group was the main determinant in directing the hydrogenation.

Although we had considerable quantities of the ‘all cis’ **24** and ‘phenyl cis’ **23** esters, the amount of ‘phenyl trans’ **22** was relatively small in comparison. However, Taylor<sup>26</sup> found that it was possible to obtain more of the phenyl trans isomer, by isomerizing compound **23** or **24** using a catalytic amount of sodium ethoxide in ethanol (Scheme 20).



**Scheme 20:** Isomerization of **23** to **22**

The isomerization occurs by abstraction of the acidic proton at the 2-position which is alpha to both the phosphoryl and phenyl groups. Under these conditions, the reaction mixture at

the two isomers, the less sterically hindered trans isomer was clearly the thermodynamically favored product. By isomerizing some of the cis esters, we were able to obtain significant quantities of the trans ester **22**.

The cis and trans nature of isomers **22-24** were readily determined on the basis of NMR data. For example, the ‘all-cis’ (**24**) and ‘phenyl-cis’ isomers (**23**) could be readily distinguished from the “phenyl-trans” isomers (**22**) since the cis isomers are symmetrical meso compounds and their phospholane ring carbons appear as only two sets of doublets in the  $^{13}\text{C}$ -NMR as opposed to 4 sets of doublets for the unsymmetrical phenyl-trans esters. We expected that the “all-cis” and “phenyl-cis” isomers would be readily distinguished on the basis of their  $^1\text{H}$ -NMRs since the methylene and methyl protons of the ethoxy groups should have very different chemical shifts and this was indeed the case (Figure 2). For example, in the “all-cis” isomer, **24**, the methylene protons ( $\text{H}_a$ ) of the ethoxy group appear considerably more upfield ( $\delta$  3.19-3.35) than is normally found with a phosphorus ethyl ester (typically  $\delta$  3.9-4.4) (Figure 2C). This is because in the “all cis” isomer, the ethyl group is on the same side of the phospholanate ring as the two phenyl groups. Thus, the methylene protons are in the “face” of the two phenyl rings and are therefore considerably shielded and are even further upfield than the benzylic phospholane ring protons ( $\text{H}_b$ ) ( $\delta$  3.33-3.51). In the case of the “phenyl-cis” isomer, **23**, the ethyl group is on the opposite side of the phospholane ring as the phenyl groups. Thus, the methylene protons appear much further downfield and have chemical shifts that one would expect to have for a “normal” phosphinate ethyl ester ( $\delta$  3.94-4.12) and are much further downfield than the benzylic protons ( $\delta$  3.2-3.4, Figure 2A). In the

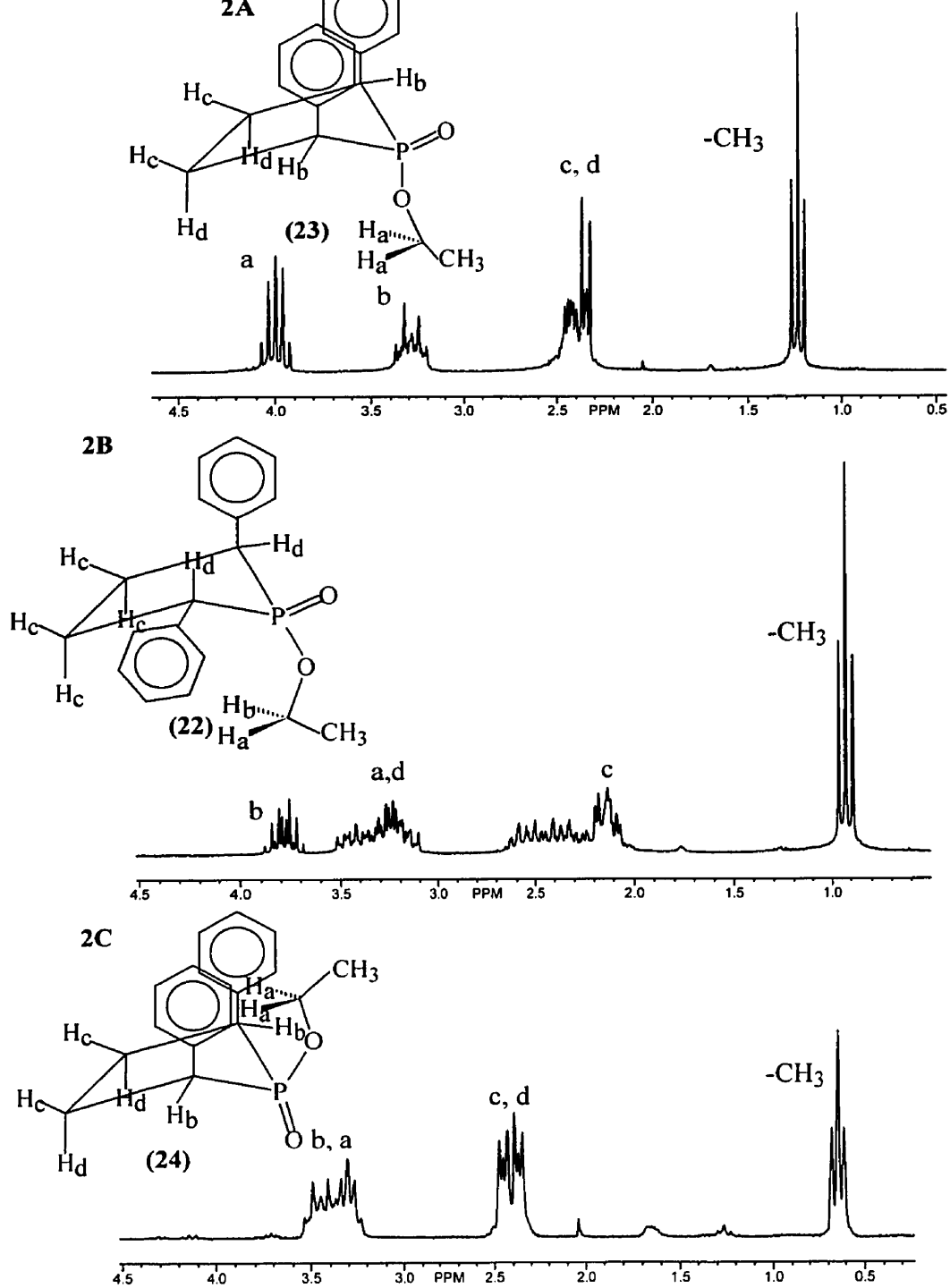


**Figure 2: Differences in  $^1\text{H}$  NMR spectra of isomers 22-24**

equivalent ( $H_a$  and  $H_b$  in Figure 2B): the ester is not symmetrical and only one of the phenyl rings is on the same side of the phospholane ring as the ethoxy group. One methylene proton  $H_b$ , appears as a complex multiplet at  $\delta$  3.8-4.2 ppm which is a ‘normal’ chemical shift for a phosphinate ethyl ester. However, the other methylene proton  $H_a$ , appears further upfield as a complex multiplet at 3.5 ppm. Thus, one of the methylene protons is shielded because it is in the ‘‘face’’ of one of the phenyl rings while the other methylene proton is oriented away from the phenyl ring and has a ‘‘normal’’ chemical shift. The stereochemical relationship between all subsequent isomeric compounds reported in this study were readily determined in a similar manner simply by examining the chemical shift of the  $-\underline{CH}_2-O-P$  protons and by  $^{13}C$  NMR.

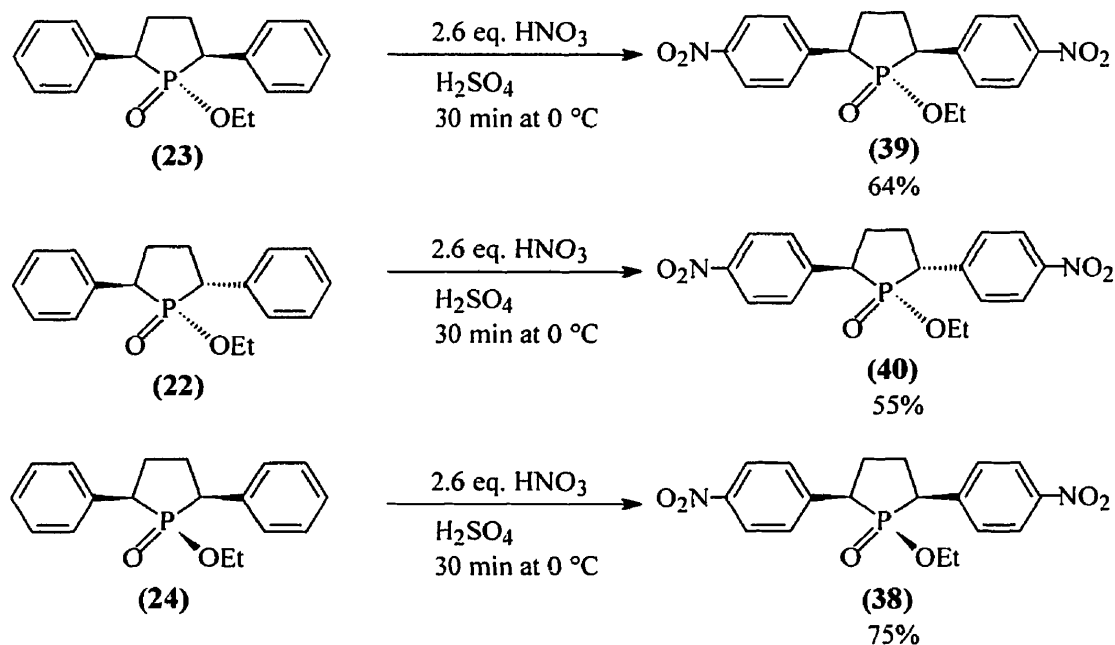
It is important to note that the *trans*-2,5-diaryl esters, and all subsequent ‘‘phenyl *trans*’’ derivatives exist as enantiomers due to the chiral centers at the 2 and 5 carbons on the phospholanate ring. No effort was made to obtain enantiomerically pure ‘‘phenyl *trans*’’ compounds since the haptens were not chiral at the phosphorous center and the substrates did not possess any chiral carbon centers.

Crucial to the success of this approach was our ability to bis-nitrate the phenyl rings in the *para*-position without obtaining large quantities of other isomers such as *ortho*-nitrated material. Nitration at the *ortho* position competes with *para* nitration and is statistically favored since there are two *ortho* positions for every one *para*. Consequently, we suspected that obtaining the desired bis-(*p*-nitrophenyl) species, **38-40** or **29-30**, (Scheme 13 or 14) might be problematic. As outlined in Schemes 13 and 14, the nitration step could be performed at various stages of the synthesis. We reasoned that it would be better to attempt

species. If the nitration reaction was not successful on isomers **22-24**, then it is unlikely that it would work any better at a later stage in the synthesis.

There are numerous methods and reagents now available for performing electrophilic aromatic nitrations.<sup>47</sup> However, we wished to use a method that was as selective as possible for the *para* position and could be performed with readily available and inexpensive materials. Although there are no methods that are completely *para*-selective, a review of the literature revealed that perhaps the most effective and economical method for *para*-nitrating phenyl rings<sup>47-49,53</sup> was with the classical nitration reagent, H<sub>2</sub>SO<sub>4</sub>/HNO<sub>3</sub>. We therefore subjected isomers **22-24** to these conditions and found, much to our surprise, that we were able to obtain the desired bis-*para*-nitrated species, **38-40** in reasonable to good yields: 55% for **40**, 64% for **39**, and 75% for **38** (Scheme 21). The di-*p*-nitrophenyl species could be easily isolated from other isomeric products using either chromatography or recrystallization. Our ability to obtain significant quantities of the bis-*para*-nitrated isomers was most likely a result of the *ortho* position being relatively sterically hindered by the phospholane ring. Indeed, the difference in yields between **38-40** can be accounted for on the basis of steric factors. In the trans-2,5-diphenyl ester **22**, only the phospholane ring obscures the *ortho* positions from attack by the nitronium ion on one of the phenyl rings. In the phenyl cis compound **23**, the proximity of the other phenyl ring to themselves serves to hinder the approach of the electrophile. In the ‘all cis’ **24**, steric hindrance is provided by both the phenyl rings themselves and the ethoxy group. This rationale accounts for the increasing yields obtained in going from the “phenyl trans”, to the “phenyl cis” and finally to the “all cis”

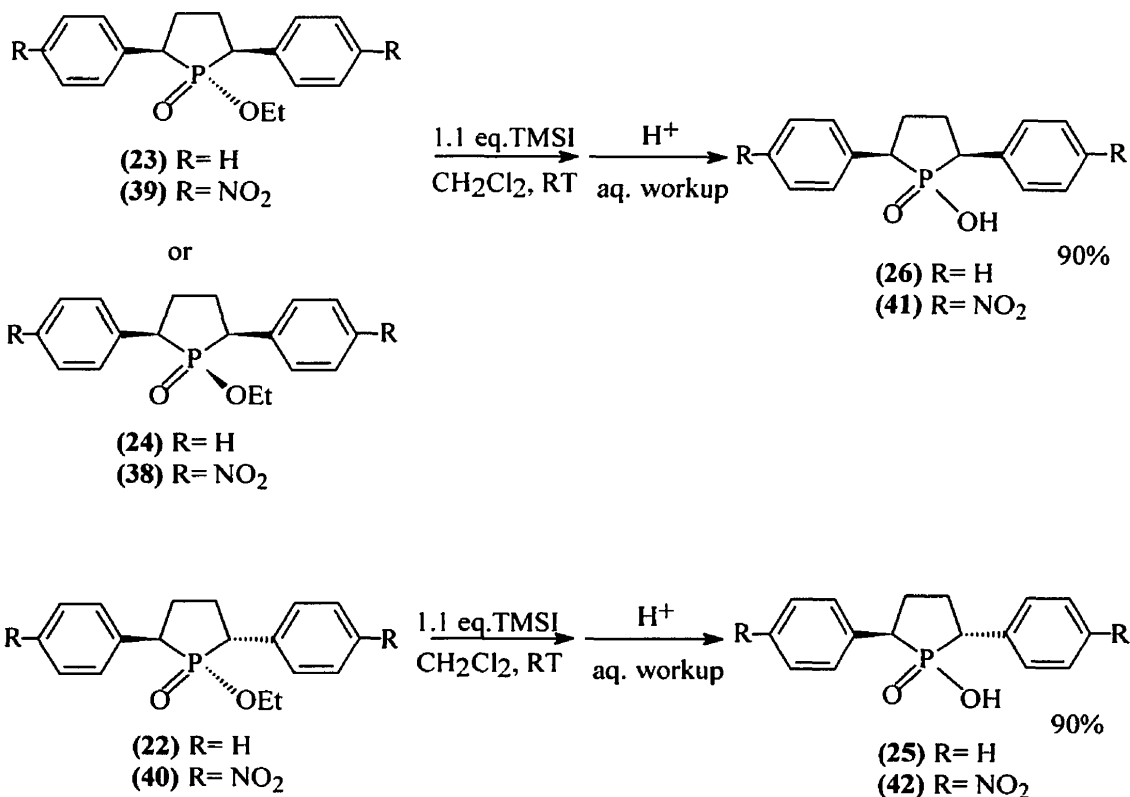




**Scheme 21:** Nitration of ethyl esters **22-24**

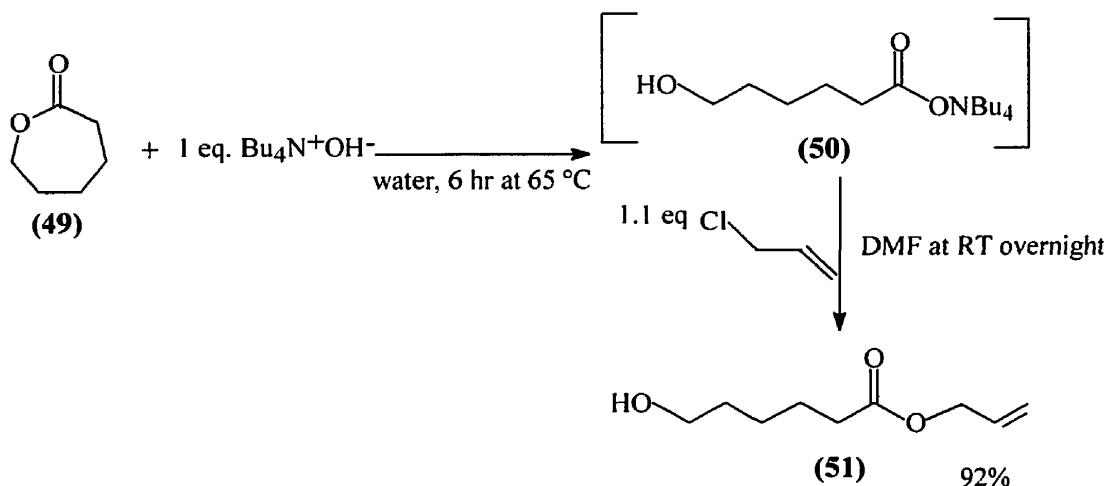
Since we were able to obtain significant quantities of the nitrated isomers **38-40**, we decided to use **38-40** for constructing the desired TSAs. Thus, the ethyl esters were converted into the free acids, **41** and **42**, in 90% yield, by formation of the silyl ester with trimethylsilyl iodide followed by an aqueous workup and acidification. The ‘all cis’, **38**, and ‘aryl cis’, **39**, compounds gave identical free acid products (Scheme 22).

With suitable quantities of the free acids in hand, the next step was to attach the six carbon linker chain. The acid group on the linker arm had to be protected to prevent it from interfering in the coupling reaction. In the original synthesis of **13** and **14** (Scheme 10 and 11), Taylor<sup>26</sup> used the benzyl protecting group which was removed by hydrogenation. This



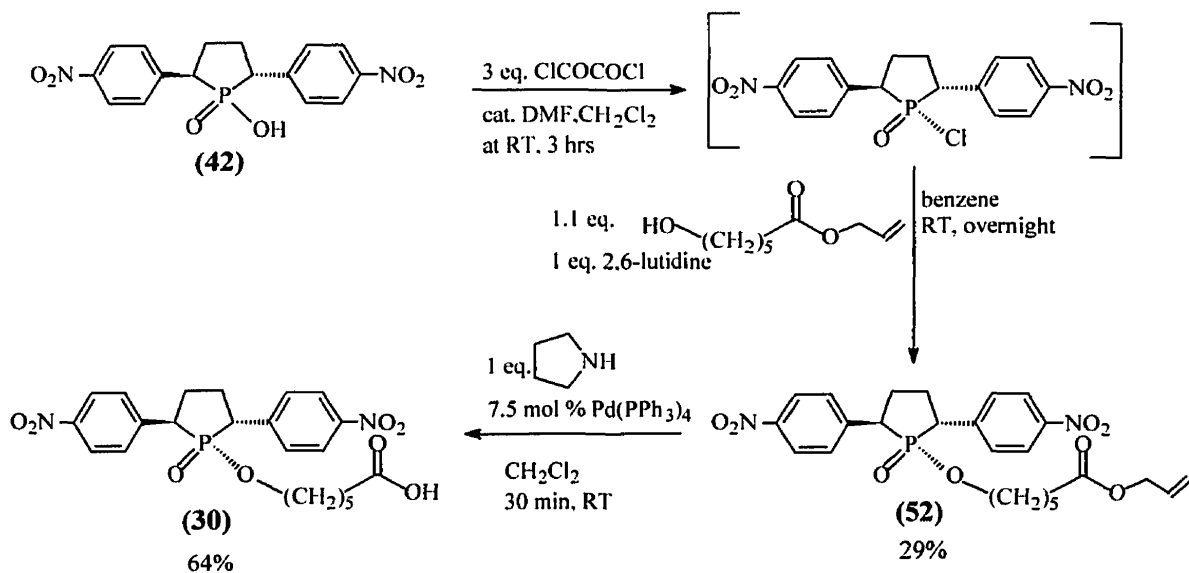
**Scheme 22:** Conversion of ethyl esters to acids

protecting group could not be used in the synthesis of **29** and **30** since hydrogenation would also result in converting the nitro groups to amino groups. Consequently, we decided to use an allyl protecting group since it can be removed under very mild conditions using tetrakis(triphenylphosphine) palladium as a catalyst with either dimedone or pyrrolidine as a mild nucleophile.<sup>50</sup> Thus, we synthesized the allyl-protected linker chain 6-hydroxy-allyl-hexanoate, **51** (Scheme 23). This was accomplished by hydrolyzing  $\epsilon$ -caprolactone, **49**, to the hydroxy acid, **50**, using tetrabutylammonium hydroxide. The resulting salt was reacted with



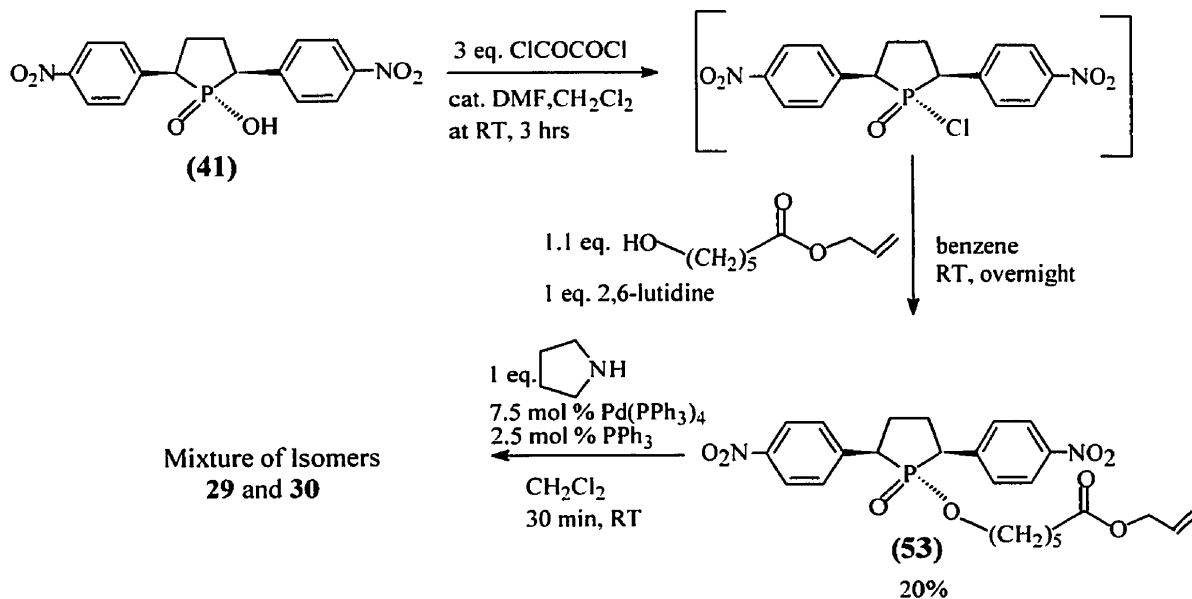
**Scheme 23:** Synthesis of 6-hydroxy-allyl hexanoate **51**

For attaching the linker arm to the nitrated acids **41** and **42**, we initially chose the procedure that Taylor<sup>26</sup> employed for the attachment of the linker arm to the unnitrated acids **25** and **26** (Scheme 11). This involved converting the acids to the acid chlorides using oxalyl chloride and a catalytic amount of DMF followed by reaction with an appropriately protected hydroxy acid linker arm in benzene in the presence of a tertiary amine base. Using this procedure with the trans acid, **42**, and the linker arm **51**, we were able to construct the protected trans TSA precursor **52** in a 29% yield (Scheme 24). To obtain the final trans TSA, **30**, we only needed to deprotect the carboxylic acid group. To accomplish this, we reacted **52** with pyrrolidine in the presence of a catalytic amount of tetrakis-(triphenylphosphine)-palladium (Scheme 24). The deprotection proceeded in 64% yield, but trace amounts of triphenylphosphine and its oxide persisted despite numerous chromatographic separations.



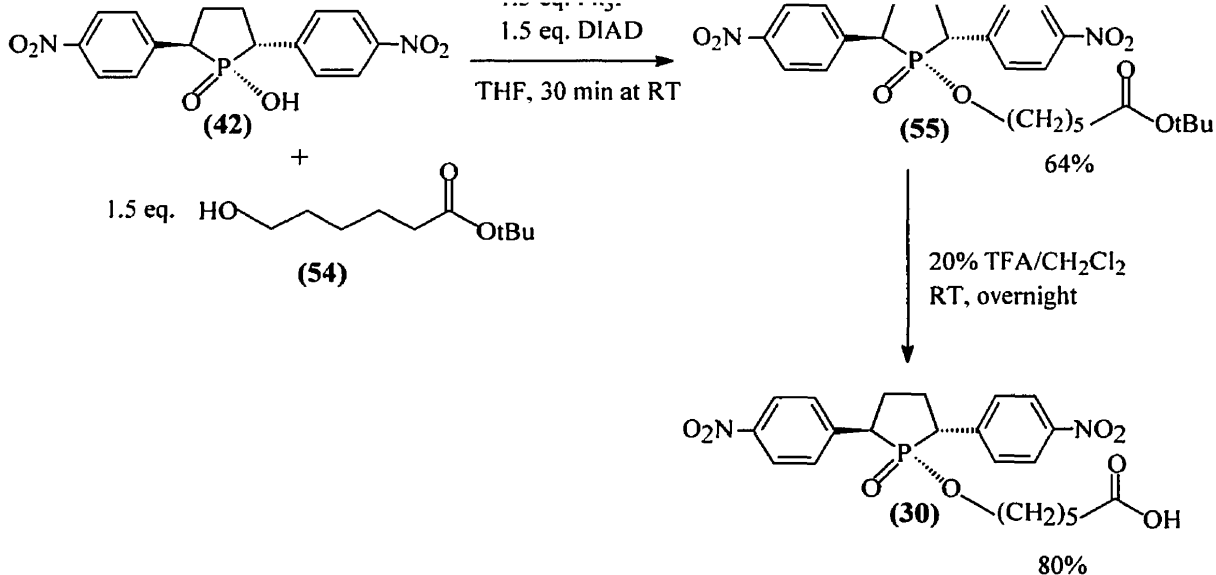
**Scheme 24:** Synthesis of **30** via an acid chloride coupling

When we attempted to attach the linker arm **51** to the cis acid **41** using the acid chloride procedure the yield of cis TSA precursor, **53**, dropped to 20% (Scheme 25). We were also able to detect significant quantities of the trans isomer **52**. This is in contrast to the results obtained by Taylor for the synthesis of **28**, the non-nitrated analogue of **53**, in which the desired ‘phenyl-cis’ species (Scheme 11) was obtained exclusively. Thus, it appears that the presence *p*-NO<sub>2</sub> groups increased the acidity of the benzylic protons to the extent that they were easily abstracted by the 2,6-lutidine used in the reaction. This resulted in some of the desired ‘aryl-cis’ product to isomerize to the more thermodynamically favored ‘aryl-trans’ form, **52**. We also found that this isomerization also occurred during the removal of the allyl group from **53**. This was most likely a result of the pyrrolidine abstracting the benzylic protons. Consequently, separation of the two isomers was not possible. As with the trans



**Scheme 25:** Synthesis of **29** via an acid chloride coupling

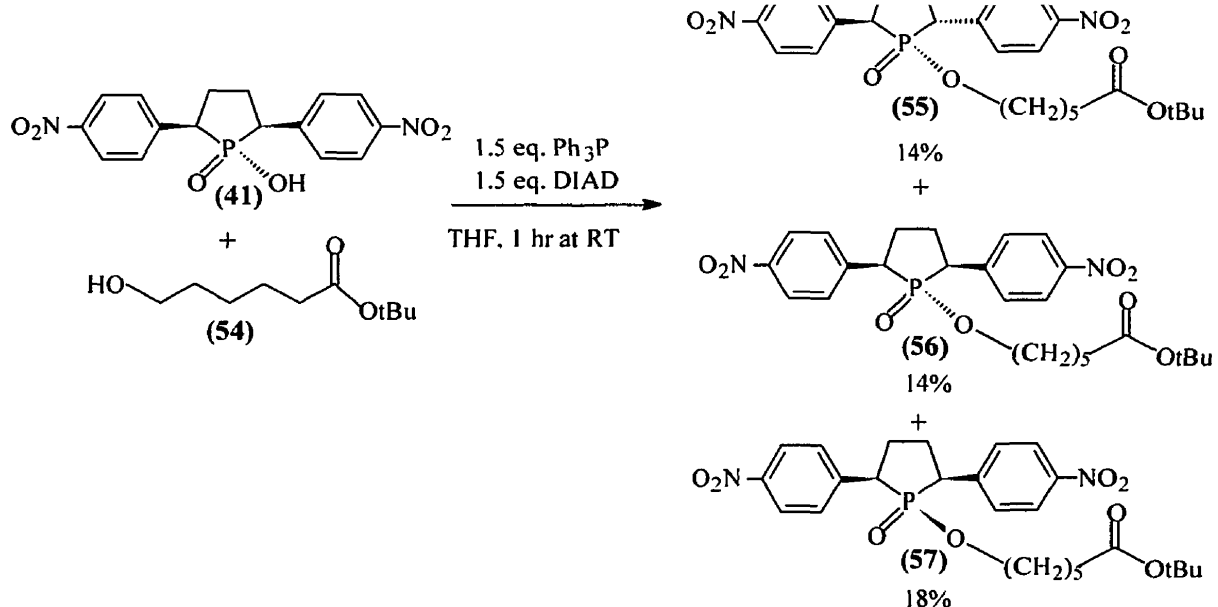
Due to the low yields obtained using the acid chloride coupling procedure and the problems encountered with isomerization, we decided to couple the linker chain using a Mitsunobu coupling procedure that has been used for the synthesis of phosphonate esters.<sup>51</sup> The Mitsunobu procedure for the synthesis of phosphonate esters involves reacting an alcohol and a phosphonic acid in the presence of triphenylphosphine and diisopropylazido dicarboxylate (DIAD). This is a very mild procedure and does not require the addition of any exogenous base. We also decided to use a *t*-butyl protecting group in the linker arm instead of the allyl protecting group since the *t*-butyl group can be removed using mild acid<sup>50</sup> and so isomerization of the *cis* ester should not occur during the deprotection process.



**Scheme 26:** Synthesis of **30** via a Mitsunobu coupling

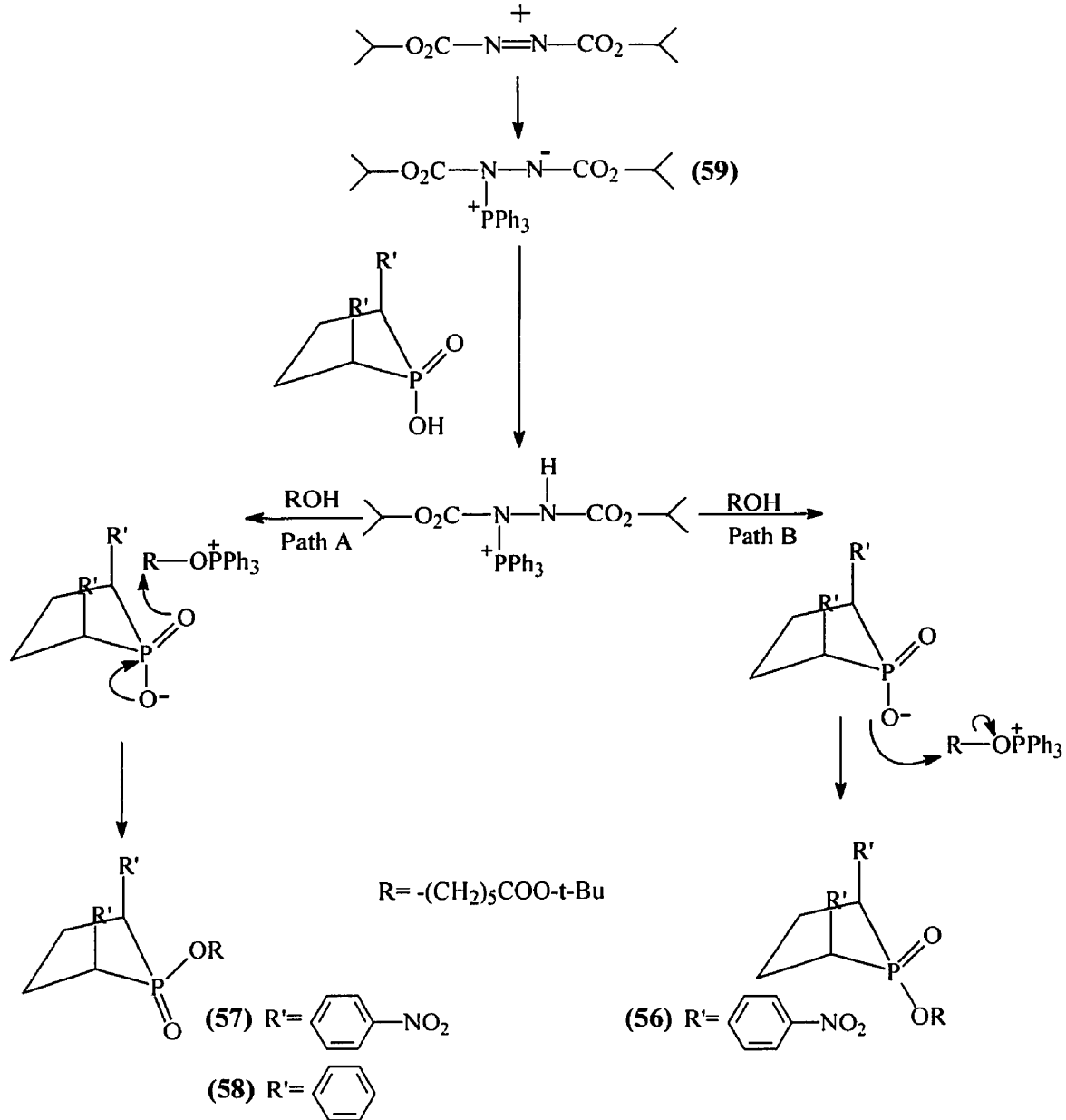
When the Mitsunobu reaction was performed with the acid **42**, and the t-butyl protected linker chain **54**<sup>34</sup>, the desired product **55** was obtained in 64% yield. Deprotection of the acid was carried out in 20%TFA/CH<sub>2</sub>Cl<sub>2</sub> yielding the desired trans TSA, **30**, in an 80% yield (Scheme 26). However, when the coupling reaction was performed with the ‘aryl cis’ acid **41**, the results were disappointing. Although the reaction yielded all three isomers **55-57**, the desired ‘aryl cis’ product, **56**, was isolated in only a 14% yield (Scheme 27).

The results of the Mitsunobu reaction with the cis acid (**41**) were unexpected since no exogenous base was added to the reaction mixture that would result in isomerization. The currently accepted mechanism for the Mitsunobu reaction involves an attack of the acid component on an *in situ* generated alkoxyphosphonium salt (Scheme 28) using cis acid **41** as an example. We had anticipated that with the cis acid, we would obtain exclusively the ‘aryl



**Scheme 27:** Mitsunobu coupling with **41**

“*cis*” product **56**, since we anticipated that attack of the phosphinic acid on the alkoxyphosphonium salt would occur from the least sterically hindered side of the phosphinic acid as shown in pathway B in Scheme 28. Formation of the “all-*cis*” product **57** (pathway A, Scheme 28) would not occur due to steric reasons. Were the three isomeric products that were obtained in the reaction solely a result of an isomerization of the desired “aryl *cis*” product or does the Mitsunobu reaction produce both “aryl *cis*” and “all *cis*” products followed by isomerization? In order to better understand the results from the coupling to the *cis* acid, we performed the Mitsunobu reaction with non-nitrated acid **26** (Scheme 28) whose ester we anticipated would not be susceptible to isomerization. *Surprisingly, we isolated the least thermodynamically stable “all *cis*” ester **58** (Scheme 28) in a 60% yield with no other*



**Scheme 28:** Mechanism of Mitsunobu coupling

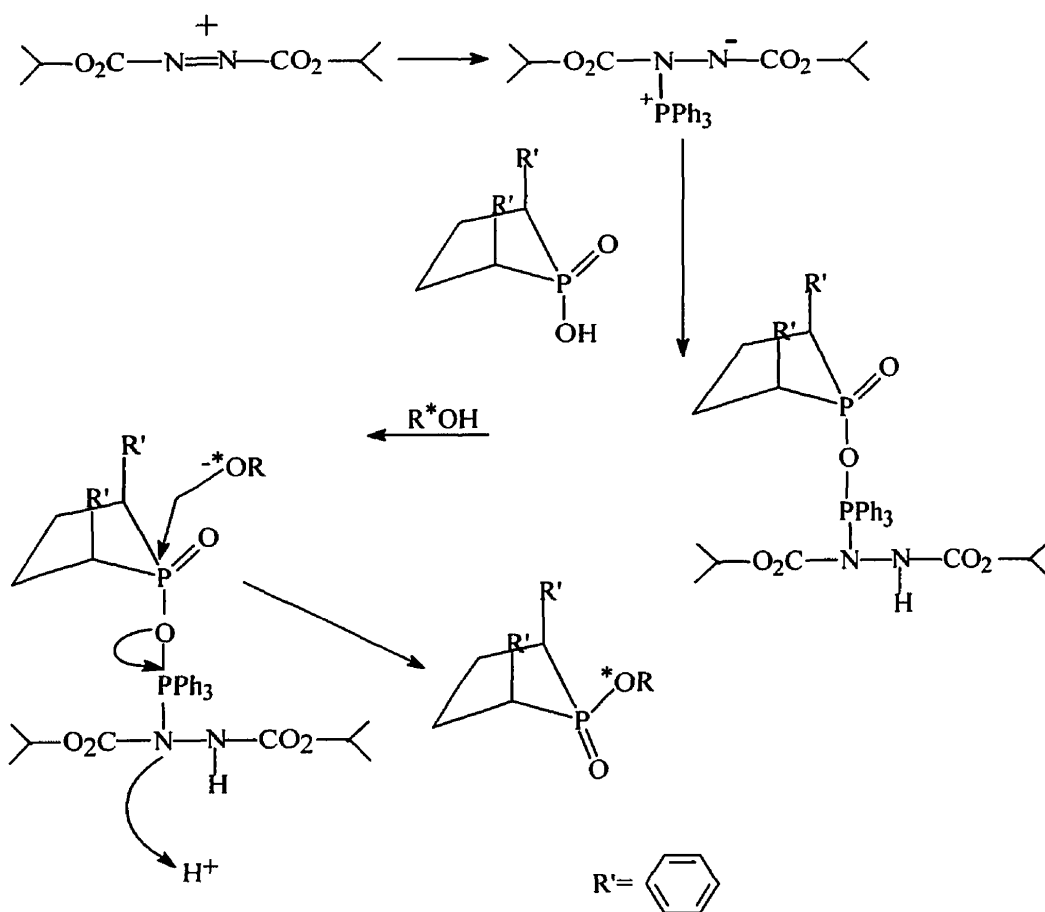
*detectable products.* Thus, the results we obtained in using the nitrated acid, **41**, were evidently a result of the increased acidity of the benzylic protons. It is likely that the “all cis”



The presence of some unprotonated betaine (**59** in Scheme 28) may be sufficient to catalyze the isomerization process.

These results with **26** were somewhat surprising. If the currently accepted mechanism for the Mitsunobu reaction (Scheme 28) is correct, then the Mitsunobu coupling favors approach of the alcohol from the more sterically hindered side of the phospholanate ring which is unlikely. An alternative mechanism is that the betaine deprotonates the acid and forms the phosphonium salt. Due to the size of the ylid formed between DIAD and triphenylphosphine, the phosphonium salt must form on the face of the phospholanate ring opposite the phenyl groups (Scheme 29). Deprotonation of the alcohol yields the better alkoxy nucleophile which is forced to approach the phosphorous center away from the DIAD-triphenylphosphine adduct. If the reaction is performed using an  $^{18}\text{O}$  labeled alcohol, the products should include  $^{18}\text{O}$  labeled triphenylphosphine oxide if the mechanism by Campbell is correct. If our mechanism is correct, the label should appear on the ester product. The results would be easily determined using either  $^{31}\text{P}$  NMR or mass spectrometry. An  $^{18}\text{O}$  atom adjacent to a phosphorous atom causes the signal to shift upfield. Analysis by mass spectrometry would reveal larger isotopic signals in either the triphenylphosphine oxide peak or the ester product signal.

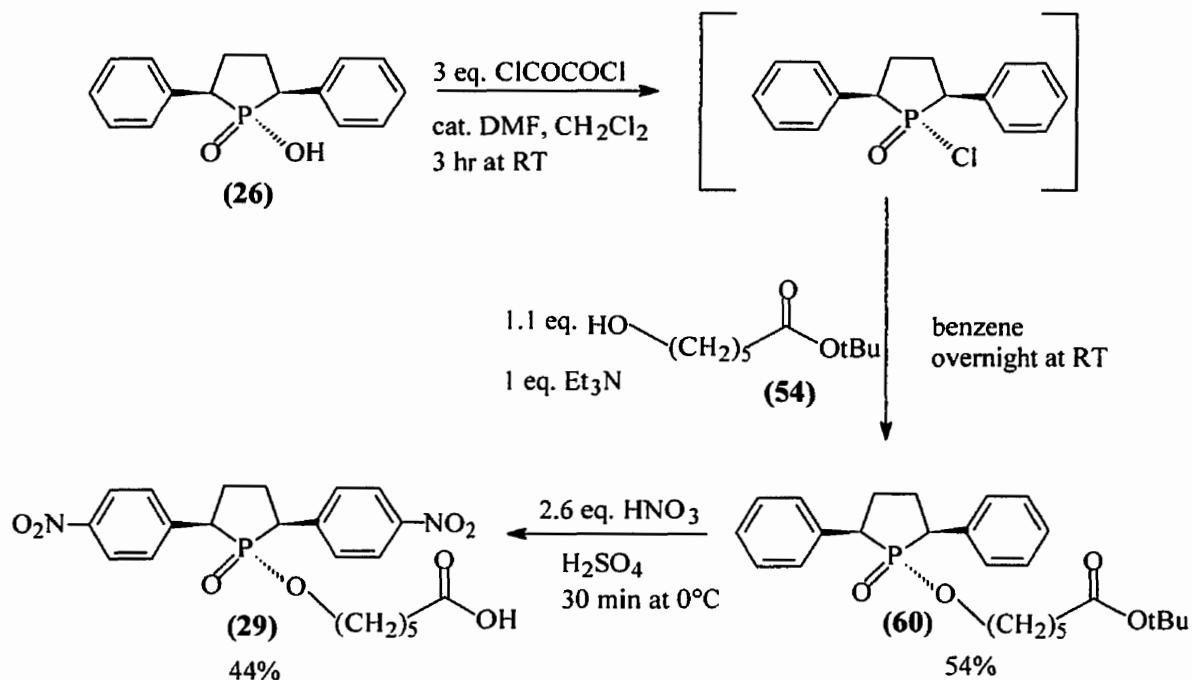
It was clear that the Mitsunobu coupling procedure would not be suitable for forming the cis TSA and an alternative approach towards was required. Taylor<sup>26</sup> had previously demonstrated that the non-nitrated “aryl-cis” ester, **28**, (Scheme 11) could be obtained using the acid chloride procedure. However, we have shown that this procedure was incompatible



**Scheme 29:** Alternate mechanism for the Mitsunobu coupling

with the nitrated acid (Scheme 25). With the success in selectively nitrating the ethoxy esters (38-40) at the *para* position, we reasoned that we could generate the nitrated cis TSA by nitrating the original non-nitrated cis hapten (13 in Scheme 11). Thus, the t-butyl protected linker chain was attached to the non-nitrated acid, 26, using the phosphochloride approach yielding 60 exclusively in a 54 % yield. We reasoned that, since the t-butyl group is sensitive to acid, we could obtain the desired cis TSA in a single step since the nitration

TSA in a 58% yield which after HPLC purification gave pure product in 44% yield (Scheme 30).



**Scheme 30: Synthesis of 29**

### 3.2 Hapten Isomerization Studies

The ease by which the cis esters isomerize raised some concerns as to whether it would be possible to obtain antibodies to the cis TSA (**29**). More specifically, we were concerned that **29** would isomerize to **30** during the conjugation (to the carrier protein) and immunization processes and mainly antibodies specific to the trans TSA, **30**, would be obtained. What we required was some assurance that the cis isomer would be sufficiently

able to survive the conjugation process as well as the immunization process and to elicit cis-specific antibodies.

We considered two methods for following the isomerization process of **29** to **30**. The most obvious experiment would be to follow the reaction by  $^{31}\text{P}$  NMR since the aryl cis and trans isomers have slightly different chemical shifts. This method is not without some drawbacks. Due to sensitivity issues, a fair amount of TSA would be required (20-30 mg) in order to maximize the signal to noise ratio. In addition, the experiments must be carried out in a buffered aqueous solution. This has the disadvantage that the NMR pulse and decoupling sequences often cause such solutions to heat up and the isomerization rate may be accelerated. The alternative procedure was to use HPLC which has far greater sensitivity. We discovered that the cis and trans TSAs (**29** and **30**) have sufficiently different retention times on a normal phase analytical HPLC column with ethyl acetate as an eluent. The cis isomer has a retention time of 3.9 minutes whereas the trans isomer has a retention time of 5.9 minutes as seen in Figure 3 when injected separately and simultaneously from ethyl acetate solutions. To rapidly verify that we could indeed follow the isomerization, we began with a 500  $\mu\text{M}$  solution of the cis hapten in 0.1 NaOH. Aliquots of the reaction were quenched with HCl, at various time intervals and the reaction mixture was extracted into ethyl acetate and injected into the HPLC. Immediately obvious is the increase in retention times of each isomer. This is most likely due to the fact that the isomers were extracted from an acidified aqueous solution into the ethyl acetate phase which thus becomes saturated with water. The chromatograms after time intervals of 10 minutes, 1 hour, and 1 day are shown in Figure 4 and the results are summarized in Table 1. It can be seen that under such harsh conditions that isomerization

since the three values over the 24 hour period are all within experimental error. The equilibrium value determined in this experiment is slightly different from the value obtained in the isomerization studies of the non-nitrated ethyl esters (22-24) determined by Taylor. In the isomerization of the 'phenyl cis' ethyl ester 22 to the trans product 23 in EtOH, it was found that 87% was in the trans form at equilibrium. However, with 29, in an 0.1 N NaOH solution, approximately 75% of the TSA is in the trans form at equilibrium. These discrepancies may be attributed to a number of factors the most obvious being the difference in solvents (EtOH vs water). The linker chain is also a larger than an ethyl group which would favor more of the cis product being present at equilibrium.

**Table 1** Isomerization Studies in 0.1 N NaOH

Incubation Period	% Cis Isomer (29)	% Trans Isomer (30)
10 minutes	24	76
1 hour	22	78
1 day	26	74

In order to mimic the *in vivo* conditions, as well as those encountered during the conjugation process, we chose to study the extent of isomerization at physiological pH (pH 7.5) in potassium phosphate buffer. Figure 5 shows the chromatograms recorded after incubation periods of 25 min, 1, 3, 7, and 11 days in phosphate buffer at pH 7.5. The results are summarized in Table 2. After a week at pH 7.5, only 8% of the cis hapten had been isomerized to the trans form. The results showed that sufficient quantities of the cis hapten

**Table 2** Isomerization Studies in Potassium Phosphate Buffer at pH 7.5

Incubation Period	% Cis Isomer (29)	% Trans Isomer (30)
25 min	100	0
1 day	100	0
3 days	97	3
1 week	92	8
11 days	86	14

We also determined the extent of isomerization of the cis TSA at pH 8.5 in a sodium bicarbonate buffer. This experiment was intended to simulate the conditions that are often employed during the process of screening the monoclonal antibodies for hapten binding. The HPLC chromatograms from this study are shown in Figure 6 and the results are summarized in Table 3. It can be seen that the isomerization occurs considerably faster at pH 8.5. After 3.5 days, only 48% of the cis hapten remained. In light of this data, screening for hapten binding will have to be performed at pH lower than 8.5.

**Table 3** Isomerization Studies in NaHCO<sub>3</sub> Buffer at pH 8.5

Incubation Period	% Cis Isomer (29)	% Trans Isomer (30)
20 minutes	100	0
3.5 days	48	52
8 days	29	71

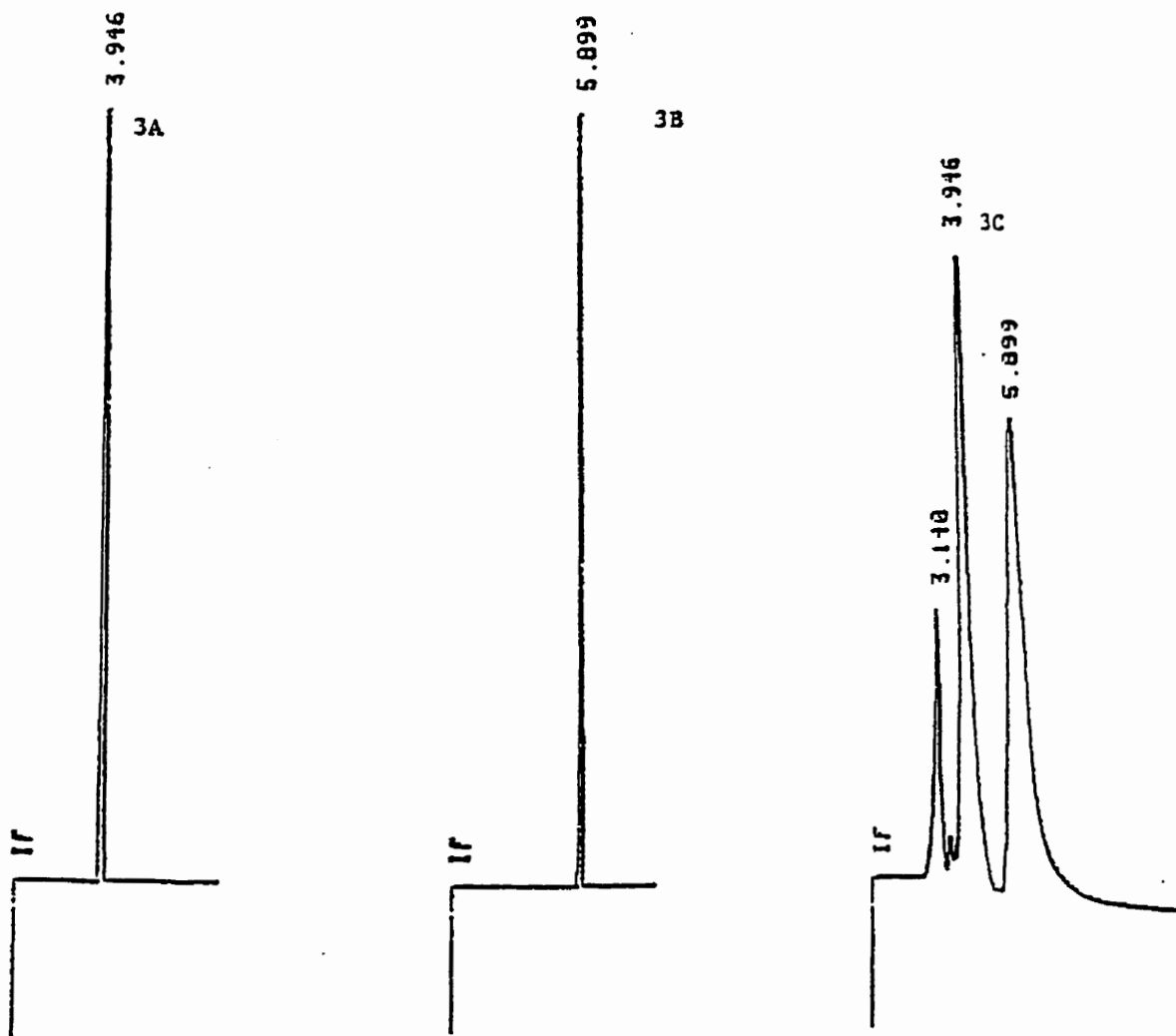
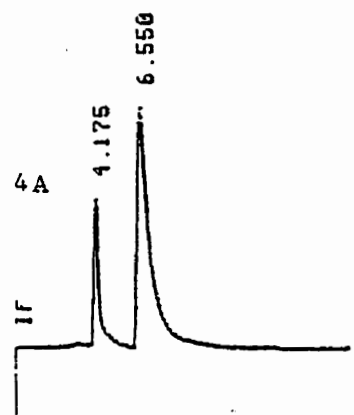
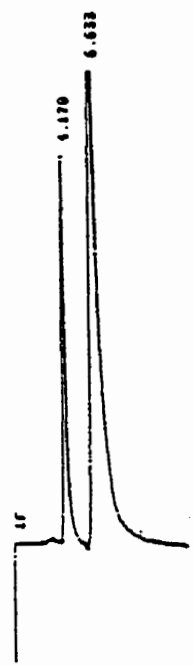


Figure 3: HPLC chromatograms of (A) 29, (B) 30, and (C) 29 and 30

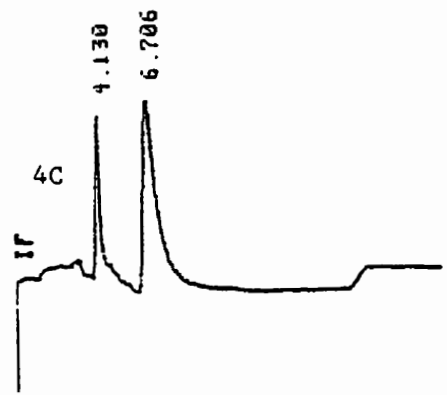


RT	AREA	TYPE	WIDTH	AREA%
4.175	1815478	PB	.351	23.64499
6.550	5862529	PB	.724	76.35501

4B



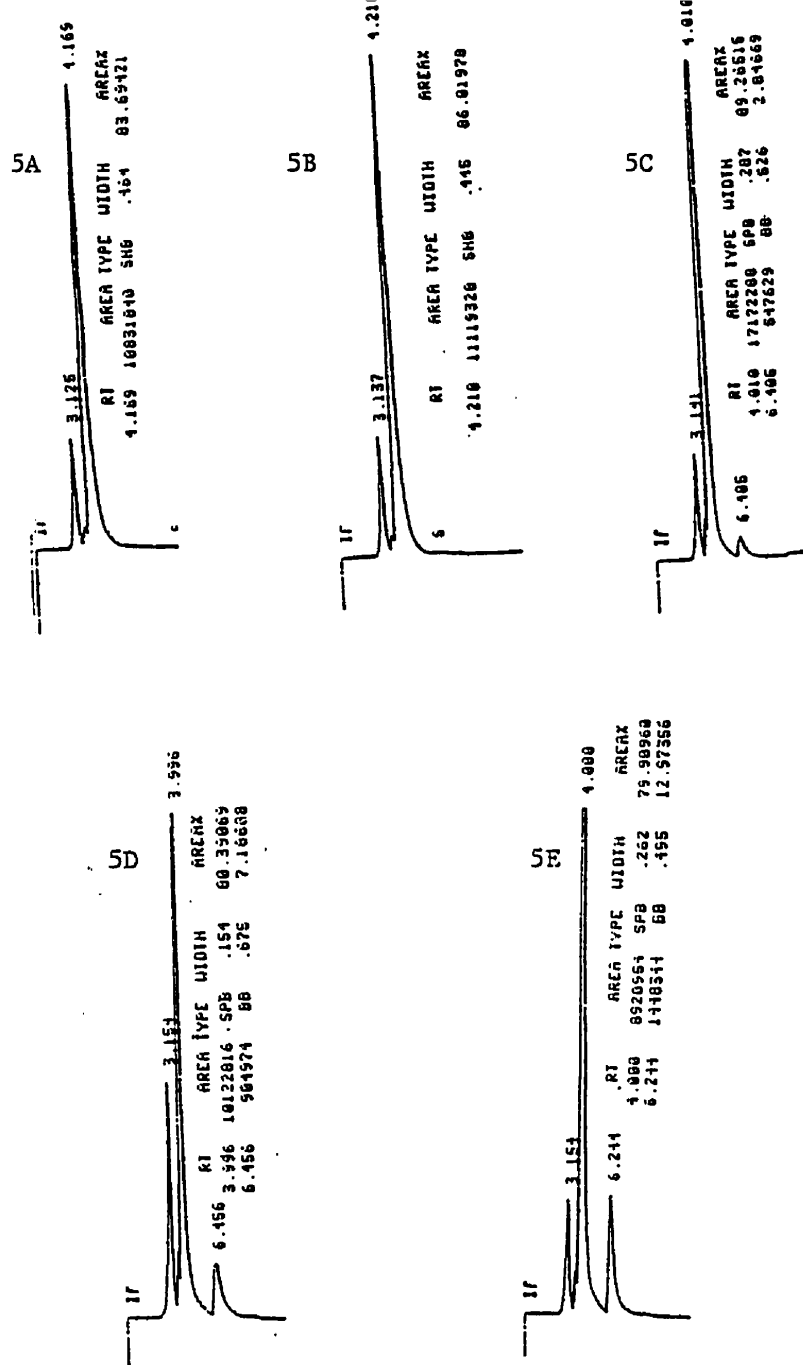
RT	AREA	TYPE	WIDTH	AREA%
4.170	1690194	PB	.324	21.58619
6.633	6139747	PB	.796	78.41382



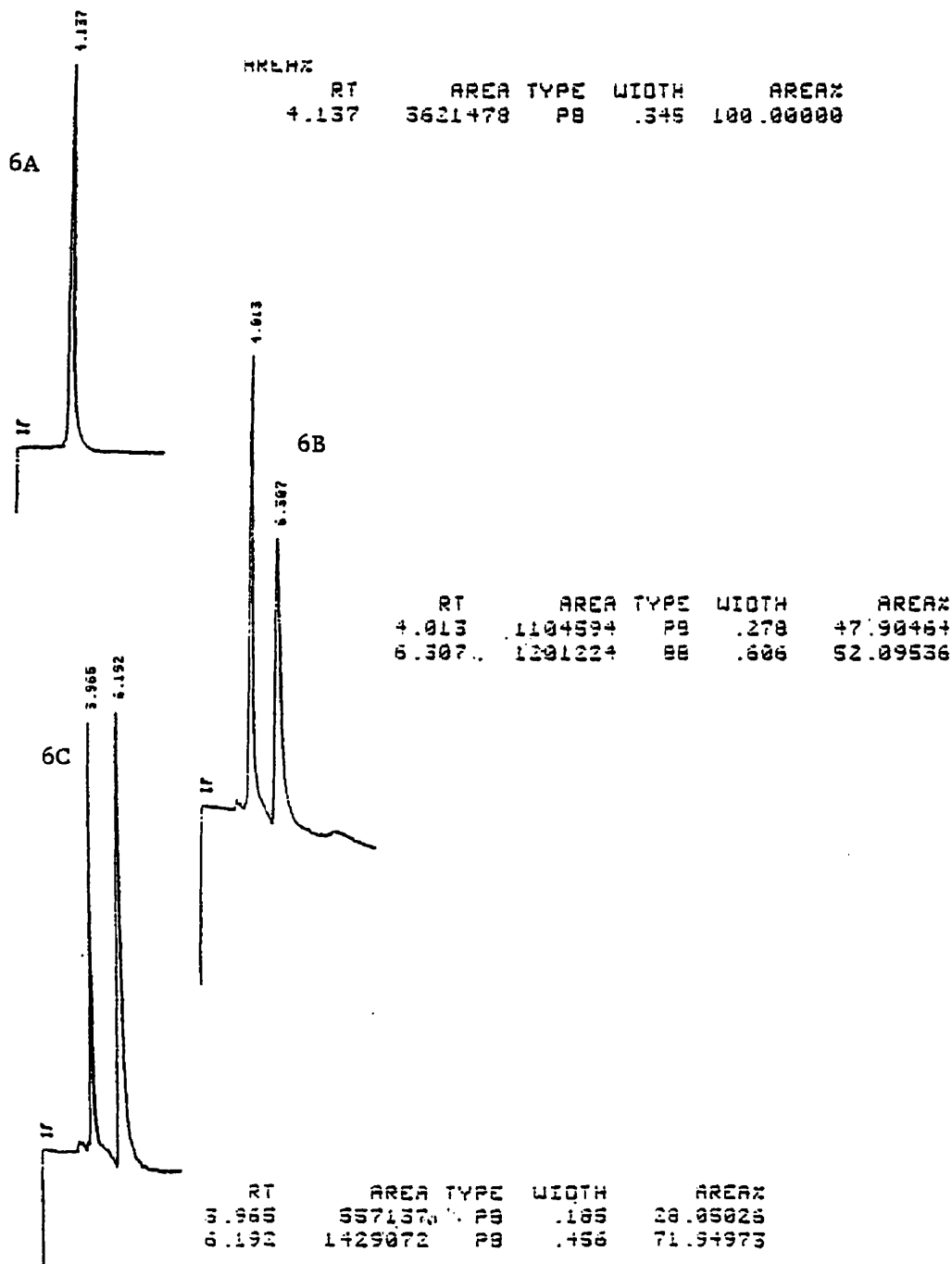
RT	AREA	TYPE	WIDTH	AREA%
4.130	456396	PB	.325	25.86740
6.706	1307972	PB	.811	74.13251

Figure 4: HPLC chromatogram of cis TSA 29 in 0.1 N NaOH after (A) t = 10 min, (B) t = 1 hour, and (C) t = 1 day



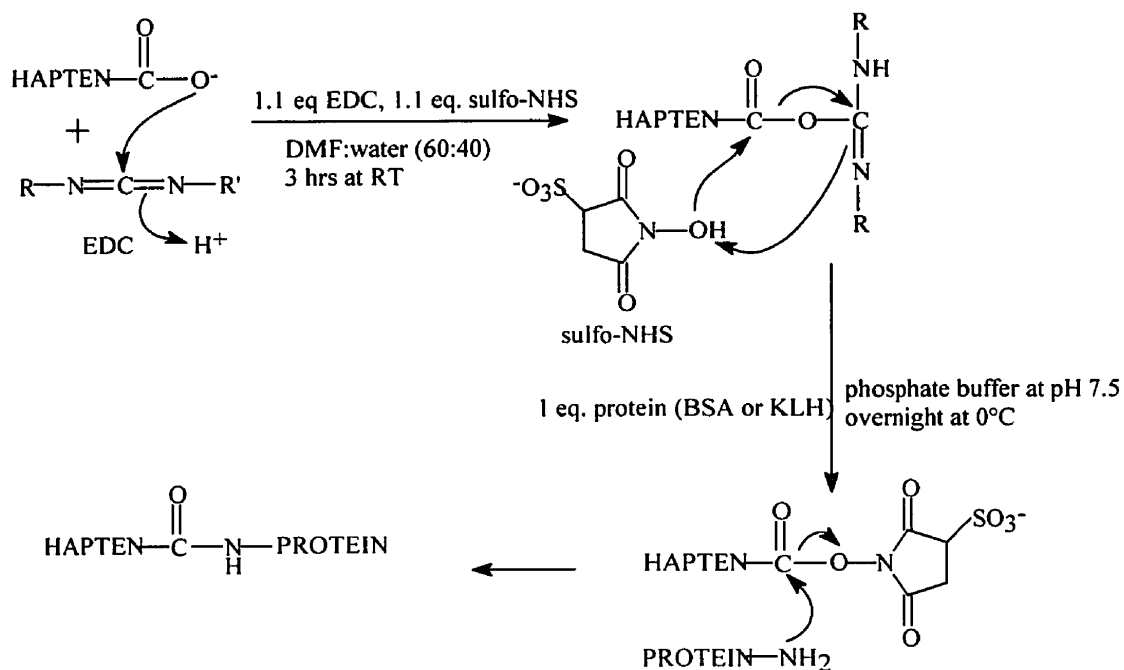


**Figure 5:** HPLC chromatograms of cis-TSA 29 in sodium phosphate buffer at pH 7.5 at (A) t = 25 min (B) t = 1 day (C) t = 3 days (D) t = 1 week (E) t = 11 days



**Figure 6:** HPLC Chromatograms of cis TSA 29 in sodium bicarbonate buffer at pH 8.5 at (A) t = 20 minutes (B) t = 3.5 days (C) t = 8 days

Being small molecules, **29** and **30** must be attached to a carrier protein in order to generate an immune response. We chose bovine serum albumin (BSA) and keyhole limpet hemocyanin (KLH) as the carrier proteins since these are commonly used as carrier proteins for monoclonal production and antibody screening. KLH conjugates are commonly used for immunization, while BSA conjugates are used to screen the antibodies for hapten binding. Two different carrier proteins are used so that one can distinguish between antibodies that recognize the carrier protein (KLH) but not the hapten.



**Scheme 31:** Conjugation of TSA's to carrier proteins

The reaction used to conjugate the haptens is shown in Scheme 31. The procedure

using the EDC coupling agent in a DMF-water solution.<sup>54</sup> The active ester is then reacted with the carrier proteins in phosphate buffer at pH 7.5 at 0°C. The amines of the lysine residues attack the carbonyl group to form the amide linkage.

Subsequent analysis of the BSA-hapten conjugates using the procedure of Habeeb<sup>35</sup> revealed that the conjugation procedures proceeded extremely well. We obtained 19 cis haptens per BSA and 11 trans haptens per BSA. We did not determine the conjugation efficiency for the KLH conjugates due to the presence of some precipitate which interferes with the Habeeb procedure. This is common when working with KLH and it is standard procedure to determine the conjugation efficiency for the BSA conjugates only<sup>52</sup> and assume that since the conjugation works with BSA then it worked equally well with KLH.

#### **3.4 Crystal Structure of trans-2,5-diphenyl phospholanic acid**

A vital part of our hapten design was the endocyclic C-P-C bond angle, since it would determine how much strain the abzymes would exert upon the substrates. Crystal structures obtained by other workers on similar compounds cited endocyclic bond angles at the phosphorous center of 98° for cyclic phosphates<sup>22</sup> and 95° for phospholanic acid.<sup>27</sup> Thus we anticipated that the endocyclic CPC bond angle of our TSAs to be in the range of 95-98°. We were able to grow crystals of the trans acid **25** in methylene chloride. The crystal structure of **25** was determined by Alan Lough from the Chemistry Department at the University of Toronto and is shown in Figure 7. The endocyclic C-P-C bond angle measures 97.7° and is in the expected range. The presence of the p-NO<sub>2</sub> groups is not expected to affect the bond angle value for the nitrated TSAs. Additional crystal structure data is included in Appendix 1.

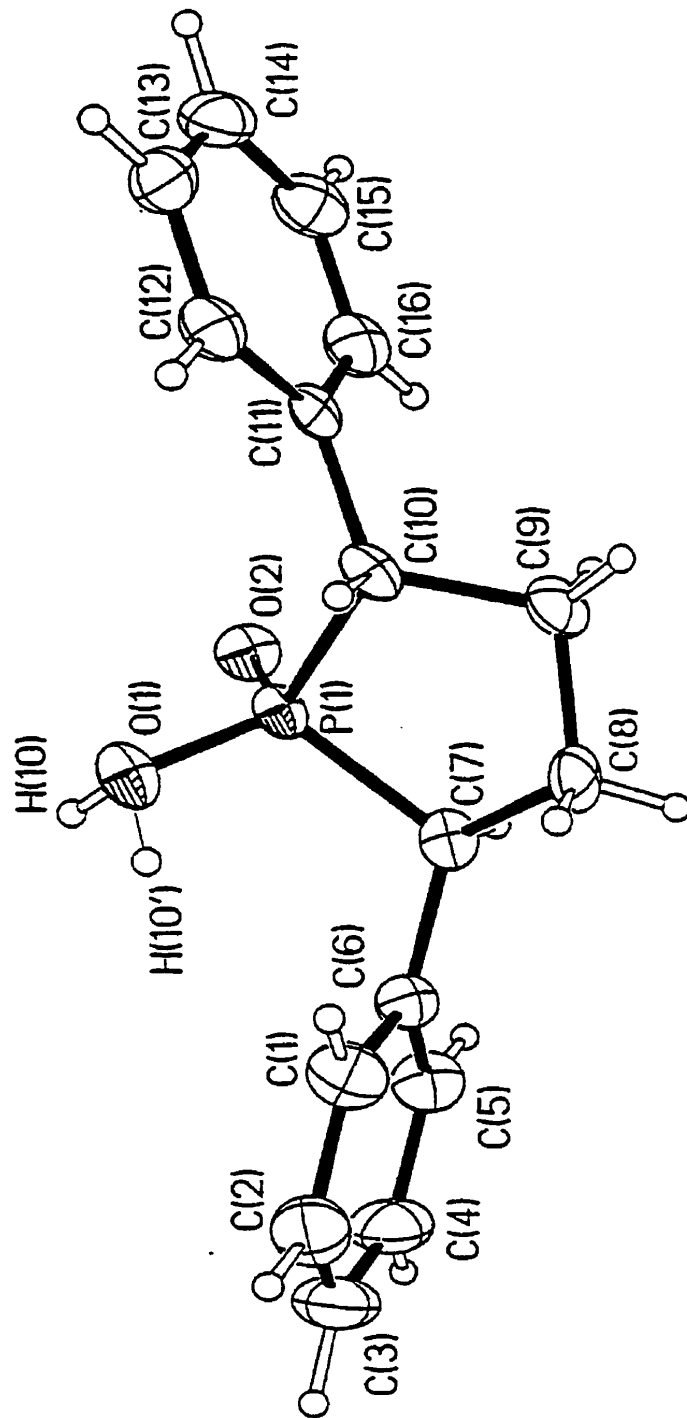
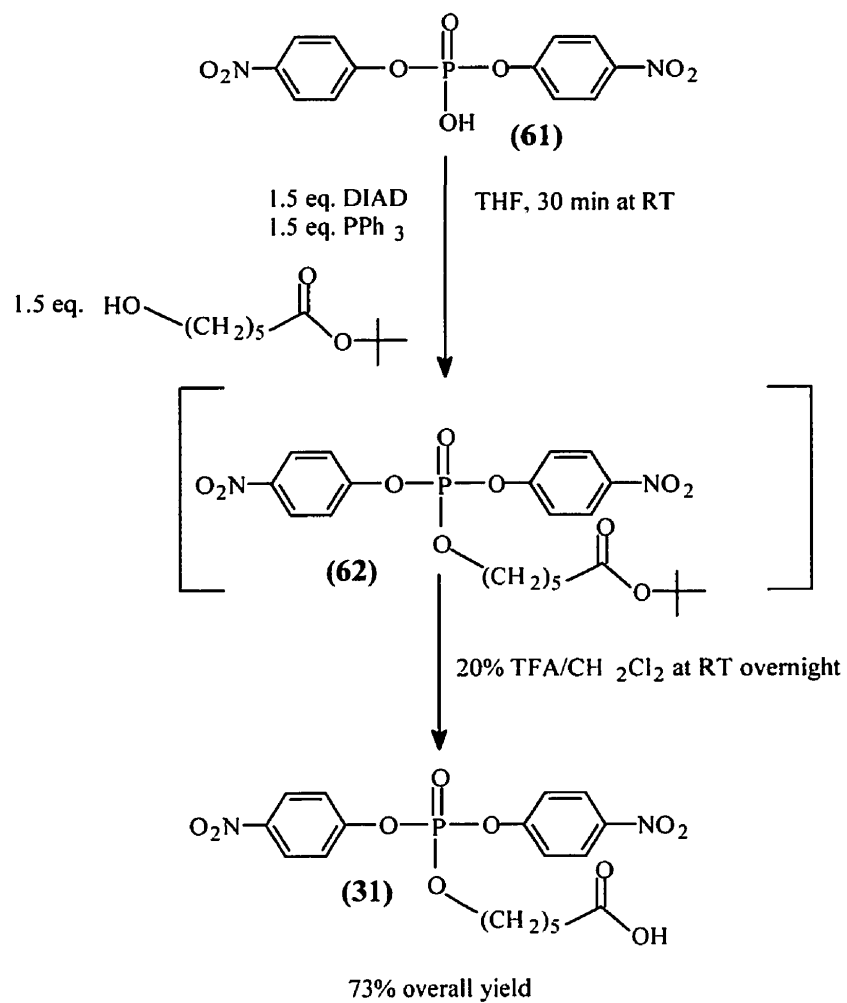


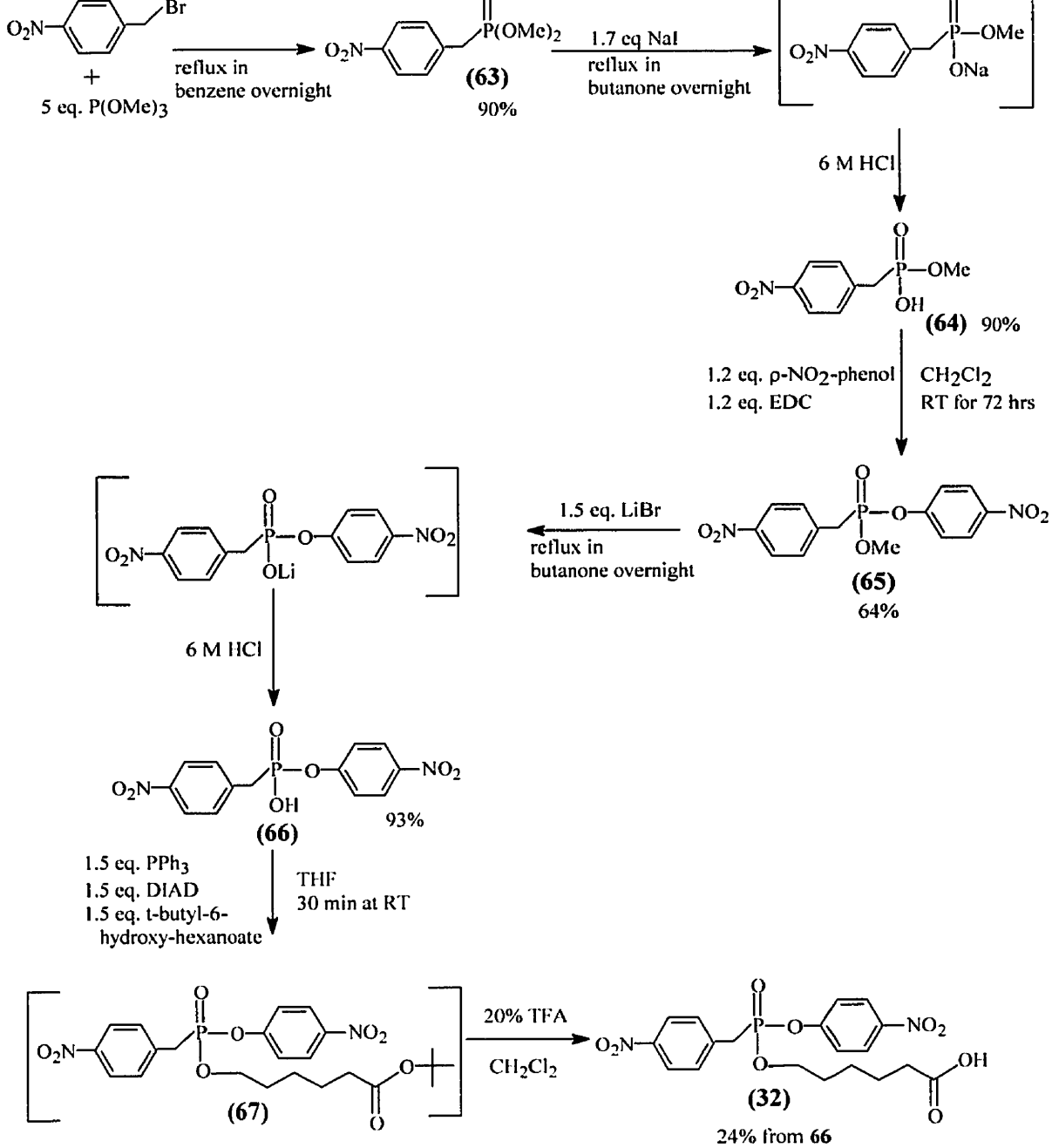
**Figure 7:** Crystal structure of trans 2,5-diphenyl phosphonic acid (25)

The synthesis of the substrates proved to be fairly straightforward. The phosphotriester **31** was synthesized as shown in Scheme 22. The starting material bis-*p*-nitrophenylphosphate (**61**) was purchased from Aldrich. Using the Mitsunobu reaction, the *t*-butyl protected linker chain, **54**, was attached. Due to the slow but constant decomposition of the triester, **62**, trace amounts of *p*-nitrophenol were constantly present, and could not be removed by chromatography thus preventing the isolation of pure **62**. It was only upon deprotection of the acid that the desired phosphate substrate **31** and *p*-nitrophenol could be easily separated. The synthesis proceeded in an overall 73% yield.

The synthesis of the phosphonate substrate **32** was more involved and is outlined in Scheme 33. We began by generating dimethyl *p*-nitrobenzylphosphonate, **63**, via an Arbuzov reaction between *p*-nitrobenzylbromide and trimethyl phosphite in 90% yield. One of the methyl groups of **63** was removed by reaction with sodium iodide in butanone to generate the monosodium salt, which was converted directly to the free acid, **64**, in a 90 % yield. We then used EDC to attach the *p*-nitrophenol group in 64% yield. All that remained was to attach the linker chain. This was accomplished by removing the remaining methyl group by refluxing **65** in the presence of LiBr in butanone followed and converting the lithium salt to the free acid, **66**, in a 93% yield. The Mitsunobu reaction was then used to couple the *t*-butyl protected linker chain to form the protected substrate **67**. Once again, the *p*-nitrophenol was difficult to separate from **67**. Thus, crude **67** was subjected to a 20% TFA/CH<sub>2</sub>Cl<sub>2</sub> solution which resulted in the removal of the *t*-butyl group and formation of the desired phosphonate substrate **32** which was readily purified. The overall yield from the acid **66** to the final



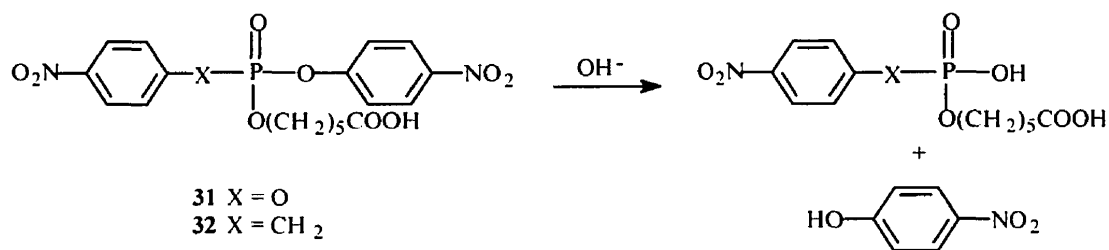
**Scheme 32:** Synthesis of phosphate substrate **31**



**Scheme 33: Synthesis of phosphonate substrate 32**



In order to be able to determine if any antibodies raised to TSA's **29** and **30** are capable of catalyzing the hydrolysis of substrates **31** and **32**, it is necessary to determine the rate at substrates **31** and **32** hydrolyze in the absence of antibody. Consequently, we determined the rate of hydrolysis of both substrates in a sodium bicarbonate buffer at pH 9 since this is the pH at which we wished to screen the antibodies for catalytic activity. These stability studies are preliminary results in order to approximate the rate of reaction of our substrates. Since *p*-nitrophenol is produced as a hydrolysis product (Scheme 34), it was possible to monitor the course of the reactions by following the increase in absorbance at 405 nm as a function of time. The results were analyzed using the Graft software package which fitted the data to a first order rate equation (Figures 8-9). Under these conditions, the phosphate substrate hydrolyzes with a half-life of approximately 9 hours while the phosphonate substrate has a half-life of approximately 14 hours. These results indicate that the substrates are sufficiently stable enough to be used for screening the antibodies for catalytic activity. They are, however, sufficiently labile to be susceptible to antibody catalysis.



**Scheme 34:** Hydrolysis of substrates **31** and **32**

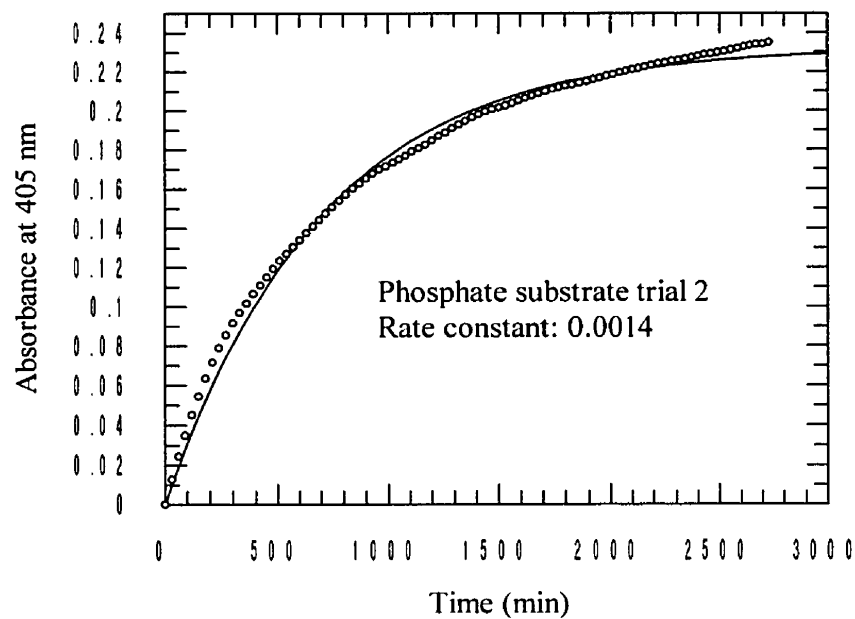
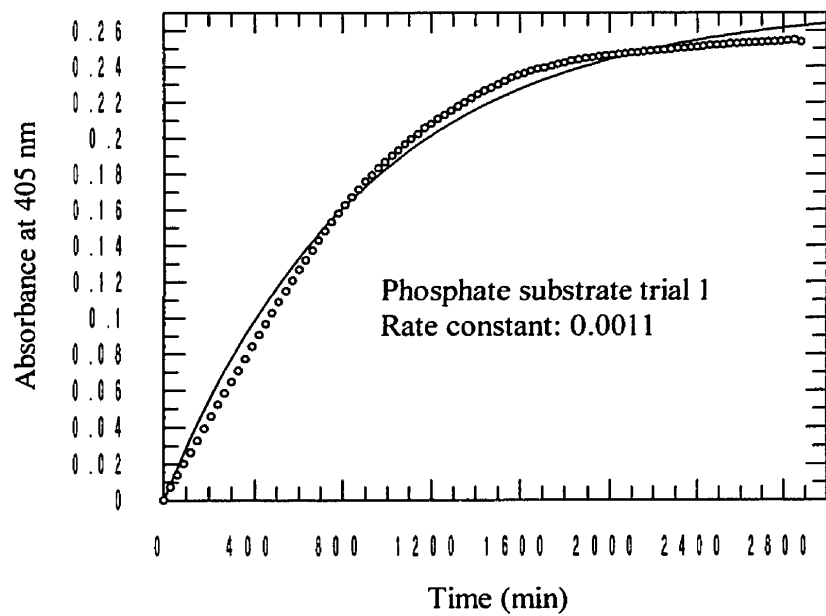


**Figure 8:** Duplicate plots of absorbance at 405 nm as a function of time for the hydrolysis of phosphate substrate **31**

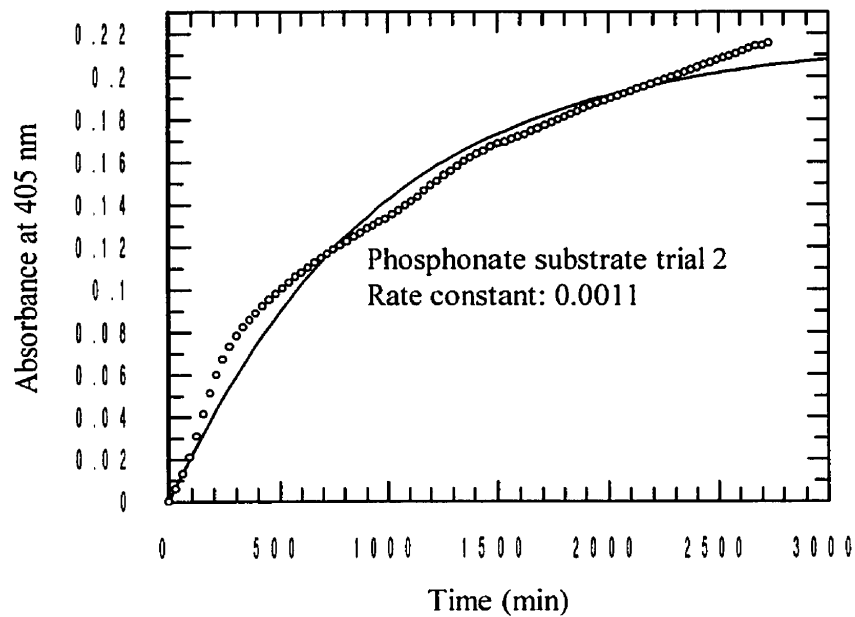
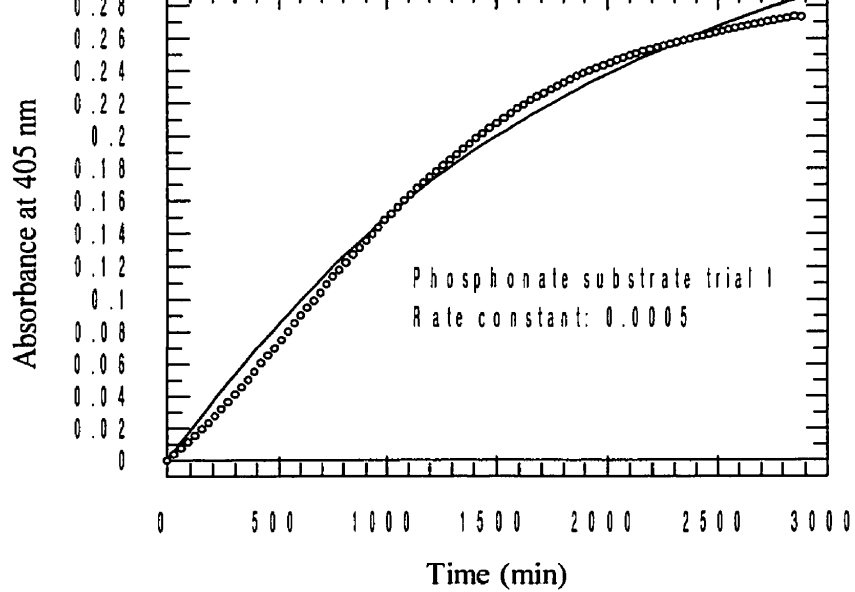


**Figure 9:** Duplicate plots of absorbance at 405 nm as a function of time for the hydrolysis of phosphonate substrate 32

In summary, we have described the synthesis of two novel 2,5-diarylphosphonate esters and discussed their potential as TSAs for generating phosphotriesterase antibodies. These TSAs are designed to mimic both a strained ground state and the transition state for phosphotriester hydrolysis. The strained nature of these TSAs was confirmed by an X-ray crystal structure of one of the TSA precursors. The stability of these haptens has been assessed and judged to be adequate for both the purposes of conjugation and immunization. Antibodies obtained from these studies will be examined for their ability to catalyze the hydrolysis of substrates **31** and **32** which we have synthesized and found to be suitable substrates for the antibody-catalyzed reaction. The TSA's have been conjugated to carrier proteins and sent to the laboratory of Prof. Jeremy Lee, for monoclonal antibody production. Antibodies specific for these TSAs will be sent to our laboratory where they will be screened for catalytic activity. Should any abzymes be obtained from these studies, they will shed light as to the role of strain in enzyme-catalyzed reactions. In addition, these studies will lay the ground work for the generation of abzymes of that could be used for the detoxification of organophosphorus-based toxins.

1. Jencks, W.P. "*Catalysis in Chemistry and Enzymology*" McGraw-Hill, New York, **1969**.
2. Pollack, S.J.; Jacobs, J.W.; Schultz, P.G. *Science* **1986**, 234, 1570.
3. Tramantano, A.; Janda, K. D.; Lerner, R.A. *Science* **1986**, 234, 1566.
4. Tramantano, A.; Janda, K. D.; Lerner, R.A. *Proc. Natl. Acad. Sci.* **1986**, 83, 6736.
5. Lerner, R.A.; Benkovic, S. J.; Schultz, P. G. *Science* **1991**, 252, 659.
6. Tawfik, D. S.; Lindner, A. B.; Chap, R.; Eshhar, Z.; Green, B. S. *Eur. J. Biochem.* **1996**, 1329/3.
7. Shokat, K. M.; Leuman, C. J.; Sugawara, R.; Schultz, P. G. *Nature* **1989**, 338, 269.
8. Thatcher, G. R. J.; Kluger, R. *Adv. Phys. Org. Chem.* **1989**, 25 99.
9. Rosenblum, J. S.; Lo, L. C.; Li, T.; Janda, K. D.; Lerner, R. A. *Angew. Chem. Intl. Ed. Engl.* **1995**, 34, n20, 2275.
10. Lavey, B. J.; Janda, K. D. *J. Org. Chem* **1996**, 61, 7633.
11. Walsh, C. "*Enzymatic Reaction Mechanisms*" W. H. Freeman and Co., San Francisco, **1979**.
12. Fersht, A. "*Enzyme Structure and Mechanism 2nd Ed.*" W. H. Freeman and Co., New York, **1985**.
13. Palmer, T. "*Understanding Enzymes 4th Ed.*" Prentice Hall Ellis Horwood, New York, **1995**.
14. Voet, D. G.; Voet, J. G. "*Biochemistry*" John Wiley and Sons, Inc., Toronto, **1995**.

15. Blake, C. C. F.; Johnson, L. N.; Mann, G. F. R.; North, A. C. F.; Phillips, D. C.; Sarma, V. R. *Proc. R. Soc. London Ser. B* **1967**, 167, 378.
16. Warshel, A.; Levitt, M.; *J. Molec. Biol.* **1975**, 92, 279.
17. Ghosh, P.; Shabat, D.; Kumar, S.; Gryszpan, F.; Li, J.; Noodleman, L.; Keinan, E. *Nature* **1996**, 382, 339.
18. Smith, R. M.; Weiner, D. P.; Chaturvedi, N. C.; Thimblin Jr., M. D.; Raymond, S. J., Hansen, D. E. *Bioorganic Chemistry* **1995**, 23, 397.
19. Yuan, P.; Plourde, R.; Shoemaker, M. R.; Moore, C. L.; Hansen, D. E. *J. Org. Chem.* **1995**, 60, 16, 5360.
20. Covitz, F.; Westheimer, F. H. *J. Am. Chem. Soc.* **1963**, 85, 1773.
21. Westheimer, F. H. *Acc. Chem. Res.* **1968**, 1, 70.
22. Chiu, Y.H.; Lipscomb, W. N. *J. Am. Chem. Soc.* **1969**, 91, 4150.
23. Kluger, R. H.; Taylor, S. D. *J. Am. Chem. Soc.* **1990**, 112, 6669.
24. Taylor, S. D.; Kluger, R. H. *J. Am. Chem. Soc.* **1992**, 114, 3067.
25. Taylor, S. D. PhD. Thesis, Department of Chemistry at the University of Toronto **1991**.
26. Taylor, S. D. Unpublished results.
27. Alver, E.; Koge, H. M. *Acta. Chem. Scand.* **1969**, 23, 1101.
28. Holmes, R. R. "Pentacoordinated Phosphorus. ACS Monograph 175" American Chemical Society, Washington, D. C., **1980**, vol. 1, Chp. 2.
29. Prezhdo, V. V., Prezhdo, O. V.; Vaschenko, E. V. *J. Mol. Struct.* **1996**, 385, 137.
30. Kalinov, S. M.; Rostovskaya, M F.; Vysotskii, V .I. *Zh. Obsch. Khim.* **1988**, 58, 783.
31. McCormack, W. B. U.S. Patents 2,663,737, **1953**; *Chem. Abst.* **1955**, 49, 7601.

32. Mouritzel, R. *Synthetic Reaction Methods for Organic Chemistry*, 10, 1, 10.
33. Tebby, J. C. ed. "CRC Handbook of Phosphorous-31 Nuclear Magnetic Resonance Data"  
CRC Press, 1991.
34. Larock, R. C.; Leach, D. R. *J. Org. Chem.* **1984**, 49, 2144.
35. Habeeb, A. F. S. A. *Anal. Biochem.* **1966**, 14, 328.
36. Grafit 3.0 from Erithacus Software.
37. Akiyama, S.; Tajima, K.; Nakatsuji, S.; Nakashima, K.; Abiru, K.; Watanabe, M. *Bull. Chem. Soc. Jpn.* **1995**, 68, 2043.
38. Harmons; Parsons; Cooke; Gupta; Schoolenberg *J. Org. Chem.* **1969**, 34, 3684.
39. Quin, L.D. "Heterocyclic Chemistry of Phosphorous" John Wiley and Sons Inc., New York, **1981**.
40. Cadogan, J. I. G. *Quart. Rev., Chem. Soc.*, **1962**, 16, 208.
41. Cadogan, J. I. G. *Acc. Chem. Res.* **1972**, 5, 303.
42. Quin, L.D.; Gratz, J. P.; Barket, T. P. *J. Org. Chem.* **1968**, 33, 1034.
43. Quin, L.D.; Barket, T. P. *Chem. Commun.*, **1967**, 914.
44. Razumova, N. A.; Evtikhov, Z. L.; Petrov, A. A. *J. Gen. Chem. USSR* **1969**, 39, 1388.
45. Razumova, N.A.; Bagrov, F.V.; Petrov, A. A. *J. Gen. Chem. USSR* **1969**, 39,2305.
46. Bodalski, R.; Pietrusiewicz, K. M.; Koszuk, J. *Tetrahedron* **1975**, 31, 1907.
47. Olah, G.A.; Malhotra, R.; Narang, S.C. "Nitration Methods and Mechanisms" VCH Publishers, New York, **1989**.
48. March, J. "Advanced Organic Chemistry - Reactions, Mechanisms, and Structure 3rd Ed."  
John Wiley and Sons, Toronto, **1985**.

*and Synthesis*” Plenum Press, New York, **1993**.

50. Kocienski, P. J. “*Protecting Groups*” Thieme, New York, **1994**.

51. Campbell, D. A.; Bermak, J. C. *J. Org. Chem.* **1994**, 59 658.

52. S. D. Taylor Personal Communication.

53. Robertson, G. R. *Org. Synth.* **I**, **1932**, 389.

54. Janda, K. D.; Weinhouse, M. I.; Schloeder, D. M.; Lerner, R. A.; Benkovic, S. J. *J. Am.*

*Chem. Soc.* **1990**, 112, 1274.



Appendix A contains supplemental data for the crystal structure of trans 2,5-diphenyl phospholanic acid.

	page
Crystal data and structure refinement	A(ii)
Atomic Coordinates	A(iii)
Bond Lengths and Angles	A(iv)
Anisotropic Displacement Parameters	A(v)
Hydrogen Coordinates and Isotropic Displacement Parameters	A(vi)

Identification code	39739
Empirical formula	$C_{16}H_{17}O_2P$
Formula weight	272.27
Temperature	293(2) K
Wavelength	0.71073 Å
Crystal system	Monoclinic
Space group	C2
Unit cell dimensions	$a = 22.559(2)$ Å $\alpha = 90^\circ$ $b = 5.7077(5)$ Å $\beta = 105.445(2)^\circ$ $c = 11.3422(9)$ Å $\gamma = 90^\circ$
Volume, Z	1407.7(2) Å <sup>3</sup> , 4
Density (calculated)	1.285 Mg/m <sup>3</sup>
Absorption coefficient	0.190 mm <sup>-1</sup>
F(000)	576
Crystal size	0.15 × 0.15 × 0.25 mm
$\theta$ range for data collection	1.86 to 28.27 <sup>o</sup>
Limiting indices	-29 ≤ h ≤ 24, -7 ≤ k ≤ 6, -14 ≤ l ≤ 15
Reflections collected	4459
Independent reflections	2778 ( $R_{int} = 0.0445$ )
Absorption correction	Semi-empirical
Refinement method	Full-matrix least-squares on $F^2$
Data / restraints / parameters	2778 / 1 / 192
Goodness-of-fit on $F^2$	1.032
Final R indices [ $I > 2\sigma(I)$ ]	$R1 = 0.0605$ , $wR2 = 0.1210$
R indices (all data)	$R1 = 0.0878$ , $wR2 = 0.1335$
Absolute structure parameter	-0.1(2)
Extinction coefficient	0.0022(11)
Largest diff. peak and hole	0.420 and -0.485 eÅ <sup>-3</sup>

Table 2. Atomic coordinates [ $\times 10^4$ ] and equivalent isotropic displacement parameters [ $\text{\AA}^2 \times 10^3$ ] for 1.  $U(\text{eq})$  is defined as one third of the trace of the orthogonalized  $U_{ij}$  tensor.

	x	y	z	$U(\text{eq})$
P(1)	1809(1)	2296(2)	392(1)	22(1)
O(1)	1954(1)	-325(5)	649(3)	29(1)
O(2)	2013(1)	3274(5)	-670(2)	27(1)
C(1)	2519(2)	1179(9)	3435(4)	37(1)
C(2)	3004(2)	340(9)	4373(4)	44(1)
C(3)	3566(2)	1477(9)	4637(4)	48(1)
C(4)	3645(2)	3394(9)	3974(4)	46(1)
C(5)	3158(2)	4265(8)	3043(4)	33(1)
C(6)	2589(2)	3124(7)	2771(3)	26(1)
C(7)	2065(2)	4110(7)	1760(3)	24(1)
C(8)	1461(2)	4692(8)	2103(4)	31(1)
C(9)	949(2)	4851(8)	917(4)	31(1)
C(10)	983(2)	2612(7)	189(3)	23(1)
C(11)	593(2)	2488(8)	-1114(3)	24(1)
C(12)	210(2)	564(7)	-1507(4)	29(1)
C(13)	-169(2)	434(8)	-2681(4)	37(1)
C(14)	-170(2)	2204(10)	-3502(3)	39(1)
C(15)	224(2)	4097(9)	-3146(4)	38(1)
C(16)	606(2)	4234(8)	-1966(4)	32(1)

Table 3. Bond lengths [Å] and angles [°] for 1.

P(1)-O(2)	1.506(3)	P(1)-O(1)	1.542(3)
<u>P(1)-C(10)</u>	1.824(3)	<u>P(1)-C(7)</u>	1.827(4)
C(1)-C(6)	1.374(6)	C(1)-C(2)	1.392(6)
C(2)-C(3)	1.385(7)	C(3)-C(4)	1.366(7)
C(4)-C(5)	1.397(6)	C(5)-C(6)	1.398(5)
C(6)-C(7)	1.519(5)	C(7)-C(8)	1.550(5)
C(8)-C(9)	1.526(5)	C(9)-C(10)	1.534(6)
C(10)-C(11)	1.506(5)	C(11)-C(16)	1.394(6)
C(11)-C(12)	1.395(6)	C(12)-C(13)	1.380(6)
C(13)-C(14)	1.373(6)	C(14)-C(15)	1.388(7)
C(15)-C(16)	1.388(6)		
O(2)-P(1)-O(1)	114.6(2)	O(2)-P(1)-C(10)	112.5(2)
O(1)-P(1)-C(10)	106.1(2)	O(2)-P(1)-C(7)	111.9(2)
O(1)-P(1)-C(7)	112.7(2)	<u>C(10)-P(1)-C(7)</u>	97.7(2)
C(6)-C(1)-C(2)	121.0(4)	C(3)-C(2)-C(1)	119.5(4)
C(4)-C(3)-C(2)	120.1(4)	C(3)-C(4)-C(5)	120.7(5)
C(4)-C(5)-C(6)	119.5(4)	C(1)-C(6)-C(5)	119.2(4)
C(1)-C(6)-C(7)	122.2(4)	C(5)-C(6)-C(7)	118.5(4)
C(6)-C(7)-C(8)	116.7(3)	C(6)-C(7)-P(1)	116.0(3)
C(8)-C(7)-P(1)	103.5(3)	C(9)-C(8)-C(7)	107.5(3)
C(8)-C(9)-C(10)	106.9(3)	C(11)-C(10)-C(9)	117.3(4)
C(11)-C(10)-P(1)	115.3(2)	C(9)-C(10)-P(1)	102.1(2)
C(16)-C(11)-C(10)	117.8(3)	C(16)-C(11)-C(10)	122.2(4)
C(12)-C(11)-C(10)	120.0(4)	C(13)-C(12)-C(11)	121.6(4)
C(14)-C(13)-C(12)	120.2(4)	C(13)-C(14)-C(15)	119.4(4)
C(16)-C(15)-C(14)	120.6(4)	C(15)-C(16)-C(11)	120.4(4)

Symmetry transformations used to generate equivalent atoms:

Table 4. Anisotropic displacement parameters [ $\text{\AA}^2 \times 10^3$ ] for 1.

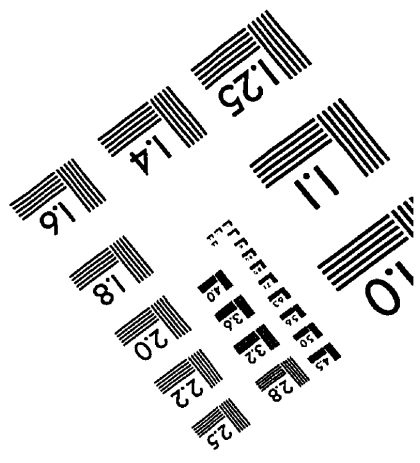
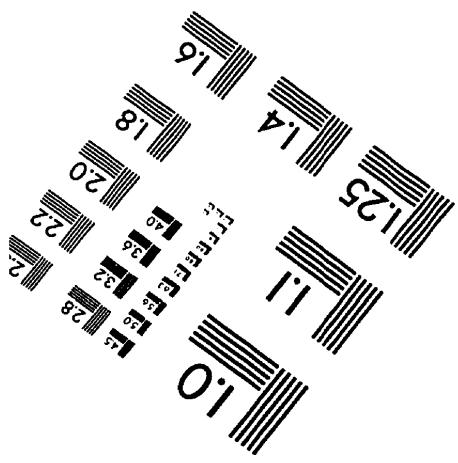
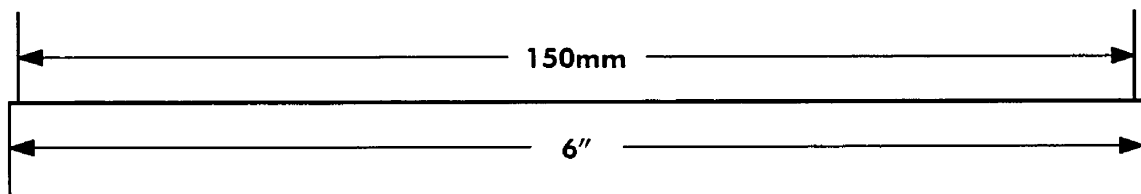
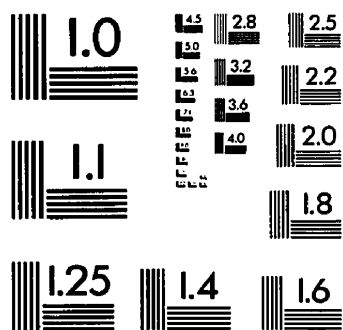
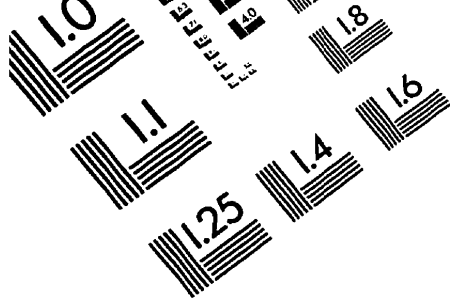
The anisotropic displacement factor exponent takes the form:

$$-2\pi^2 [ (ha^*)^2 U_{11} + \dots + 2hka^* b^* U_{12} ]$$

	U11	U22	U33	U23	U13	U12
P(1)	12(1)	24(1)	32(1)	1(1)	10(1)	0(1)
O(1)	16(1)	31(2)	44(2)	2(1)	15(1)	1(1)
O(2)	17(1)	36(2)	32(1)	1(1)	13(1)	-4(1)
C(1)	35(3)	38(3)	38(2)	7(2)	10(2)	0(2)
C(2)	61(3)	43(3)	32(2)	11(2)	18(2)	9(2)
C(3)	39(3)	66(4)	33(2)	6(2)	-1(2)	15(2)
C(4)	30(3)	66(3)	37(2)	-3(2)	-2(2)	5(2)
C(5)	24(2)	40(3)	36(2)	1(2)	9(2)	-5(2)
C(6)	21(2)	32(2)	26(2)	0(2)	8(2)	0(2)
C(7)	20(2)	22(2)	34(2)	-1(2)	12(2)	-5(2)
C(8)	26(2)	36(3)	36(2)	-9(2)	14(2)	5(2)
C(9)	18(2)	36(3)	40(2)	-1(2)	10(2)	4(2)
C(10)	13(2)	26(2)	34(2)	4(2)	12(1)	2(2)
C(11)	13(2)	30(2)	31(2)	-3(2)	11(1)	6(2)
C(12)	21(2)	33(3)	37(2)	1(2)	14(2)	5(2)
C(13)	28(2)	45(3)	39(2)	-11(2)	12(2)	2(2)
C(14)	25(2)	57(3)	34(2)	-5(3)	4(2)	8(3)
C(15)	31(2)	48(3)	38(2)	8(2)	14(2)	6(2)
C(16)	22(2)	33(2)	43(2)	0(2)	14(2)	0(2)

Table 5. Hydrogen coordinates (  $\times 10^4$  ) and isotropic displacement parameters ( $\text{\AA}^2 \times 10^3$ ) for 1.

	x	y	z	U(eq)
H(10)	2285(13)	-636(24)	517(53)	33(18)
H(10')	2121(25)	-509(15)	1379(9)	33(18)
H(1)	2142(2)	411(9)	3254(4)	44(13)
H(2)	2950(2)	-973(9)	4818(4)	51(14)
H(3)	3891(2)	935(9)	5263(4)	50(14)
H(4)	4027(2)	4125(9)	4143(4)	70(17)
H(5)	3212(2)	5594(8)	2608(4)	42(13)
H(7)	2214(2)	5584(7)	1498(3)	35(12)
H(8A)	1369(2)	3475(8)	2625(4)	49(14)
H(8B)	1502(2)	6169(8)	2540(4)	12(9)
H(9A)	1006(2)	6222(8)	453(4)	21(10)
H(9B)	552(2)	4967(8)	1091(4)	56(14)
H(10)	855(2)	1314(7)	631(3)	19(9)
H(12)	211(2)	-659(7)	-966(4)	12(9)
H(13)	-425(2)	-856(8)	-2913(4)	63(16)
H(14)	-431(2)	2136(10)	-4288(3)	45(12)
H(15)	232(2)	5283(9)	-3703(4)	25(11)
H(16)	872(2)	5499(8)	-1742(4)	29(11)



**APPLIED IMAGE, Inc**  
1653 East Main Street  
Rochester, NY 14609 USA  
Phone: 716/482-0300  
Fax: 716/288-5989

© 1993, Applied Image, Inc., All Rights Reserved